Project title: Implications of Medical Low Dose Radiation Exposure

Grant Agreement Number: 755523

Call identifier: NFRP-2016-2017

Topic: NFRP-9

Deliverable 2.15

Organ dose conversion coefficients for the estimation of patient doses from CT for attenuation correction and anatomic localisation in multi-modality imaging

Lead partner:	UGent
Author(s):	Gwenny Verfaillie, Klaus Bacher
Work Package:	WP2
Estimated delivery:	31 October 2021
Actual delivery:	31 October 2021
Type:	Report
Dissemination level:	Public

This project has received funding from the Euratom research and training programme 2014-2018 under grant agreement No 755523.

Table of contents

Abbreviations

3D	Three-dimensional
AC	Attenuation Correction
ACL	Attenuation Correction and anatomical Localisation
AI	Artificial Intelligence
ATCM	Automatic Tube Current Modulation
CT	Computed Tomography
CTDI	Computed Tomography Dose Index
DICOM	Digital Imaging and Communication in Medicine
DLP	Dose-Length Product
FOV	Field of View
HVL	Half-Value Layer
HU	Hounsfield (scale) Unit
MC	Monte Carlo
PACS	Picture Archiving and Communications System
PET	Positron Emission Tomography
ROI	Region Of Interest
SPECT	Single Photon Emission Computed Tomography
SSDE	Size-Specific Dose Estimate
WB	Whole-Body
WED (D_w)	Water Equivalent Diameter

1 Introduction

In nuclear medicine, positron emission tomography (PET) and single photon emission tomography (SPECT) imaging reveal important functional information. However, they often lack morphological data needed to localise the disease [1]. The combination of PET or SPECT with x-ray computed tomography (CT) provides essential anatomical information, thereby improving the quality and confidence in the nuclear medicine diagnosis [2]. Today, hybrid imaging modalities such as PET/CT and SPECT/CT are well-established tools in nuclear medicine departments and play a vital role in the daily workflow of clinicians [3, 4].

The risks from PET/CT and SPECT/CT are generally far outweighed by the benefits of the procedure when used appropriately. However, dual-modality imaging results in increased radiation exposures due to the combined dose from the CT component and the radiopharmaceutical. In nuclear medicine, CT acquisitions may be performed for different reasons. Hence, depending on the clinical task at hand and the image quality requirements, the radiation dose to the patient may differ. For attenuation correction and localisation of the emission data, the CT dose can be relatively small. However, for hybrid systems with diagnostic capabilities, higher exposure levels are more likely. In addition, multimodality examinations are often used to monitor treatment response which require multiple examinations. It is thus important to be aware of the additional dose to the patient from the CT component of the scan [5-9].

Most PET/CT and SPECT/CT systems have separate protocols for diagnostic-, localisation- and/or attenuation correction-exclusive purposes.

Deliverable 2.15 is part of Task 2.3 “Dose evaluation and optimisation of multimodality imaging” of the MEDIRAD project, and is more specifically linked to Subtask 2.3.2 “Patient organ dose estimation and optimisation of chest multimodality protocols”. It aims to propose conversion coefficients for the estimation of CT dose to the breast (female), heart, liver, lungs, kidneys, thyroid, esophagus, ribs and spine of adult patients undergoing a PET/CT or SPECT/CT examination by considering patient size, automatic tube current modulation and specific CT scanner characteristics with the use of patient-specific voxel models. This was done for the most frequently performed PET/CT and SPECT/CT examinations in nuclear medicine, taking into account the clinical purpose of the CT scan.

Specific CT scanner characteristics can be determined in multiple ways. Therefore, the influence of X-ray spectrum determination and shaped filter modelling on estimated CT organ doses was studied as well. In addition, the CT image data on which the patient-specific computational models are based may be limited. The latter influence on the estimation of CT organ doses is discussed in this report.

2 Materials and Methods

To estimate patient-specific organ doses from CT in hybrid nuclear medicine imaging, Monte Carlo simulations were performed. As proposed in Deliverable D2.14 [10], the validated patient-specific dose calculation tool ImpactMC (version 1.6, CT Imaging GmbH ©, Erlangen Germany) was used [11-13]. It combines Monte Carlo algorithms with scanner specific parameters and patient CT images. The latter are used as patient-specific voxel models. In this way, the software calculates individualised 3D dose distributions, considering all relevant photon interaction processes [11, 12]. Delineation of the organs of interest makes it possible to estimate patient-specific organ and tissue doses. To obtain organ dose conversion factors, these patient-specific dose estimations are correlated with patient characteristics or specific dose indicators. A general overview of this process is given in Figure 1.

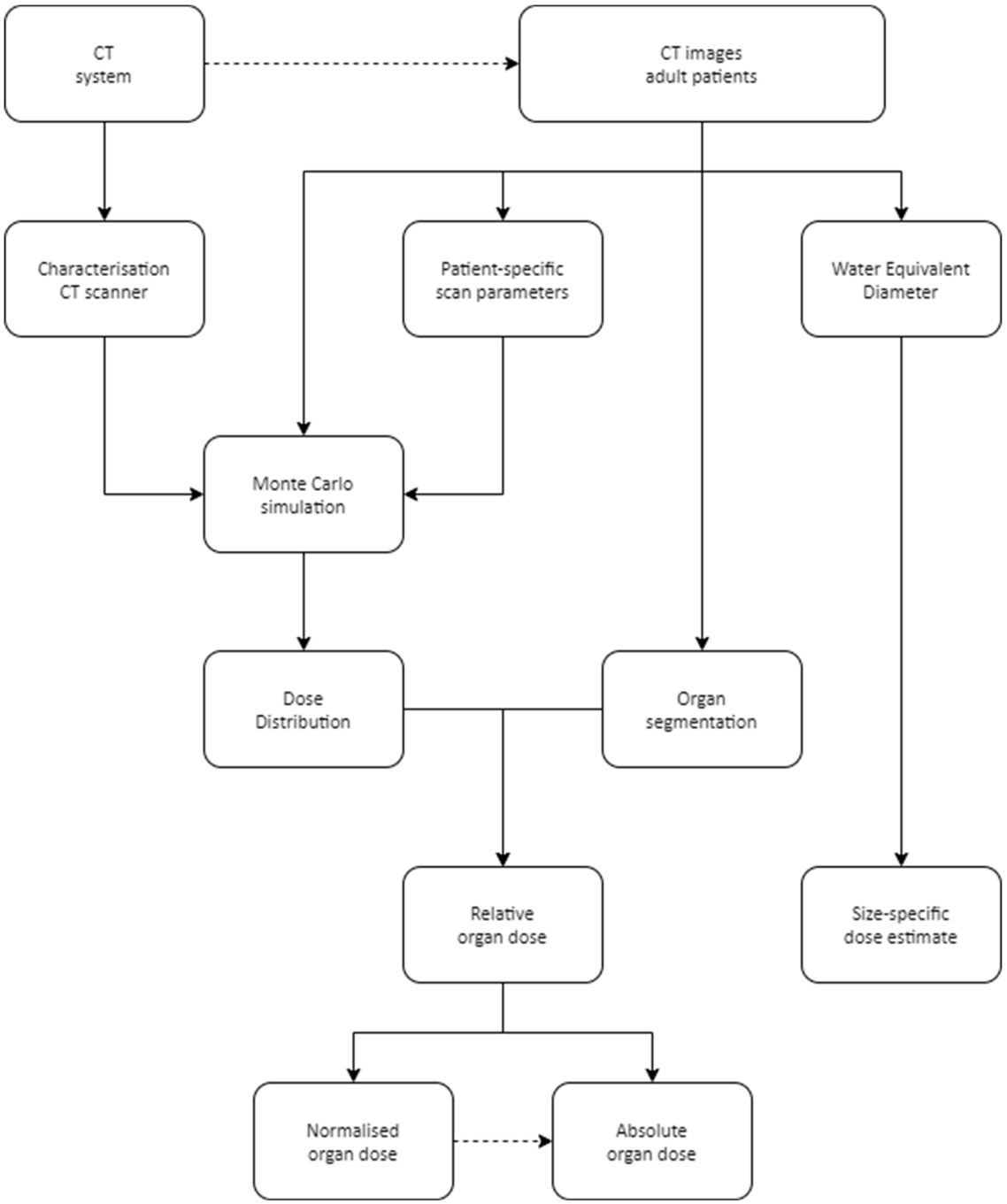

Figure 1: Overview of the followed procedure to obtain patient-specific organ dose estimations.

2.1 Collection of patient CT scans

For individualised dose calculations of CT scans in multi-modality imaging, patient-specific voxel models were set up based on clinical CT data. The retrospective use of the CT images was approved by the institutional ethical committee. To be suitable for accurate dose estimations, the reconstructed Field of View (FOV) of the CT scans must include the entire cross-section of the patient. Otherwise, missing tissue parts in the CT scans FOV will affect x-ray absorption and transmission through the patient model, which will result in dose inaccuracies [10].

CT images of 100 adult patients, acquired during a whole-body PET/CT examination, were collected retrospectively. The fifty male and female patients were chosen in such a way to assure a wide variety in Body Mass Index (BMI). In addition, CT data of 100 adult patients who underwent a SPECT/CT examination were gathered as well. This was done for the most performed SPECT/CT examinations. For each study, an equal number of male and female patients was selected.

All images were selected and extracted from the institutional Picture Archiving and Communication System (PACS). To comply with the current General Data Protection Regulation (GDPR) rules, all CT data was anonymised according to the hospitals anonymization policy before extraction from the PACS. This means that patient-related information, represented by unique identifiers (tags), in the DICOM header of the images was completely removed or replaced by de-identifiable information. Only data concerning patient sex, age, length and weight was kept.

2.2 CT scanner characterisation

For scanner-specific dose computations, the Monte Carlo software ImpactMC also needs some scanner specific information as input parameters. This includes information on the geometric, spectral and shaped filter characteristics of the CT scanner. In addition, the air kerma measured free-in-air in the isocenter of the CT gantry needs to be defined as well since the calibration of the simulation software is based on it.

2.2.1 Geometric characteristics

Geometrical specifications of the CT scanner of hybrid imaging devices (Table 1) were extracted from the technical reference manual of the system. However, in most cases these parameters can also be derived from specific data elements, DICOM tags, in the DICOM header of the CT images.

Table 1: Geometrical characteristics of the CT scanner of hybrid imaging systems.

	Hybrid imaging device	Focus to Isocenter Distance CT (mm)	Fan angle CT (rad)	Beam collimation CT (mm)
PET/CT	Siemens Biograph mCT Flow	595	0.7955	CT protocol dependent
	GE Discovery MI	541	0.8658	CT protocol dependent
SPECT/CT	Siemens Symbia Intevo T16	535	0.8744	CT protocol dependent
	Siemens Symbia Intevo Bold	535	0.8744	CT protocol dependent
	Siemens Symbia Intevo 6	535	0.8744	CT protocol dependent
	GE Discovery NM/CT 670	541	0.8658	CT protocol dependent

2.2.2 Spectral characteristics

An important input for Monte Carlo dose simulations is the spectrum of the X-ray beam, which is defined by its tube potential and the first half-value layer (HVL). As already described in Deliverable D2.14 [10], the Monte Carlo software ImpactMC expects the spectrum to be specified as the number of photons at each energy level. Therefore, each line in the spectrum text file has the following structure:

energy e (in keV), number of photons in the spectrum in energy bin e

The number of photons, binned in 1 keV steps, did not have to be normalised because normalisation will be done by the software, if necessary.

To obtain the X-ray beam spectrum of each tube potential (i.e. 70 kV, 80 kV, 100 kV, 110 kV, 120 kV, 130 kV and 140 kV, depending on the specific hybrid CT scanner), different possibilities exists (Figure 2). For the best results, quantitative spectral information is provided by the manufacturer that can be directly used as input for the Monte Carlo dose simulations. A second option is to use manufacturer's data, such as the anode angle and amount of filtration (materials and thicknesses), to create an artificial spectrum. Therefore, several spectrum generators exist such as the ImpactMC integrated spectrum generator (based on work of Tucker *et al.* [14]) and SpekCalc (based on work of Poludniowski *et al.* [15]). However, manufacturer's data are not always available and therefore the methodology as described by Turner *et al.* [16] for equivalent energy spectra in CT was used. Based on experimental derivation of the first half-value layer, an equivalent spectrum was generated with a MATLAB code (Mathworks, USA) with added SPEKTR tool [17].

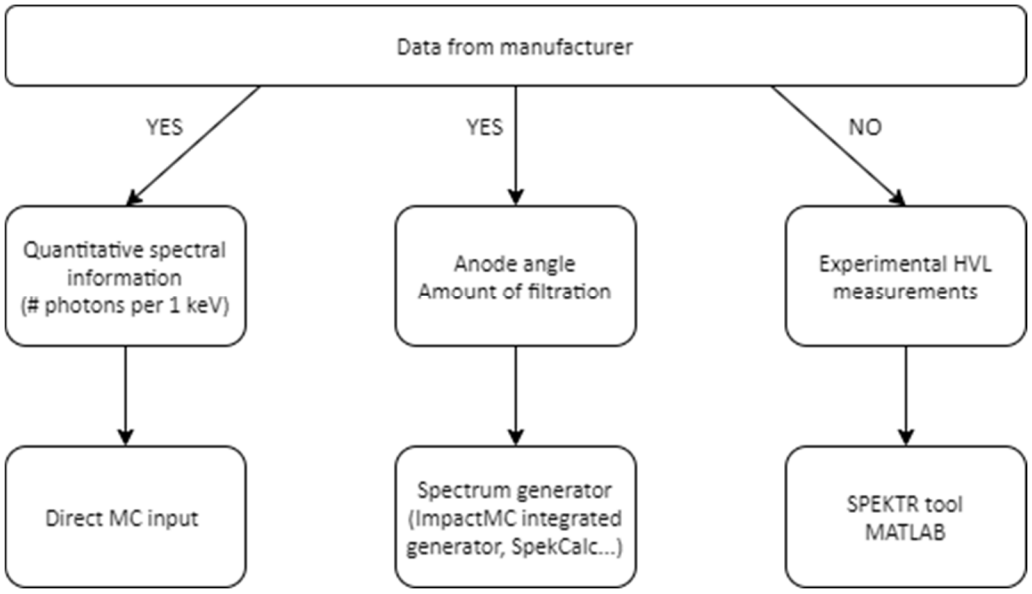

Figure 2: Schematic overview of different possibilities to obtain X-ray beam spectrum for each tube voltage.

The impact of X-ray beam spectra quantitatively provided by the manufacturer or generated by spectrum generators (such as SpekCalc and the MATLAB SPEKTR tool based on half-value layer measurements) on CT organ doses obtained by Monte Carlo simulations is studied in more detail in Chapter 3.

2.2.3 Shaped filters

The Monte Carlo software ImpactMC allows including a shaped bowtie filter. The first option is to define the shaped filter material and density and describe the shape in function of the material thickness with varying fan angle at the X-ray source. However, this requires data from the manufacturer that they are not always willing to share. To overcome this problem, it is also possible to characterise the shaped filter as transmittances or measured dose values.

Because of the difficulty to obtain the necessary information from the manufacturer, bowtie profiles were characterised based on dose measurements. Therefore, the set-up as shown in Figure 3 was used. In order to fix the X-ray tube at the 12 o'clock position dose measurements were performed in scout or topogram modus. A calibrated pencil beam ionisation chamber (Model 10X6-3CT, Radcal Corporation, USA), clamped to a laboratory stand, was initially positioned free-in-air at the scanner's isocenter. Dose measurements were incrementally obtained by moving the laboratory stand in 1 cm intervals in the +x direction. Since the bowtie filter is symmetric, only one side of the bowtie filter needs to be defined together with the focus to isocenter distance and the increment distance between the measurement points. However, due to uncertainties in positioning dose measurements were also performed in the -x direction. The dose at each increment position is then calculated as the mean of the measured dose values in the +x and -x direction at the same distance from the isocenter.

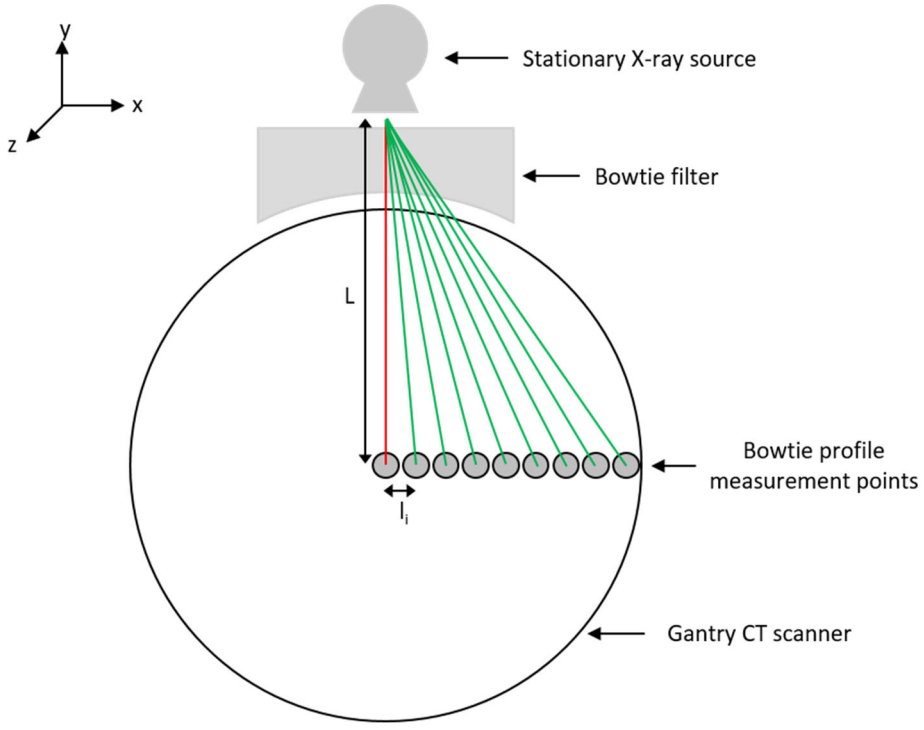

Figure 3: Set-up of CT bowtie profile dose measurements, with L the focus to isocenter distance and l_i the distance between the measurement points (figure based on [16]).

A CT scanner may have multiple bowtie filters. Which one is used depends on the clinical task. It is thus important to perform the bowtie profile dose measurements within the same scan protocol as the Monte Carlo dose simulations.

As for the X-ray beam spectra, the impact of bowtie filters defined by the manufacturer or based on dose measurements on CT organ doses obtained by Monte Carlo simulations is studied in more detail in Chapter 3.

2.2.4 Air kerma

The air kerma was calculated for each tube voltage available. A calibrated pencil beam ionisation chamber (Model 10X6-3CT, Radcal Corporation, USA), clamped to a laboratory stand, was positioned free-in-air at the scanner's isocenter. By measuring the dose-length product (DLP) of a circular scan without table feed, the air kerma can be calculated as followed:

$$K_{Air}\left[\frac{mGy}{100\ mAs}\right] = 10^6 \cdot \frac{DLP\ [Gy \cdot cm]}{collimation[mm] \cdot I[mA] \cdot t[s]} \quad (1)$$

with tube current I, rotation time t and $collimation$ the actual beam collimation measured with self-developing Gafchromic film.

2.3 Patient-specific scan parameters

Although all scan parameters mainly depend on the clinical acquisition protocol, some partially depend on the patient as well. For the Monte Carlo software ImpactMC this includes the number of rotations needed to cover the scan range and the performance of the tube current modulation.

2.3.1 Scan range

ImpactMC requires entries for both the start position of the CT scan in the z direction and the number of rotations needed to cover the total scan range. Both can be derived from the information embedded in the DICOM headers of the CT images.

To calculate the number of rotations, the scan length has to be known. For this, the position of the patient in the z direction of the first and last reconstructed slice in the scan range is extracted from DICOM tag "0020,0032" (Image Position Patient). Taking into account the table increment and the total beam collimation, the number of rotations needed for the CT acquisition is calculated.

To get all necessary data from the CT images automatically, a macro for the open source software Fiji (Fiji Is Just ImageJ) was developed. This macro extracted data from the DICOM header of the images that could be used directly as input for the Monte Carlo dose simulation or could be used to calculated some of the other input parameters such as the number of rotations.

2.3.2 Tube current modulation

All modelled hybrid CT scanners are capable to perform fixed tube current and tube current modulated acquisitions. As already mentioned in Deliverable D2.14 [10], the DICOM header of each reconstructed image (z) included a unique tube current (mA) value along with the corresponding table position. Each tube current value is the average of the angularly and longitudinally modulated values applied over the gantry rotation used to reconstruct this z-th image.

The same ImageJ macro as mentioned in section 2.3.1 also extracted the tube current value from the DICOM header of each reconstructed image. For tube current modulation, the Monte Carlo software expects the tube current values to be stored in a separate text file with the number of specified tube current values equal to:

$$Number\ of\ projections\ per\ rotation \times Number\ of\ rotations \quad (2)$$

The number of projections per rotation can be chosen freely. However, the larger this number the longer it takes for a simulation to be completed. To compile a text file with enough tube current values and a sufficient number of projections per rotation to ensure speed and accuracy, a Python algorithm was developed.

2.4 Monte Carlo dose simulations

In nuclear medicine, clinical protocols specific for examinations of the chest are mostly not present. Therefore, Monte Carlo simulations were performed for the most frequently performed PET/CT and SPECT/CT examinations. Most of these include the thoracic region completely or partially.

2.4.1 General

To perform patient-specific dosimetric computations with the Monte Carlo software ImpactMC, patient CT scans were used as input volume. For each PET/CT and SPECT/CT examination, the specific settings of the CT scan were translated to the corresponding parameter values in the Monte Carlo software. The number of rotations was calculated based on the length, beam collimation and pitch of the CT scan (see Section 2.3.1). To ensure the speed and accuracy of the Monte Carlo simulation, the number of X-rays depositing energy was chosen to be 10^{10} for all simulations. The resulting dose distributions were exported as DICOM format.

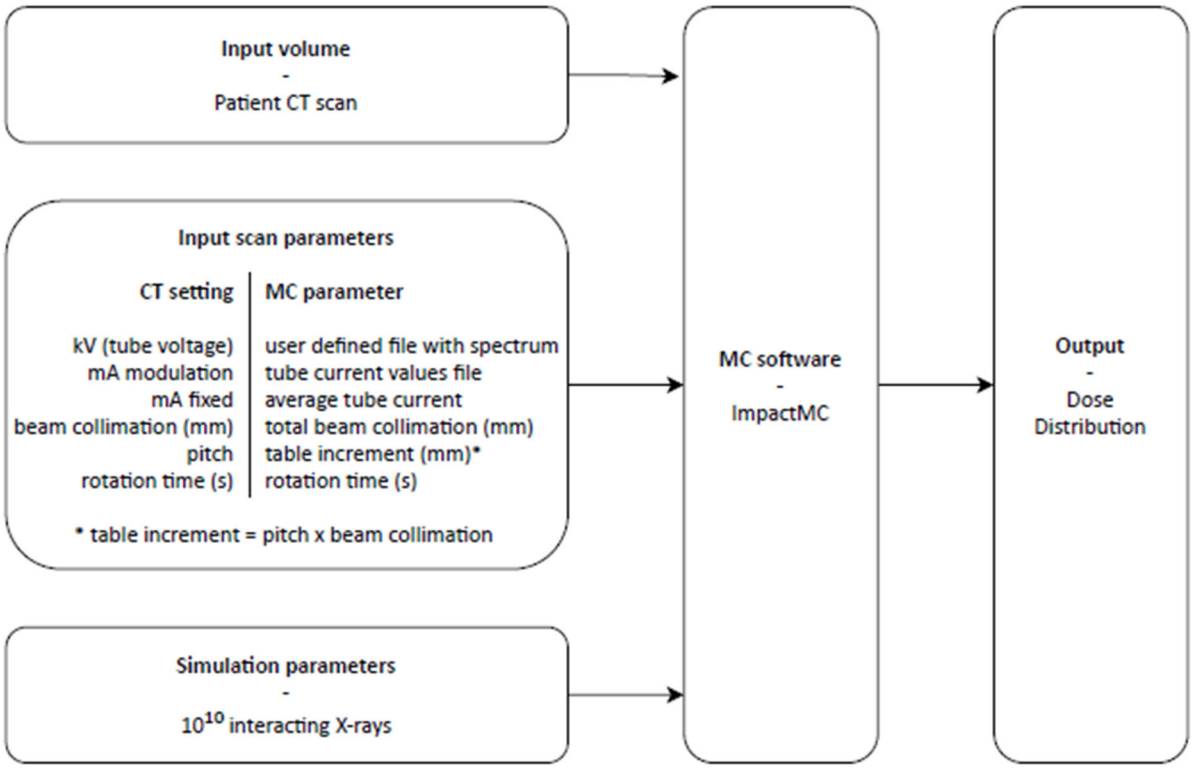

Figure 4: Overview of the input needed for Monte Carlo (MC) dose calculations with ImpactMC and the resulting output.

2.4.2 PET/CT

The most frequently performed PET/CT studies are whole-body (WB) examinations in which the body is scanned from head to mid-thigh. In contrast to conventional radiology where the purpose of a CT scan is purely diagnostic, the CT scan of a whole body PET/CT examination may serve for attenuation correction and anatomical localisation as well. Depending on the clinical task, CT images with a lower image quality and corresponding lower dose may be sufficient.

In this study, diagnostic and localisation CT scans were simulated for 100 patients undergoing a whole-body PET/CT examination on a Siemens Biograph mCT Flow and GE Discovery MI PET/CT. Compared to the diagnostic CT scan, localisation CT scans are performed at a lower tube voltage (80 kV versus 120 kV), lower tube current-time product and larger pitch. Although in clinical practice automatic tube current modulation (ATCM) is always applied, a simulation with and without tube current modulation was performed for each model. In the first simulation, a different tube current value was applied for each individual tube rotation. In the second simulation, the tube current was kept constant in all tube rotations throughout the entire examination length. Simulations without automatic tube current modulation were performed at a tube current-time product of 100 mAs.

2.4.3 SPECT/CT

SPECT/CT examinations are divided according to the anatomical region studied. As for PET/CT, the purpose of the CT scan may be diagnostic, for anatomical localisation or only for attenuation correction of the functional SPECT images. The most performed SPECT/CT examinations in the chest region are ventilation/perfusion lung scans and cardiac scans. Other frequently performed SPECT/CT studies are examinations of the cervical and lumbar spine.

Ventilation/perfusion lung scans are carried out to evaluate the circulation of air and blood within a patient's lungs. The CT scan performed during such an examination only serves attenuation correction and anatomical localisation purposes. Monte Carlo simulations of 30 patient models were performed for a GE Discovery NM/CT 670 at 100 kV, which is the clinical used tube voltage, and with a fixed tube current value.

Cardiac SPECT/CT examinations consist of two steps usually performed on two consecutive days. At the first day, a resting examination is performed while at day two a stress scan is taken. In contrast to the resting examination where the CT scan is always an attenuation correction (AC) CT with tube current modulation, the stress CT may be as well an AC CT with tube current modulation or a Calcium (Ca) scoring CT with fixed tube current. Because of the higher tube current, needed for the clinical image quality, the CTDI of the Ca-scoring CT is higher. Monte Carlo dose calculations for 32 patients (17 women and 15 men) were performed for both the AC CT and Ca-scoring CT performed at a Siemens Symbia Intevo T16.

Cervical and lumbar spine SPECT/CT examinations may be performed with a localisation or diagnostic CT. Differences in CT settings are a higher pitch, larger collimation and lower tube current range for the localisation CT. The length of a localisation CT is normally the full SPECT field. Depending on the agreements made at the nuclear medicine department, the length of a diagnostic CT may be adjusted according to the SPECT image and clinical indication. Diagnostic and localisation CT simulations were performed for both a Siemens Symbia Intevo Bold and Intevo 6. The latter consists of a 6-slice CT while the first has a 16-slice CT part. This was done for 20 patients undergoing a CT scan of the cervical spine and for 20 patients undergoing a lumbar spine examination.

2.5 Delineation of organs

The radiosensitive organs and tissues of interest are the breast (for females), heart, liver, lungs, kidneys, ribs, thyroid, spine and esophagus. To delineate these organs, the open source software tools Fiji (or ImageJ) and 3D Slicer were utilised. Figure 5 gives an overview of the steps followed to segment the organs of interest.

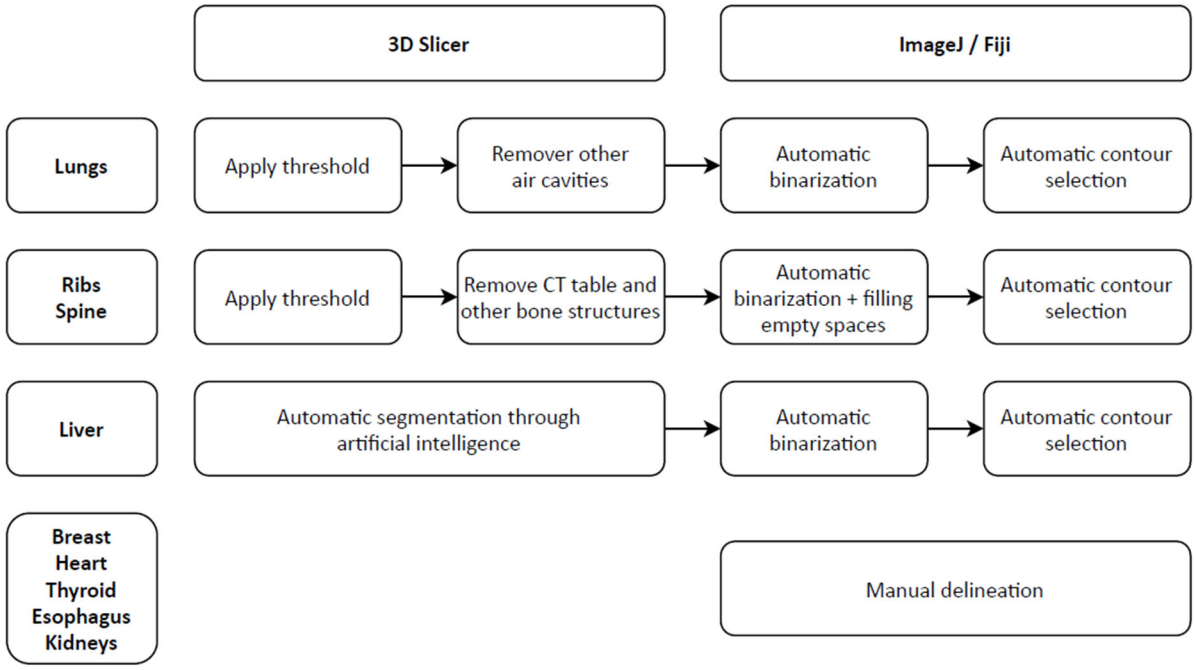

Figure 5: Schematic overview of the followed organ segmentation procedure. If necessary, the automatic contour selection of the spine can be followed by manual removement of the spinal cord.

Structures that were semi-automatically delineated were lungs, bones (ribs/spine) and the liver (Figure 6). Therefore, the CT images of the patient were first imported in the software package 3D Slicer. For the lungs, ribs and spine threshold techniques were applied. In case of the lungs, other air cavities such as air gaps in the esophagus and intestine were segmented as well. To remove these structures, the segmentation was shown in 3D and the 'scissors' tool was used. Small structures could also be removed by utilising the 'remove small islands' or 'keep selected island'-function. The threshold applied for bones also segmented the contour of the CT table, which could be easily removed by using the scissor tool. The same could be done for bone structures other than the ribs and spine. For the liver, the artificial intelligence (AI) tool, implemented in 3D Slicer Version 4.11 or later, was used. Each of these segmentations were then exported to a binary labelmap in DICOM format. Algorithms developed for the image processing software ImageJ (or Fiji) performed the other delineation steps. This includes conversion of the labelmap to binary using the MaxEntropy method and automatic selection of the contours of the organ in each image of the binary followed by automatic saving of the created ROIs as a ZIP file. In case of the ribs and spine empty spaces produced by, among other things, bone marrow were filled as well. If necessary, the spinal cord was removed manually afterwards.

The breast, heart, kidneys, thyroid and esophagus were manually delineated using ImageJ's ROI (Region of interest) Manager for working with multiple selections. For each organ, the brightness and contrast of the image were adjusted to optimum levels. An ImageJ macro was developed to combine multiple selections in a slice into one per slice and save all selections as a ZIP file. For each organ, the ZIP file then contains one ROI per CT image containing the organ. Examples of these organ delineations can be seen in Figure 6.

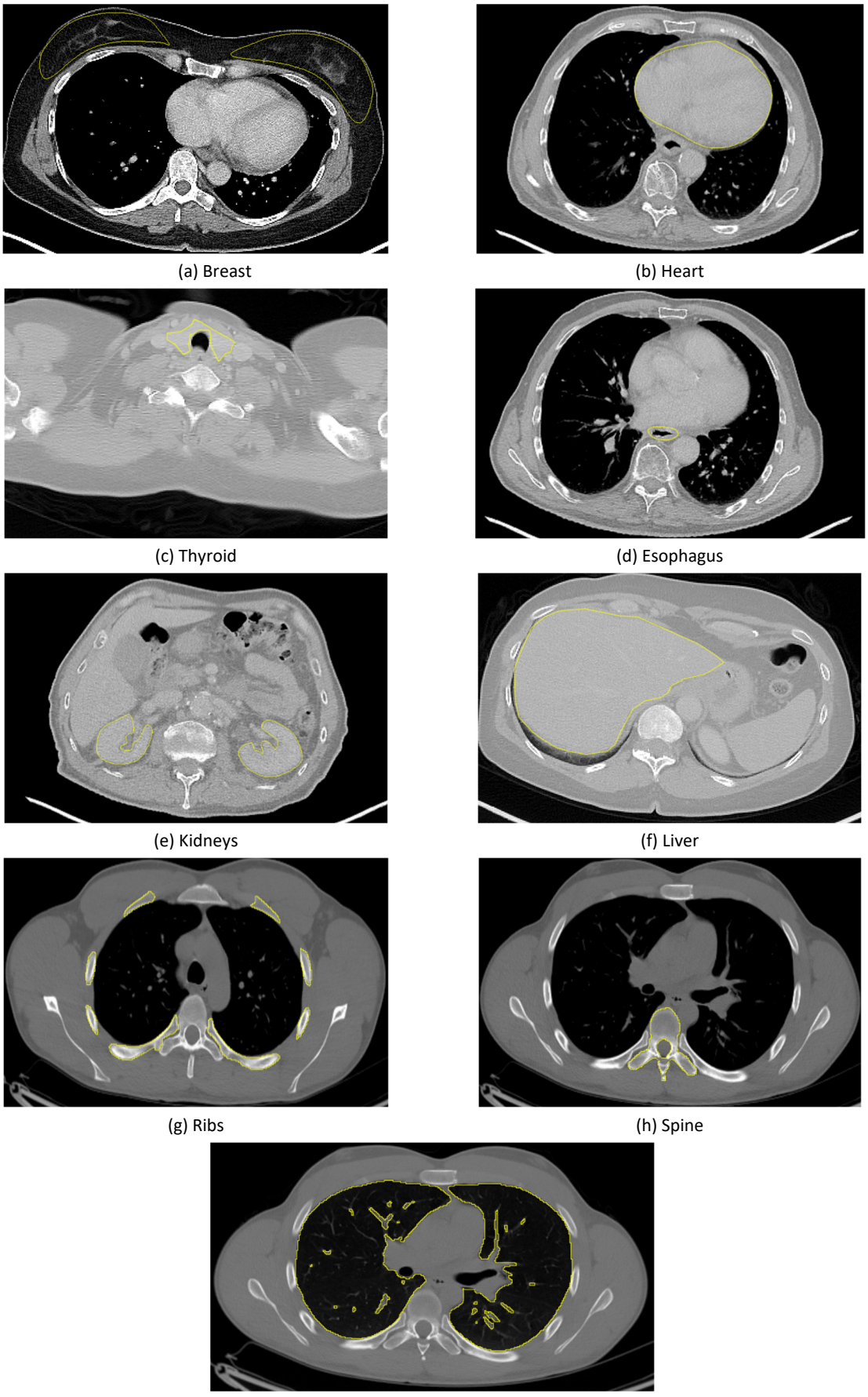

(a) Breast (b) Heart

(c) Thyroid (d) Esophagus

(e) Kidneys (f) Liver

(g) Ribs (h) Spine

(i) Lungs

Figure 6: Manual delineation of (a) breast, (b) heart, (c) thyroid, (d) esophagus and (e) kidney contours and semi-automatical delineation of (f) liver, (g) ribs, (h) spine and (i) lungs.

Automatic renaming of ROIs

Having whole-body patient CT scans available has the potential to study the influence of scan range limited CT image data on organ dose estimations. A comparison can be made between organ doses obtained by Monte Carlo simulation of for example a chest CT scan when using all whole-body CT images and only the chest CT images as input volume. This is studied in more detail in chapter 4.

Reducing the scan range to, for example, a chest CT scan, so reducing the number of CT images, is easy. However, the organ segmentations obtained by delineation of the organs on the whole-body CT images need to be adjusted. Each organ selection (ROI) has a specific name of the form 'xxxx-yyyy-zzzz.roi' (e.g. 0119-0280-0302.roi) in which the first four numbers correspond with the position of the CT image in the image stack (e.g. image 119 of 300 images). When reducing the number of CT images the position of the CT image in the image stack may change (e.g. from image 119/300 to image 19/150). The first four numbers of each ROI thus need to be changed. Due to the large number of patients and organ segmentations, doing this manually would be very time consuming. Therefore, an ImageJ macro was developed to rename all ROIs of all organ segmentations automatically for the new CT scan range.

2.6 Organ dose calculation

A Monte Carlo dose computation with ImpactMC results in a 3D dose distribution based on the physical properties (i.e. attenuation, composition and size) of the input patient CT scan. As already mentioned in Deliverable 2.14 [10], each slice in the dose volume corresponds to the same slice in the CT scan and each pixel in a specific slice of the CT volume has a corresponding dose value in the 3D dose distribution. To export the dose distribution in DICOM format, the dose was normalised to the air kerma measured free-in-air.

In this work, the organs and tissues of interest are the breast, heart, liver, lungs, kidneys, ribs, thyroid, spine and esophagus. For each organ, the contours of the organ were overlaid on the corresponding slices of the dose distribution to extract the organ dose. The dose over the whole organ (D_T) was determined as:

$$D_T = \sum_{i=1}^{N} \left(f_{i,T} \cdot M_{i,T}\right) \quad with \quad f_{i,T} = \frac{A_{i,T}}{\sum_{i=1}^{N} A_{i,T}} \tag{3}$$

where $M_{i,T}$ is the mean dose within the contour at slice i of organ T, N the total number of slices that contain contours of organ T and $f_{i,T}$ the fractional area of each organ contour (with $A_{i,T}$ the area within the contour at slice i of organ T).

Due to the normalisation of the dose to the air kerma, dose distributions in DICOM format only contain relative dose values. To calculate absolute dose values (D_{abs}) the following equation was used

$$D_{abs}[mGy] = D_{rel}\left[\frac{mGy}{mGy}\right] \cdot K_{air}\left[\frac{mGy}{100\ mAs}\right] \cdot Q_{mean}[mAs] \tag{4}$$

where D_{rel} is the relative organ dose as calculated by equation (3), K_{air} the air kerma measured free-in-air and Q_{mean} the mean tube current-time product.

Due to the large number of Monte Carlo simulations, an algorithm was implemented in ImageJ/Fiji to provide unsupervised organ dose calculation. The flowchart of the implemented procedure is displayed in Figure 7. For each Monte Carlo simulation, the resulting relative, absolute and normalised organ doses are saved in a separate text file.

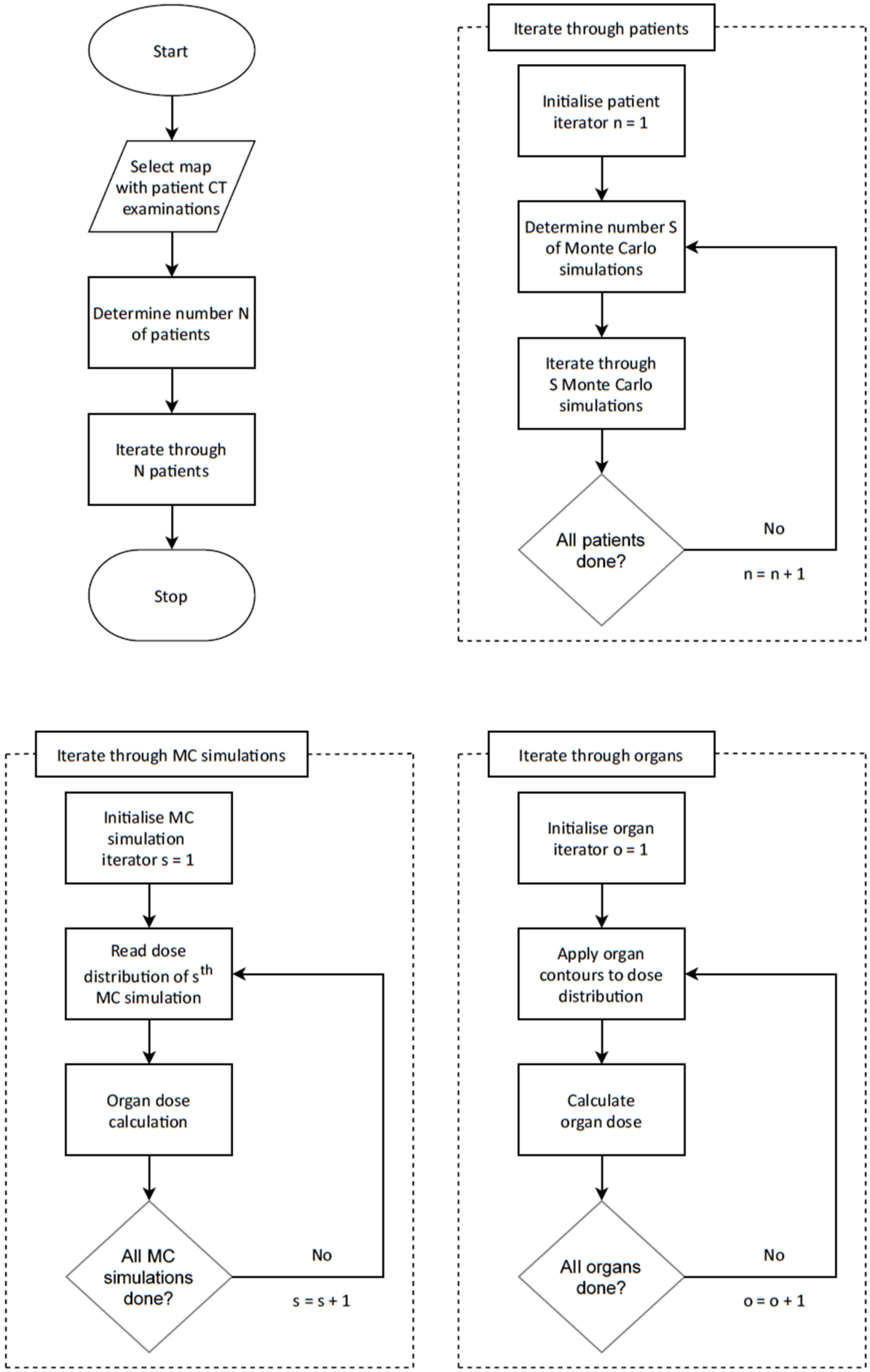

Figure 7: Flowchart of automated patient-specific organ dose calculation.

2.7 Water equivalent diameter and size-specific dose estimate

Current CT scanners display the volume computed tomography dose index ($CTDI_{vol}$) and the dose-length product, both before and after the CT scan is performed [18]. Their definition makes it possible to compare doses of similar examinations between CT scanners. Although both are sensitive to changes in scan parameters, they are displayed for a reference phantom (i.e. 16 cm head or 32 cm body CTDI phantom).

To estimate patient doses more accurately, AAPM Report No. 204 (2011) [18] introduced size-specific dose estimates (SSDE) which take into account the size of the patient. At first, the effective diameter was proposed to represent the diameter of the patient at a given location along the z-axis of the patient. However, the definition of effective diameter assumes that the patient has a circular cross section. AAPM Report No. 220 (2014) [19] recommended the water equivalent diameter (D_W) as new size metric, taking into account the X-ray attenuation of the patient. The water equivalent diameter is calculated as:

$$D_W = 2 \cdot \sqrt{\left[\frac{1}{100}\overline{CT(x,y)_{ROI}} + 1\right] \cdot \frac{A_{ROI}}{\pi}} \tag{5}$$

where $\overline{CT(x,y)_{ROI}}$ is the average Hounsfield Unit (HU) value over each x, y location in the ROI that contains the imaged patient in one slice and A_{ROI} the area of the ROI. The SSDE(z) is then calculated as:

$$SSDE(z) = a \cdot e^{-b \cdot D_W} \cdot CTDI_{vol}(z) \tag{6}$$

where a and b are exponential fit coefficients, depending on the diameter of the PMMA phantom (either 16 or 32 cm) used to measure the $CTDI_{vol}$ [18]. The mean WED and SSDE over the entire scan range is then determined as:

$$\overline{D_W} = \frac{\sum_{z=1}^{N} D_W}{N} \tag{7}$$

$$\overline{SSDE} = \frac{\sum_{z=1}^{N} SSDE(z)}{N} \tag{8}$$

where N is the total number of images in the scan range.

Accurate determination of the water equivalent diameter requires detailed delineation of the patient's body contour without including the CT table. Therefore, the procedure as described in Figure 8 was followed: After importing the CT images of the patient in the software package 3D Slicer, a threshold was applied (Figure 8a). To remove the CT table and other small structures the option 'keep largest island' was used (Figure 8b). Hereby the body shape and size was preserved. The visible segments of the patient's body were then exported to a binary labelmap in DICOM format. An algorithm developed for the image processing software ImageJ (or Fiji) performed all other delineation steps. This includes automatic conversion of the labelmap to binary using the MaxEntropy method (Figure 8c), filling empty space produced by lungs and other air cavities (Figure 8d) and automatic selection of the body outline in each image of the binary followed by automatic saving of the created ROIs as a ZIP file.

For each patient, the mean water equivalent diameter and size-specific dose estimate were then calculated based on equations (7) and (8). Due to the large number of patients, an ImageJ algorithm was developed to automate these calculations.

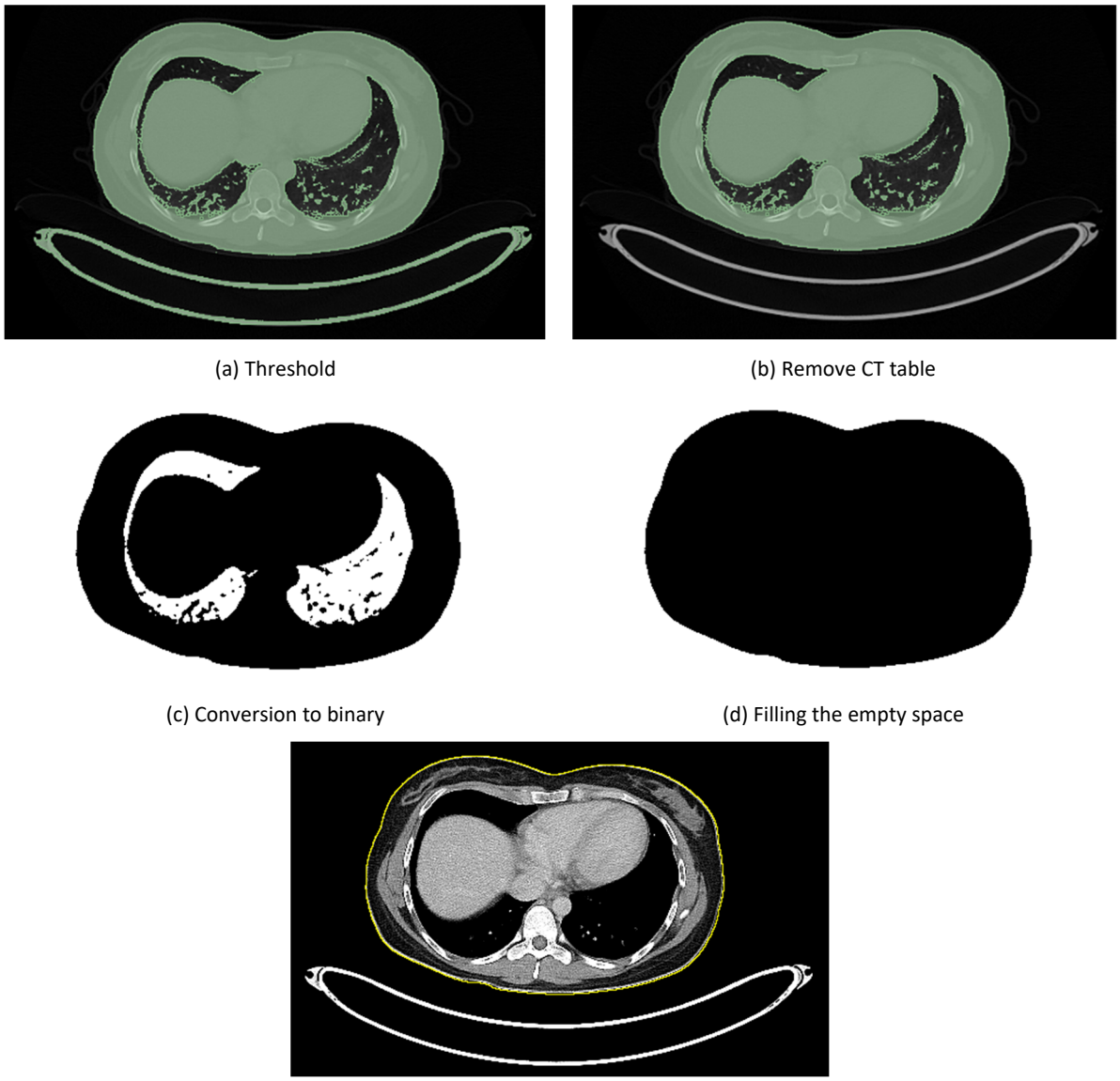

(a) Threshold

(b) Remove CT table

(c) Conversion to binary

(d) Filling the empty space

(e) Outline overlaid on original CT image

Figure 8: Delineation of the patient body contour - (a) thresholding and (b) removing the CT table using 3D Slicer, export visible segments to binary labelmap and save in DICOM format, (c) binarization of the labelmap and (d) filling the empty space using ImageJ/Fiji, automatic contour selection, (e) outline overlaid on original image.

3 Determination of X-ray spectra and modelling of shaped filters – Influence on CT organ dose

Today, Monte Carlo frameworks are the golden standard to perform patient-specific dosimetry because they allow both an accurate description of the X-ray modalities and the implementation of anatomical models. For CT examinations, characterisation of the CT scanner includes describing the geometrical, spectral and shaped filter characteristics. As already described in section 2.2, the Monte Carlo software ImpactMC expects spectral and shaped filter characteristics to be specified in a separate text file. To obtain the best results, quantitative spectral information and information on the bowtie filter material and shape is provided by the manufacturer. However, manufacturer's data is not always available. Fortunately, other methodologies exist to determine X-ray spectra and model shaped filters.

In this chapter, the influence of X-ray spectrum determination and shaped filter modelling on simulated CT organ doses is studied. Therefore, quantitative spectral and bowtie filter information as provided by the manufacturer of one of the PET/CT systems was used as well.

3.1 Determination of X-ray spectra

The spectrum of the X-ray beam is defined by its tube potential and the first half-value layer (HVL). To obtain the X-ray beam spectrum of each tube potential different possibilities exist. Paragraph 3.1.1 describes the used methods, while paragraph 3.1.2 provides a graphical comparison of the resulting X-ray spectra.

3.1.1 Methods

In this study, five X-ray beam spectra were created for each tube voltage based on:

Quantitative spectral information from the manufacturer

Quantitative spectral information specified as the number of photons at each energy level was provided by the manufacturer. Because normalisation of the number of photons is done by the Monte Carlo software if necessary, the *provided spectral information* could be directly used as input for the dose simulations.

Spectrum generators

Artificial X-ray beam spectra were created using the *ImpactMC integrated spectrum generator* (based on work of Tucker *et al.* [14]) and *SpekCalc* (based on work of Poludniowski *et al.* [15]). The user can select the tube potential, the anode angle and the amount of filtration. The latter can be selected in mm for different materials. Therefore, information on the anode angle and amount of filtration (materials and thicknesses) was provided by the manufacturer.

Half-value layer measurements

The methodology as described by Turner *et al.* [16] for equivalent energy spectra in CT only requires physical measurements and calculations. First, the half-value layer of the spectra was experimentally derived. To do this, a calibrated pencil beam ionisation chamber (Model 10X6-3CT, Radcal Corporation, USA) was placed free-in-air at the isocenter of the CT. Thin aluminium slabs with a thickness of 2, 1 and 0.5 mm were step-wise added to the beam path, until the air kerma measured was less than half the initial air kerma measured without extra aluminium. In this way, the half-value layer was determined as the amount of aluminium needed to half the initial air kerma. In order to keep the X-ray tube

stationary, measurements were performed in scout or topogram modus. The experimental set-up is illustrated in Figure 9.

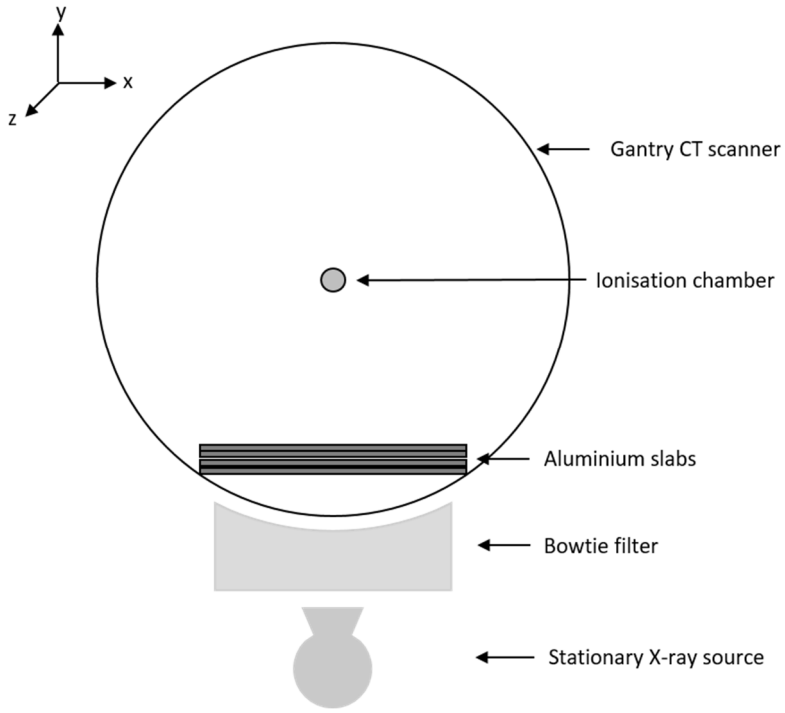

Figure 9: Set-up of half-value layer measurement (based on [16]). In case CT exposure cannot occur without the CT table in the X-ray beam path, the X-ray source and aluminium slabs are positioned laterally at the 3 o'clock position.

Secondly, an equivalent spectrum was generated with a MATLAB code (Mathworks, USA) with added SPEKTR tool [17]. The code started from a soft spectrum and iteratively adds layers of aluminium until the difference between the simulated and measured half-value layer is minimal. The resulting spectrum was binned in 1 keV steps and ready to be used in a Monte Carlo simulation.

Next to the tube potential and the amount of added filtration, the SPEKTR tool also expects the ripple factor (percentage voltage ripple) as input parameter for the generation of equivalent energy spectra. Turner *et al.* [16] used a 25% voltage ripple, while the study of Yang *et al.* [20] started with a ripple factor of 0%. In this study, *equivalent energy spectra* for CT were created applying a voltage ripple of *0%* and *25%*.

3.1.2 Graphical comparison

For each method described above, X-ray spectra were generated for each tube voltage. Figure 10 shows the equivalent spectra obtained by physical half-value layer measurements and applying a voltage ripple of 0% to the SPEKTR tool. The resulting X-ray spectra clearly consist of bremsstrahlung, yielding a continuous X-ray spectrum falling off to zero at the tube voltage. Regardless of the method of generation, characteristic radiation peaks superimposed onto the continuous spectrum are observed for tube voltages ranging from 80 kV to 140 kV. The tube and inherent filtration resulted in the visible low energy cut off. Increasing the tube voltage results in both a shift of the spectrum up and towards the right and into an increase of the maximum energy and the total number of photons. It also increases the probability of exceeding the critical value for the production of characteristic radiation.

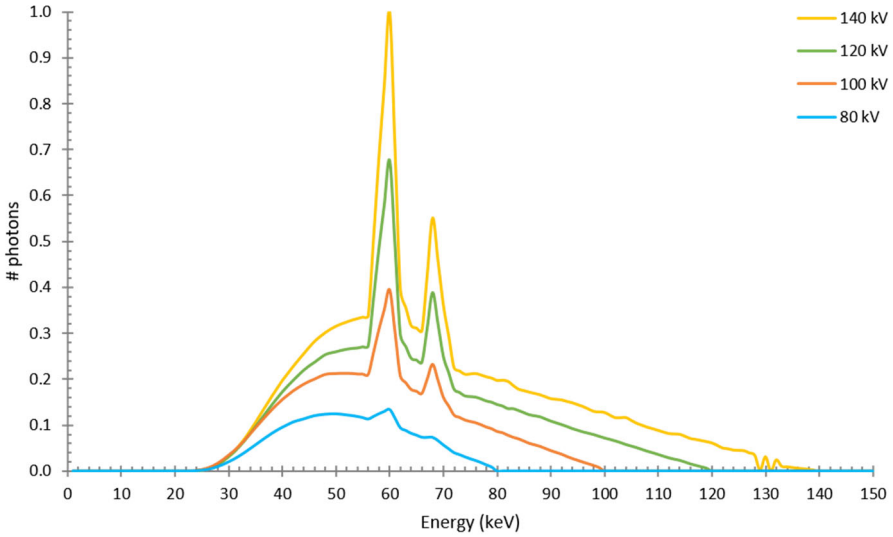

Figure 10: Normalised equivalent X-ray spectra based on half-value layer measurements and generated with a voltage ripple of 0%.

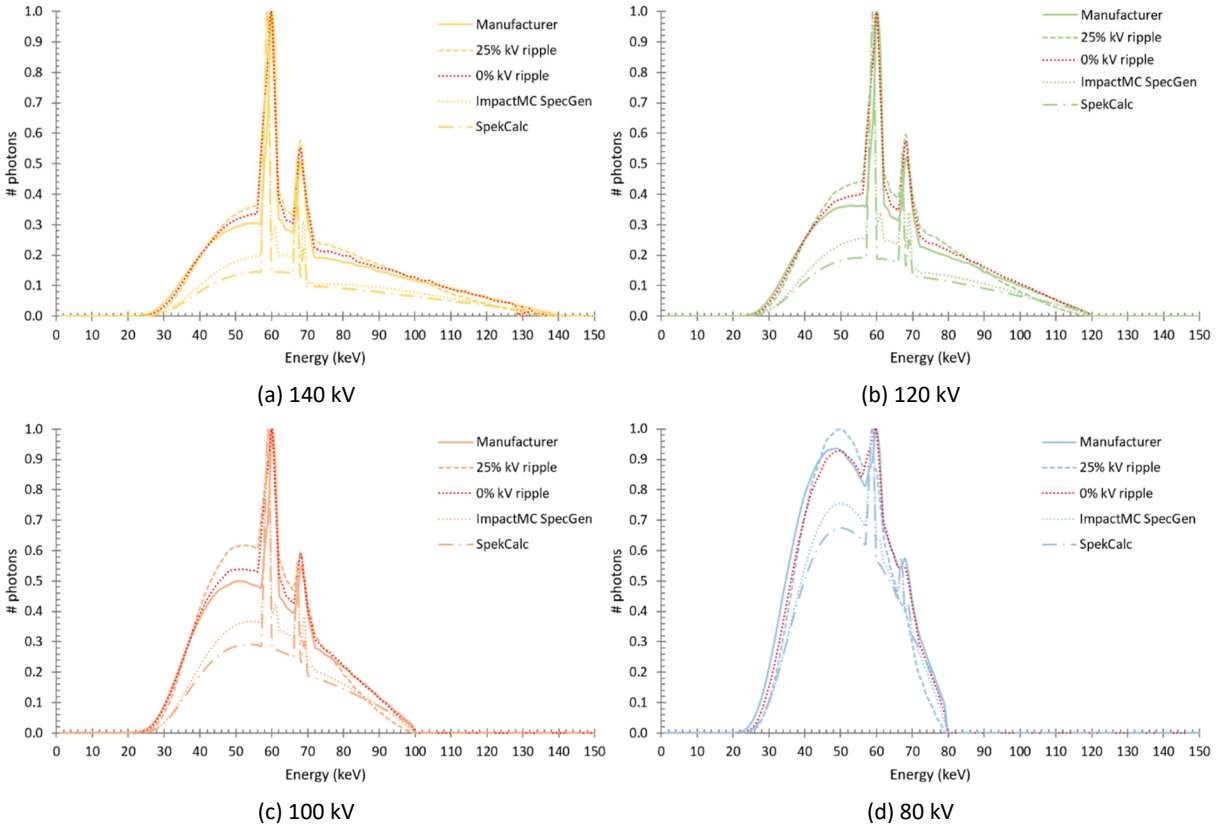

(a) 140 kV (b) 120 kV

(c) 100 kV (d) 80 kV

Figure 11: Graphical comparison of the (a) 140 kV, (b) 120 kV, (c) 100 kV and (d) 80 kV X-ray spectra provided by the manufacturer, created with the SPEKTR tool applying a 25% and 0% voltage ripple after half-value layer measurements, and generated with the ImpactMC integrated spectrum generator and SpekCalc.

To compare the generated X-ray spectra with each other for every tube voltage, each spectrum was normalised to its maximum number of photons (Figure 11). As expected, characteristic radiation peaks are superimposed at the same position of the continuous spectrum for each tube voltage independent of the method used to create the spectrum. However, a clear difference is observed in the continuous spectrum. For all tube voltages, the continuous part of the spectrum is the lowest for spectra generated with the spectrum processor SpekCalc followed by those generated with the spectrum

generator integrated in the Monte Carlo software ImpactMC. Equivalent spectra, based on half-value layer measurements, created with the SPEKTR tool and by applying a voltage ripple of 25% show the highest continuous spectrum part. At 100 kV, 120 kV and 140 kV the continuous spectrum is also slightly shifted towards the right for the spectra generated with the ImpactMC integrated spectrum generator and SpekCalc.

Visual comparison of the energy spectra shows that, for all tube voltages, equivalent spectra based on physical half-value layer measurements and with a voltage ripple of 0% resemble the most those quantitatively provided by the manufacturer (Figure 11). This indicates that when no data from the manufacturer is available, equivalent spectra generated based on the work of Turner *et al.* [16] with a 0% voltage ripple form a good alternative for the use in Monte Carlo dose simulations.

3.2 Modelling of shaped (bowtie) filters

Different possibilities exist to model shaped filters such as the bowtie filter of a CT system. For the best results, the manufacturer provides the required data. In this study, the influence of two shaped filter models on simulated organ doses is investigated.

The first bowtie model is based on data provided by the manufacturer, which defined the attenuation of the bowtie (w.r.t. the detector signal) as a function of the fan angle. This information was converted to an input file suitable for the Monte Carlo software.

The second model characterises the bowtie filter based on measured dose values. As described in paragraph 2.2.3, these dose measurements are performed with a calibrated pencil beam ionisation chamber. They are obtained by moving the ionisation chamber in 1 cm intervals from the isocenter of the CT. Since the bowtie filter is symmetric, only one side of the bowtie filter needs to be defined together with the focus to isocenter distance and the increment distance between the measurement points.

3.3 Influence of X-ray spectrum and bowtie filter on CT organ doses

The impact of the X-ray spectrum determination and bowtie filter modelling on simulated CT organ doses was studied for patients undergoing a diagnostic CT scan at 120 kV with tube current modulation as part of a whole-body PET/CT examination. Therefore, Monte Carlo simulations were performed for twenty adult patients (10 female and 10 male patients). The patient models were selected to ensure a wide variety in Body Mass Index.

For each whole-body patient model, Monte Carlo dose simulations were performed for each combination of the five generated X-ray spectra with the two bowtie filter models. These combinations are summarised in Table 2.

Table 2: X-ray spectrum and bowtie filter combinations.

X-ray spectrum and bowtie filter combination	120 kV X-ray beam spectrum	Bowtie filter
1a	Manufacturer	Manufacturer
1b	Manufacturer	Experimental

2a	Equivalent - 0% kV ripple	Manufacturer
2b	Equivalent - 0% kV ripple	Experimental
3a	Equivalent - 25% kV ripple	Manufacturer
3b	Equivalent - 25% kV ripple	Experimental
4a	ImpactMC generator	Manufacturer
4b	ImpactMC generator	Experimental
5a	SpekCalc	Manufacturer
5b	SpekCalc	Experimental

The resulting mean CT organ doses and corresponding standard deviations are shown in Figure 12. As expected, deviations in organ doses are seen between the different X-ray spectra and bowtie filter combinations. For all organs, the estimated organ doses are the smallest and the largest when using the X-ray spectrum provided by the manufacturer and generated with SpekCalc, respectively. Applying the bowtie model of the manufacturer also seems to result in lower doses for most of the organs. These differences will be discussed in more detail in the following sections.

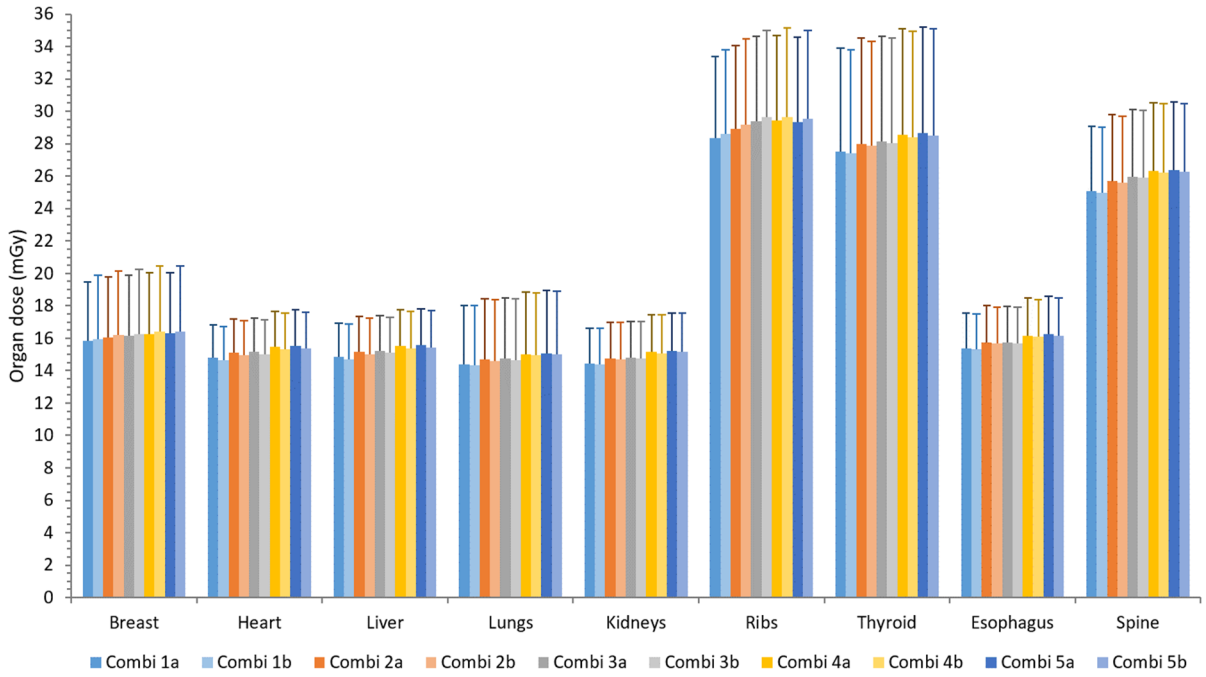

Figure 12: Estimated mean organ doses of a diagnostic whole-body CT scan for each X-ray spectrum and bowtie filter combination (with 1 - the spectrum provided by the manufacturer, 2 - the created equivalent spectrum with 0% voltage ripple, 3 - the created equivalent spectrum with 25% voltage ripple, 4 - the spectrum generated with the ImpactMC integrated spectrum generator, 5 - the spectrum generated with SpekCalc, a - the bowtie model provided by the manufacturer and b - the bowtie model characterised by dose measurements).

3.3.1 Influence of bowtie filter modelling

To study the influence of bowtie filter modelling on estimated CT organ doses in more detail the percentage difference is calculated between organ doses resulting from Monte Carlo simulations that applied the bowtie model based on data from the manufacturer and dose measurements, respectively. Therefore, it is important to keep the X-ray spectrum used for the dose simulation constant. The

assumption was made that the bowtie filter model provided by the manufacturer is the real model. This is done for each organ.

For both the absolute and normalised mean organ doses, the maximum percentage difference found over all organs is shown in Figure 13 for each X-ray spectrum. For Monte Carlo simulations performed with the X-ray spectrum provided by the manufacturer the mean organ dose lies maximum around 0.91% higher when using the bowtie model based on dose measurements compared to the bowtie model of the manufacturer. In normalised dose values, this is a difference of around 0.97%. Similar values are found for dose simulations acquired with the equivalent X-ray spectrum with a voltage ripple of 0%.

Over all, differences in CT organ doses are smaller than 1% when modelling the bowtie filter based on dose measurements. This model is thus a very good alternative when no manufacturer's data about the bowtie filter is available.

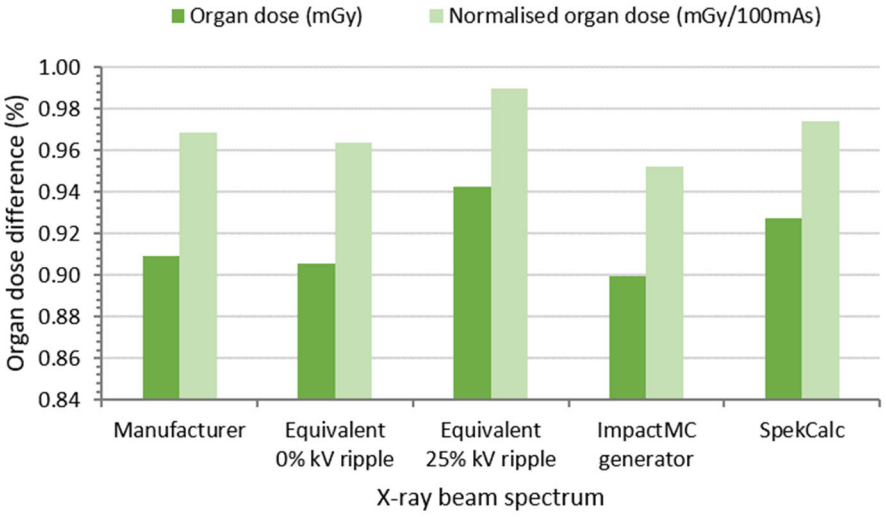

Figure 13: Maximum percentage difference in mean organ dose between the two bowtie models used for the Monte Carlo simulation of a diagnostic whole-body CT scan in hybrid imaging. Note that the assumption was made that the bowtie filter model provided by the manufacturer is the real filter model.

3.3.2 Influence of X-ray spectrum determination

The influence of the X-ray spectrum determination on estimated CT organ doses is studied in more detail by keeping the bowtie filter the same in all Monte Carlo simulations. Organ dose differences are then calculated for all simulations using one of the other four determined X-ray spectra compared to the same simulation using the X-ray spectrum provided by the manufacturer, assuming that the latter is the real spectrum. This is done for both bowtie filter models.

The maximum percentage dose difference found over all organs is shown in Figure 14. Similar results are found for both bowtie filter models when looking at the absolute and normalised organ doses. For all X-ray spectrum determination methods used, organ doses are within 6% from those resulting from simulations with the spectrum provided by the manufacturer.

Monte Carlo simulations acquired with the equivalent X-ray spectrum with a voltage ripple of 0% result in organ doses that are maximum around 2.4% higher than those obtained when using the spectrum from the manufacturer. This indicates that the methodology described by Turner *et al.* [16] for equivalent energy spectra in CT is a good alternative to characterise the spectral characteristics of the

CT scanner. The lowest difference is obtained when applying a voltage ripple of 0%, which confirms our findings based on a visual comparison of the X-ray spectra (see paragraph 3.1.2).

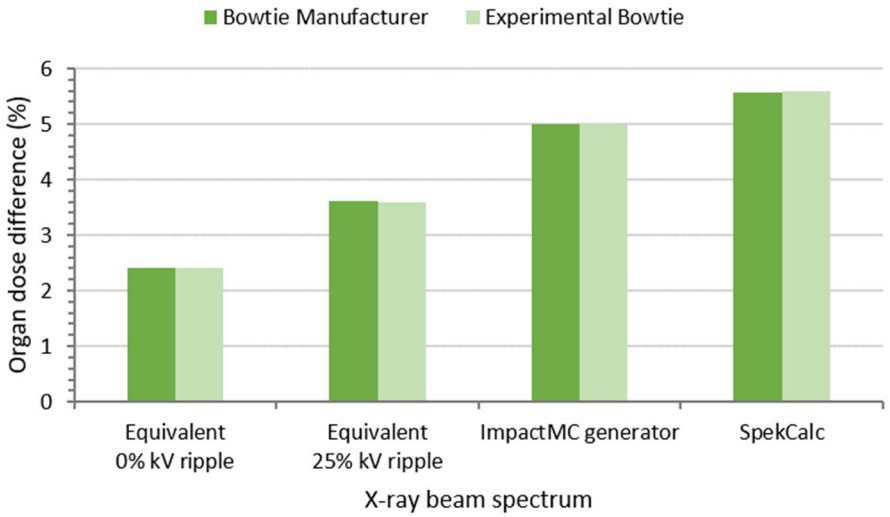

Figure 14: Maximum percentage difference in mean organ dose for the different X-ray spectra used for the Monte Carlo simulation of a diagnostic whole-body CT scan in hybrid imaging compared to simulations using the spectrum provided by the manufacturer. Note that the assumption was made that the X-ray spectrum provided by the manufacturer is the real spectrum. Results are given for simulations performed with the bowtie model from the manufacturer and experimental dose measurements, respectively.

3.3.3 Influence of bowtie filter and X-ray spectrum combination

In the end, it is important to look at the combined effect of the bowtie filter modelling and X-ray spectrum determination. Therefore, the mean organ doses of each combination described in Table 2 is compared to the combination combining both the X-ray spectrum and bowtie model provided by the manufacturer, which is considered to give the best results.

For each comparison, the maximum percentage dose difference over all organs is shown in Figure 15. Quite similar results are found when looking at the absolute and normalised organ doses. For all X-ray spectrum and bowtie filter combinations, organ doses are within 6% from those resulting from simulations with the spectrum and bowtie filter model provided by the manufacturer. Taking into account the CT dose range, these differences are rather small. Disregarding the situations that use the bowtie model from the manufacturer, organ dose differences are within 5%.

According to Figure 15, using combination 1b will results in organ doses that are maximum around 1% higher. However, this combination makes use of the X-ray spectrum provided by the manufacturer. Disregarding all situations combining the X-ray spectrum or bowtie filter model provided by the manufacturer, the best results are obtained by determining equivalent energy spectra with a voltage ripple of 0% and model the bowtie filter based on dose measurements. Organ dose difference are then within 3%. This confirms the findings stated in paragraph 3.3.1 and 3.3.2.

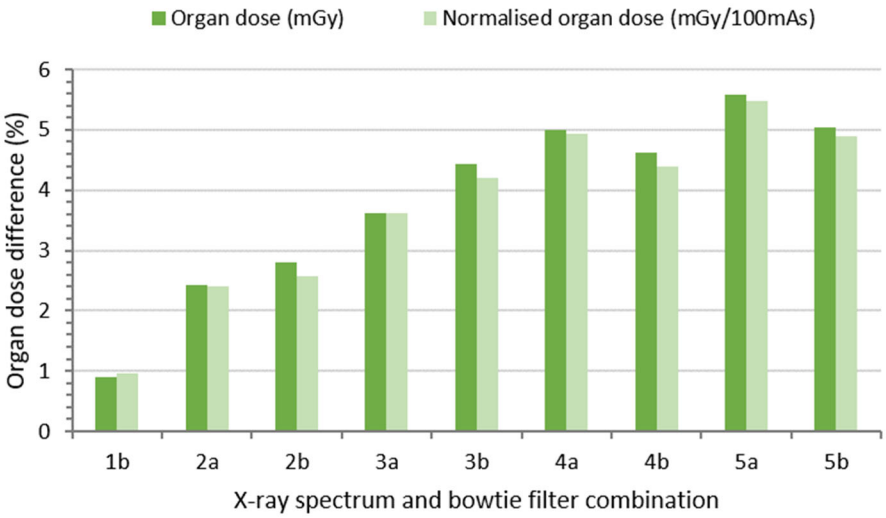

Figure 15: Maximum percentage difference in mean organ dose for all X-ray spectrum and bowtie filter combinations compared to combination 1a that combines the X-ray spectrum and bowtie filter model provided both by the manufacturer, assuming that this combination leads to the best results. Note that '1' stands for the spectrum provided by the manufacturer, '2' for the created equivalent spectrum with 0% voltage ripple, '3' for the created equivalent spectrum with 25% voltage ripple, '4' for the spectrum generated with the ImpactMC integrated spectrum generator, '5' for the spectrum generated with SpekCalc, 'a' for the bowtie model provided by the manufacturer and 'b' for the bowtie model characterised by dose measurements.

When manufacturer's data is not available, half-value layer and dose measurements are thus good alternative methods to obtain equivalent X-ray spectra and bowtie filter profiles, respectively. Monte Carlo simulations then result in estimated CT organ doses that deviate only slightly from reality. This supports our decision of adopting these methods to characterise the CT scanner's spectrum and bowtie filter in order to estimate organ doses from the CT part of hybrid nuclear medicine examinations.

4 Influence of available image data on CT organ dose estimations – Clinical practice versus scan range limited CT image data

In conventional CT, the available image data are limited to the patient's scan range, and no information exists regarding the rest of the body. The same limitation occurs in SPECT/CT imaging where the scan range of the CT examination is limited to the field of view (FOV) of the SPECT exam or shorter depending on the clinical indication. This influences the accurate incorporation of scatter in the dose calculation and the calculation of organ doses out of the field of view. Having whole-body patient CT images from whole-body PET/CT examinations available has the potential to study this influence. Therefore, Monte Carlo simulations of a chest and cardiac CT examination are performed using both the whole-body CT images and the images limited to the scan range in conventional CT as input volume. This was done for fifty patients undergoing a diagnostic CT scan with tube current modulation as part of a whole-body PET/CT examination on a Siemens Biograph mCT Flow. An equal number of male and female patients was selected.

4.1 Ventilation/perfusion lung or chest/thorax CT

4.1.1 Monte Carlo simulation CT scan

Ventilation/perfusion lung and chest/thorax CT scans are limited to the thorax region in both radiology and nuclear medicine. This means that both volumetric and dose information is missing of organs that are partially or completely out of the field of view. For organs that are completely in the scan region scatter may not be completely incorporated in the dose calculation.

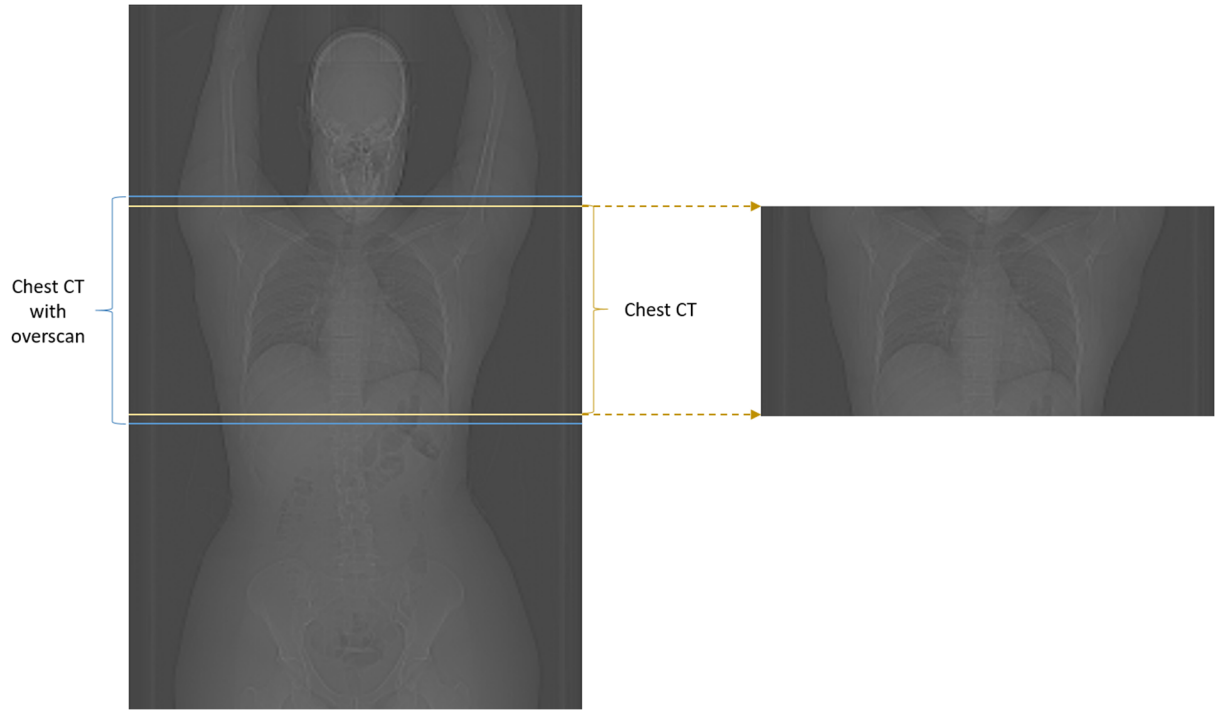

Figure 16: Simulated scan range for a chest CT with and without overscan using whole-body CT images (left) and images limited to the scan range of a conventional chest CT (right) as input volume for the Monte Carlo simulation.

To study the influence of missing CT image data on simulated CT organ doses, Monte Carlo simulations of a chest CT were performed using both the whole-body CT images and the images limited to the chest region as input volume. Figure 16 gives an indication of the scan range in the respective input volumes. This was done for fifty patients. All scan parameters, including the tube current modulation, were kept the same as those used for the diagnostic CT scan as part of a whole-body PET/CT examination on a Siemens Biograph mCT Flow.

In addition, the influence of overscan on CT organ doses is studied. Therefore, the original scan range was extended as shown in Figure 16. For this, the whole-body CT images were used as input volume for the Monte Carlo dose simulations.

4.1.2 Organ doses

Three Monte Carlo simulations were performed for each patient. The first made use of the CT images limited to the chest scan range as input volume while the second used all whole-body images for the dose simulation. This means that in the first situation scatter from the rest of the body is not incorporated and that the calculated organ doses are based on the known, for some organs limited, organ volume. The second situation resembles clinical practice the most because it contains organ information from head to mid-thigh and thus includes scatter from the rest of the body. The last Monte Carlo simulation included the principle of overscan, considered as an extension of the original chest scan range, using the whole-body image data. However, a fourth situation is distinguished as well. For all organs of interest, which are the breast, heart, liver, lungs, kidneys, ribs, thyroid, esophagus and spine, the entire organ volume is known from segmentation of the whole-body CT images. Recalculation of the organ doses, resulting from the Monte Carlo simulation with limited CT image data, for the entire organ volume is thus possible. Hereby, scatter radiation from the rest of the body is excluded. For all four situations, the normalised mean organ doses and their standard deviations are shown in Figure 17.

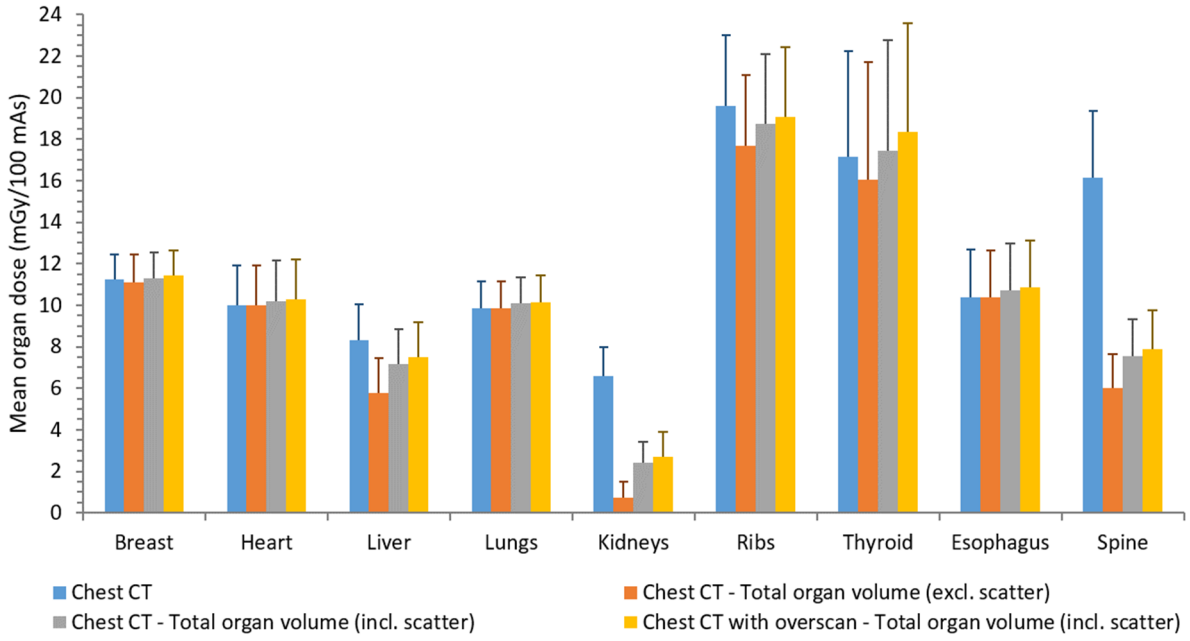

Figure 17: Monte Carlo simulated mean organ doses of a diagnostic chest CT scan with tube current modulation on a Siemens Biograph mCT Flow PET/CT using CT image data limited to a chest CT in conventional radiology (Chest CT) and taking into account the total volume of all organs but excluding scatter radiation from the rest of the body (Chest CT – Total organ volume, excl. scatter) or using whole-body CT images including the total volume of all organs and scatter radiation (Chest CT – Total organ volume, incl. scatter = clinical practice) and overscan (Chest CT with overscan – Total organ volume, incl. scatter).

Compared to organ doses calculated with limited CT image data, taking into account the entire organ volume but excluding scatter radiation from the rest of the body leads to a dose decrease for most organs. The largest decreases are observed for the kidneys (-89%) and spine (-63%) of which the largest part of their volume lies outside the field of view. For the liver the dose lies only 30% lower because more than half of the liver lies in the field of view for most patients. Even smaller differences are seen for the ribs (-10%) and thyroid (-6%) which are almost completely in the field of view. For the breast and esophagus, mean organ doses are 1% and 0.3% lower, respectively. No dose differences are observed for the heart and lungs because the CT scan covers them entirely.

Incorporating scatter from the rest of the body as well, which corresponds to the clinical practice, leads to a dose increase for all organs. For organs located in or almost completely in the field of view, such as the heart, lungs, breast and esophagus, these increases are rather small (max. +4%). For the ribs and thyroid, this increase is around 6% to 9%. The largest dose increases are observed for the spine, liver and kidneys because of the higher contribution of scatter due to a larger percentage of the organ volume located outside the field of view.

As expected, overscan induces higher organ doses resulting from the wider scan range. Compared to the previous situation, which takes into account the entire organ volume and scatter, dose increases within 5% are observed for all organs except the kidneys. For the kidneys, an increase in dose of 12% is seen which primarily originates from the fact that in percentage terms more of the organ is now in the field of view. These percentage differences are visualised in Figure 18, comparison ‘C3’.

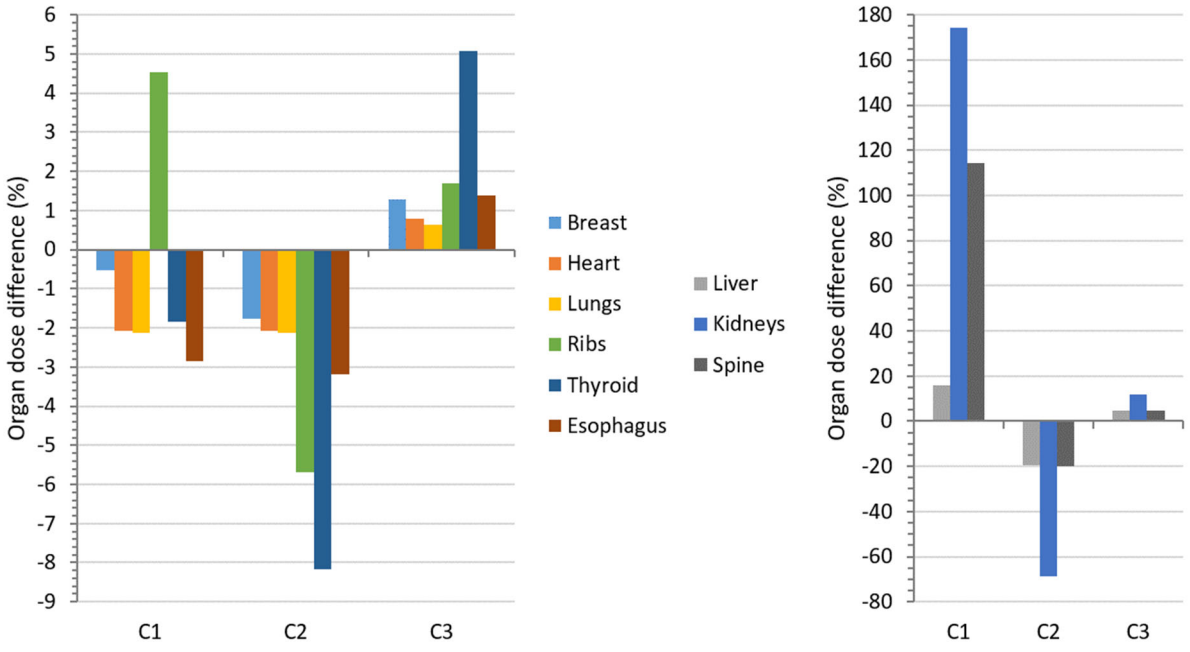

Figure 18: Percentage difference in mean organ dose for the simulated diagnostic chest CT scans with tube current modulation compared to clinical practice (C1: image data limited to a conventional chest CT compared to a chest CT having whole-body data available (all organ volumes known and including scatter radiation), C2: image data limited to a conventional chest CT but taking into account the entire volume of all organs compared to a chest CT having whole-body data available (all organ volumes known and including scatter radiation), C3: chest CT with overscan compared to chest CT without overscan using whole-body CT image data).

Figure 18 also shows the percentage differences in mean organ dose of dose simulations performed with limited CT image data with and without taking into account the entire organ volume compared to the clinical practice where scatter of the rest of body as well as the entire organ volume are incorporated (comparison ‘C2’ and ‘C1’, respectively). If patient information is thus limited to the

image data of the chest (Figure 18, comparison 'C1'), breast, heart, lung, thyroid and esophagus doses are underestimated by around 0.5% to 3% because scatter contribution from the rest of the body is ignored. The rib, liver, spine and kidney doses on the other hand are overestimated by around 5%, 16%, 114% and 174%, respectively, which is most importantly due to the missing knowledge of the entire organ volume. When the entire organ volume is taken into account, an underestimation in dose is found for all organs because now only the contribution of scatter from the rest of the body is ignored (Figure 18, comparison 'C2').

4.2 Cardiac CT

4.2.1 Monte Carlo simulation CT scan

CT image data resulting from conventional cardiac CT studies and cardiac PET/CT or SPECT/CT examinations in nuclear medicine is limited to the cardiac region. When using whole-body CT images as input volume for the Monte Carlo simulation of a cardiac CT, scatter can be accurately incorporated in the dose calculation as well as organ doses out of the field of view. Therefore, Monte Carlo simulations of a cardiac CT were performed using both the whole-body CT images and the images limited to the cardiac region as input volume. This is illustrated in Figure 19. As in the previous case, this was done for fifty patients and all scan parameters, including the tube current modulation, were kept the same as those used for the diagnostic CT scan as part of a whole-body PET/CT examination on a Siemens Biograph mCT Flow.

To study the influence of overscan, the whole-body images were used as input volume and the original scan range was extended (Figure 19).

Figure 19: Simulated scan range for a cardiac CT with and without overscan using whole-body CT images (left) and images limited to the scan range of a conventional cardiac CT (right) as input volume for the Monte Carlo simulation.

4.2.2 Organ doses

Again, three Monte Carlo simulations were performed for each patient but four organ dose calculations were compared with each other. The first dose calculation is based on the limited image data used as input volume. This means that the only information available is that embedded in the CT images of the cardiac region. Secondly, recalculation of the organ doses for the entire organ volume is done. The third dose calculation, for which the whole-body images were used as input volume, incorporates both the entire volume of all organs and scatter from the rest of the body. The fourth and last situation included the helical overscan, considered as an extension of the original cardiac scan range, using the whole-body image data. For all four situations, the normalised mean organ doses and their standard deviations are shown in Figure 20.

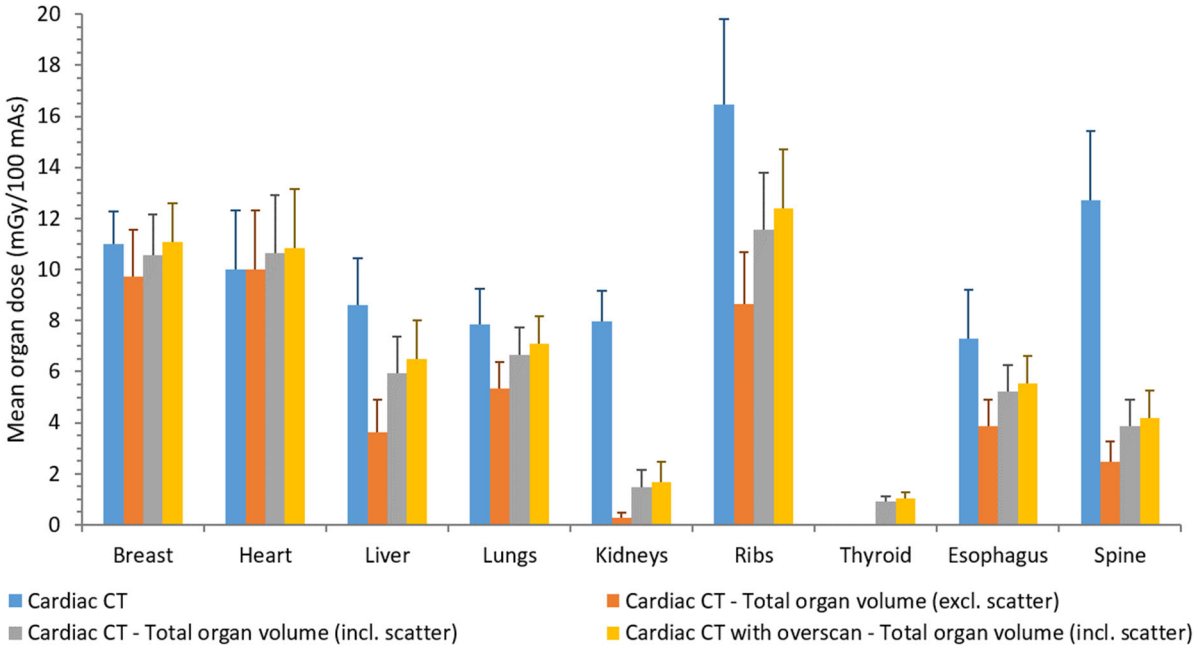

Figure 20: Monte Carlo simulated mean organ doses of a diagnostic cardiac CT scan with tube current modulation on a Siemens Biograph mCT Flow PET/CT using CT image data limited to a cardiac CT in conventional radiology (Cardiac CT) and taking into account the total volume of all organs but excluding scatter radiation from the rest of the body (Cardiac CT – Total organ volume, excl. scatter) or using whole-body CT images including the total volume of all organs and scatter radiation (Cardiac CT – Total organ volume, incl. scatter = clinical practice) and overscan (Cardiac CT with overscan – Total organ volume, incl. scatter).

Taking into account the entire organ volume but excluding scatter from the rest of the body leads to a dose decrease for most organs, compared to organ doses calculated with the limited CT image data. Of course, no dose difference is found for the heart because it lies completely within the scan range. The largest differences are observed for the kidneys (-97%), spine (-80%), liver (-58%), ribs (-47%) and esophagus (-47%). This is mainly because in percentage terms more of the organ is outside the field of view than within. The lung dose lies 32% lower because, for all patients, more than half of the lungs is in the field of view. For the breast, a difference of around 12% is found which corresponds with an almost complete coverage of the breast by the CT scan. No conclusion can be drawn for the thyroid because it is not in the scan area.

As already mentioned earlier, incorporating scatter from the rest of the body as well leads to a dose increase for all organs. These dose results resemble the clinical practice. For the heart and the breast, this increase is around 6% and 9%, respectively. Organs located more out of the field of view, like the

lungs, ribs, esophagus, spine and liver, show a dose increase ranging from 25% over 34% to 64% depending on the percentage of the organ lying within the primary exposed volume. The dose increase is the largest for the kidneys because the largest dose contribution originates from scatter. As can be seen in Figure 20, organ doses for the thyroid can now be calculated as well. However, it is important to notice that only scatter contributes to the thyroid dose.

As expected, overscan induces higher organ doses. Compared to the previous situation, which takes into account the entire organ volume and scatter, dose increases within 15% are observed for all organs. The smallest increases are found for the heart (+2%) and breast (+5%). This is because there is not much difference in percentage of the organ volume lying within the primary exposed volume compared to the other organs. These percentage differences are visualised in Figure 21, comparison 'C3'.

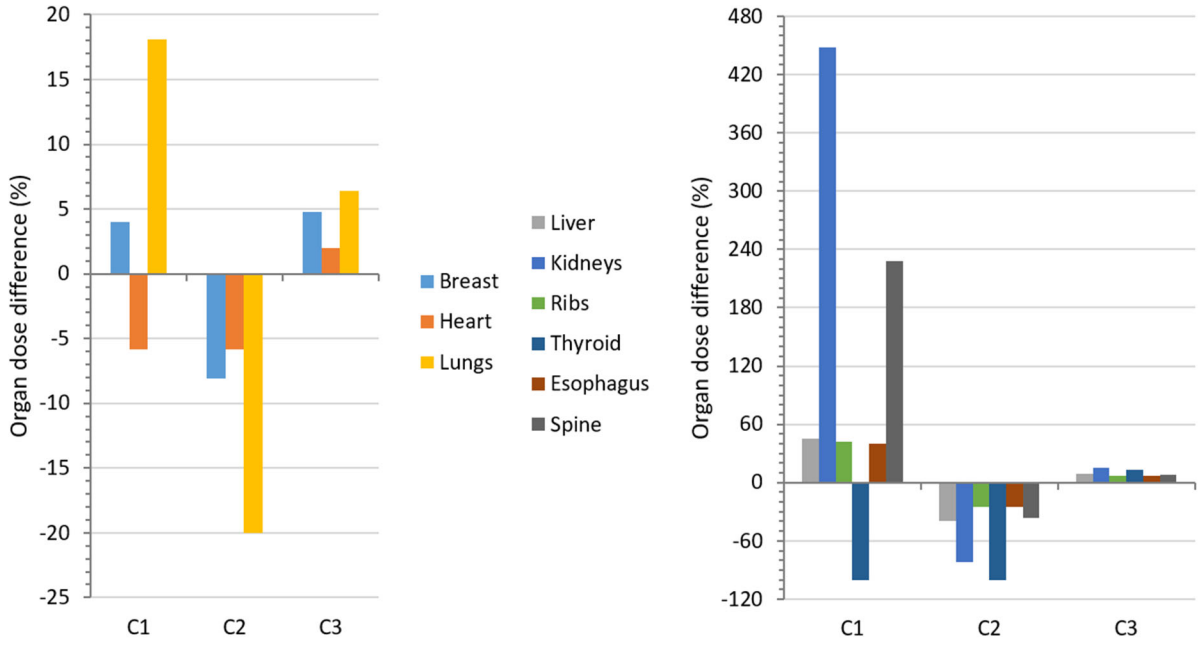

Figure 21: Percentage difference in mean organ dose for the simulated diagnostic cardiac CT scans with tube current modulation compared to clinical practice (C1: image data limited to a conventional cardiac CT compared to a cardiac CT having whole-body data available (all organ volumes known and including scatter radiation), C2: image data limited to a conventional cardiac CT but taking into account the entire volume of all organs compared to a cardiac CT having whole-body data available (all organ volumes known and including scatter radiation), C3: cardiac CT with overscan compared to cardiac CT without overscan using whole-body CT image data).

Figure 21 also shows the percentage differences in mean organ dose of dose simulations performed with limited CT image data with and without taking into account the entire organ volume compared to the clinical practice where scatter of the rest of body as well as the entire organ volume are incorporated (comparison 'C2' and 'C1', respectively). In case image data is limited to the cardiac region (Figure 21, comparison 'C1'), the heart dose is underestimated by around 6% because the scatter contribution from the rest of the body is not known. For the thyroid, the dose cannot be estimated when it is not present in the image data. Because only scatter contributes to the thyroid dose, an underestimation of 100% is found. For all other organs, the organ dose is overestimated mainly because the entire volume of the organ cannot be taken into account. As was the case for chest CT, an underestimation in dose is found for all organs when only incorporating the entire organ volume and not the contribution of scatter from the rest of the body (Figure 21, comparison 'C2').

5 CT organ doses in PET/CT

In PET/CT, whole-body examinations are the most frequently performed whereby the body is scanned from head to mid-thigh. Depending on the clinical task, a distinction can be made between studies with a diagnostic or a localisation CT scan. Although both serve for attenuation correction of the functional PET images as well, a diagnostic CT will result in higher organ doses than a localisation CT.

This chapter focuses on the calculation of the organ doses resulting from the CT part of a whole-body PET/CT examination and on their correlation with patient characteristics and dose indicators. Therefore, Monte Carlo simulations were performed for 100 patients with an equal number of male and female patients. The diagnostic CT scan was simulated with and without tube current modulation while the localisation CT was simulated at a fixed tube current. This was done for the specific scan protocols available on a Siemens Biograph mCT Flow and a GE Discovery MI.

5.1 Organ doses

Both PET/CT systems, Siemens Biograph mCT Flow and GE Discovery MI, have similar whole-body protocols present. Diagnostic CT scans are performed at a tube voltage of 120 kV while a tube voltage of 80 kV is used in case of a localisation CT. Compared to a diagnostic CT, localisation CT scans also apply a larger pitch and lower tube current-time product. For both systems, twenty-five male and female patients with varying body mass index were selected. For each patient, Monte Carlo simulations were performed of a diagnostic CT scan with and without tube current modulation and a location CT with a fixed tube current. Simulations without tube current modulation were performed at a fixed tube current-time product of 100 mAs. The resulting distribution of organ doses normalised to 100 mAs is visualised in Figure 22.

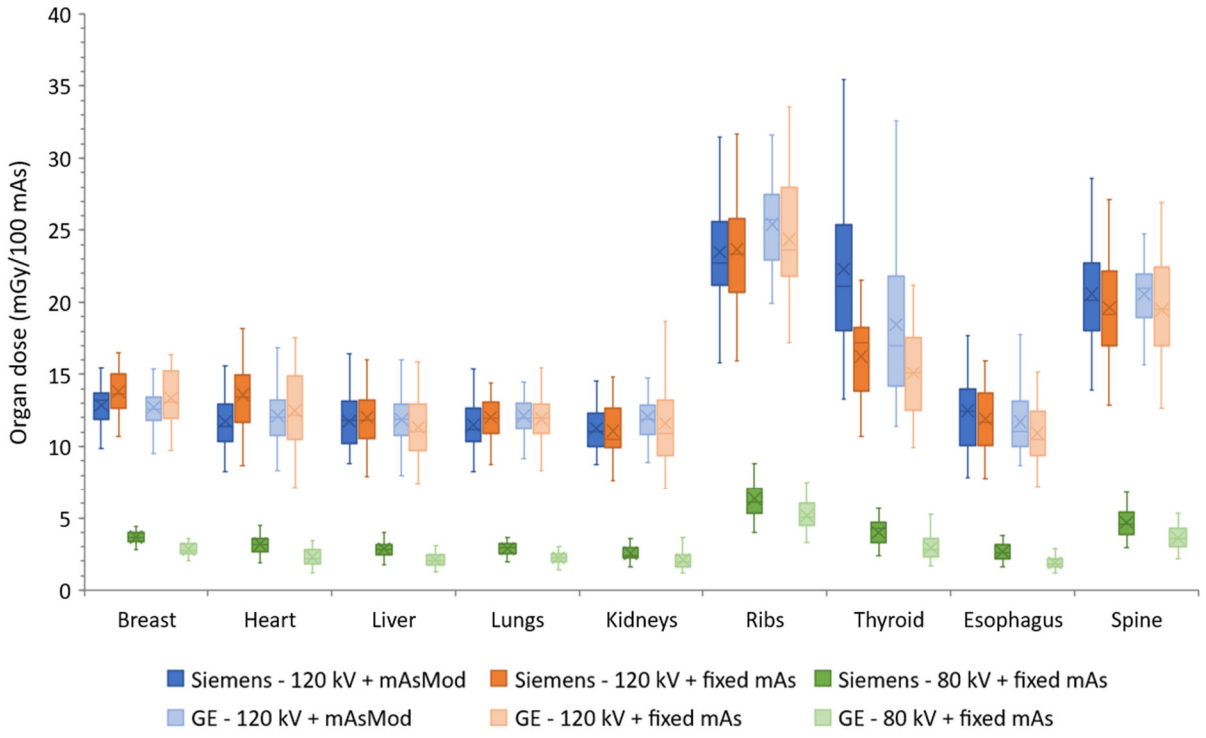

Figure 22: Distribution of the organ doses normalised to 100 mAs received by a diagnostic CT at 120 kV with and without automatic tube current modulation and a localisation CT at 80 kV with fixed tube current-time product (mAs) as part of a whole-body PET/CT examination on a Siemens Biograph mCT Flow and GE Discovery MI.

As expected are the organ doses larger for diagnostic than for localisation CT scans. This is observed for both systems. Comparing the diagnostic CT at 120 kV with the localisation CT at 80 kV, both without the use of tube current modulation, a mean dose difference of around 75% and 80% is found for the Siemens and GE PET/CT, respectively.

Applying a fixed tube current instead of tube current modulation leads, for both systems, to a mean dose increase for the breast and heart. For the Siemens PET/CT, an increase in mean dose is also seen for the liver, lungs and ribs while for the GE PET/CT a dose decrease is observed. However, these dose differences are rather small (< 5%). For all other organs of interest, a decrease in mean organ dose is found for both PET/CT devices. These differences are within 7% for the kidneys, esophagus and spine. The largest dose decrease is seen for the thyroid, which is around 27% and 18% for the Siemens and GE PET/CT, respectively. This is because the thyroid is a relatively small superficial organ. In addition, a smaller spread in thyroid doses is observed when using no tube current modulation.

Independent of the CT protocol and hybrid imaging system used, the largest doses are found for the ribs and spine because of the higher attenuation coefficient of bone. In addition, a wider spread in doses between patients is observed for these structures. For organs made up of soft tissue, superficial organs such as the thyroid and breast receive a higher dose. Note the large spread in thyroid doses, especially for a diagnostic CT scan with tube current modulation, which is probably due to the large variation in size of this small organ between patients. Similar organ doses are found for soft tissue organs located more centrally in the body.

Comparing the Siemens Biograph mCT Flow with the GE Discovery MI results in lower mean organ doses for the localisation CT of the GE PET/CT. Depending on the specific organ, doses are around 15% to 30% lower. This may be induced by the pitch of the CT protocol that is larger than one for the GE PET/CT and smaller than one for the Siemens PET/CT, respectively, 1.375 and 0.8. The other scan parameters are quite similar. For a diagnostic CT with tube current modulation, mean breast, heart, liver and spine doses differ within 4% between both PET/CT systems. Mean lung, kidney and rib doses lie 5% to 10% lower for the Siemens PET/CT while the mean esophagus dose is around 7% higher. The thyroid dose on the other hand is about 21% higher at the Siemens PET/CT. When comparing the diagnostic protocols of both systems using fixed tube current, mean doses differ within 4% for the breast, lungs, ribs and spine. For the heart, liver, thyroid and esophagus mean doses are 5% to 10% lower for the GE PET/CT while for the kidneys the mean dose is around 5% higher.

5.2 Correlation between organ doses and patient characteristics

As described in section 2.7, the patient size is characterised by its water equivalent diameter (D_w or WED) which takes into account the X-ray attenuation of the patient. The correlation between organ dose and water equivalent diameter was determined through regression analysis. The estimated regression function was of the exponential form

$$y = a \cdot e^{b \cdot x} \tag{9}$$

where the independent variable, x, corresponds to the water equivalent diameter (D_W) in centimetre (cm) which is estimated per patient as described by equation 7 (see section 2.7). The dependent variable, y, corresponds to the organ dose expressed in mGy or mGy/100mAs (normalised dose unit).

The parameters a and b were estimated for each correlation between the Monte Carlo computed organ dose and patient-specific water equivalent diameter. The coefficient of determination, R^2, was used as a measure to assess the strength of correlation between organ dose and D_W.

5.2.1 Diagnostic CT scan

Figure 23 - 26 display estimated organ doses as a function of the water equivalent diameter (D_W) for the heart, lungs, esophagus and spine of a whole-body diagnostic CT scan with tube current modulation. For each organ, the water equivalent diameter was correlated to the estimated absolute dose values and to the dose values normalised to 100 mAs. The orange line corresponds to regression associated with dose values computed using the Siemens Biograph mCT Flow model while the dashed blue lines corresponds to the GE Discovery MI model.

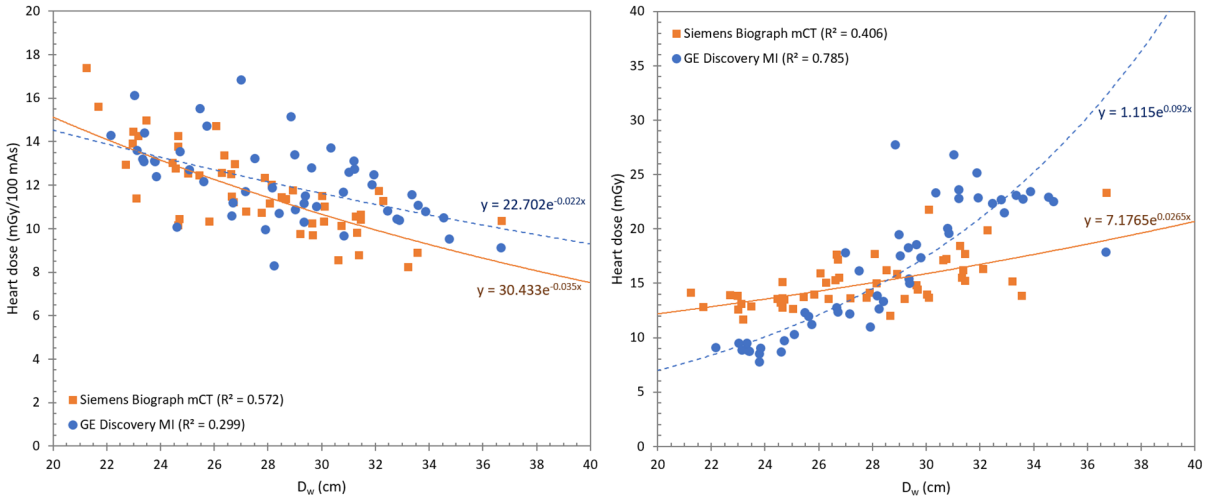

(a) Normalised dose (b) Absolute dose

Figure 23: Estimated (normalised) heart dose as a function of water equivalent diameter (D_w) for a diagnostic CT scan at 120 kV with tube current modulation as part of a whole-body PET/CT examination. Plot points are patient-specific organ doses for examinations on a Siemens Biograph mCT Flow (circles) and GE Discovery MI (squares). Associated exponential regression lines are visualised as a full and dashed line, respectively.

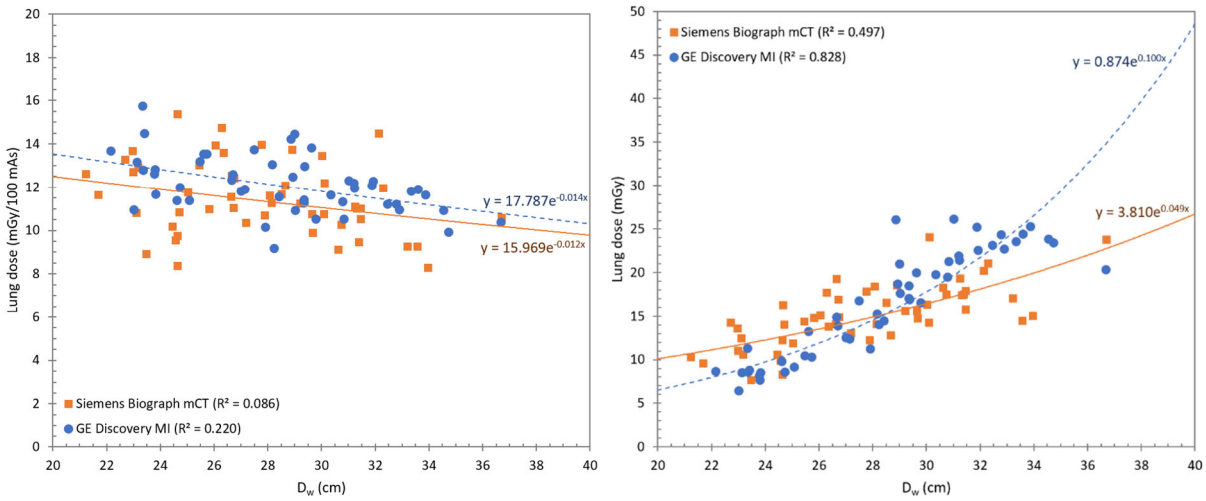

(a) Normalised dose (b) Absolute dose

Figure 24: Estimated (normalised) lung dose as a function of water equivalent diameter (D_w) for a diagnostic CT scan at 120 kV with tube current modulation as part of a whole-body PET/CT examination. Plot points are patient-specific organ doses for examinations on a Siemens Biograph mCT Flow (squares) and GE Discovery MI (circles). Associated exponential regression lines are visualised as a full and dashed line, respectively.

When looking at the regression of the normalised organ doses, stronger correlations are found for the esophagus and spine ($R^2 \geq 0.6$) than for the heart and lungs. In addition, the strength of the correlation varies with the PET/CT model especially for the heart where a much stronger correlation is found for the Siemens PET/CT than for the GE PET/CT. Taking into account the patient-specific tube current-time product results for all organs into strong correlations ($R^2 > 0.7$) for the GE Discovery MI model. For the Siemens Biograph mCT Flow, the strength of the correlation increases for almost all organs except for the esophagus and spine. There a strong decrease in strength is observed.

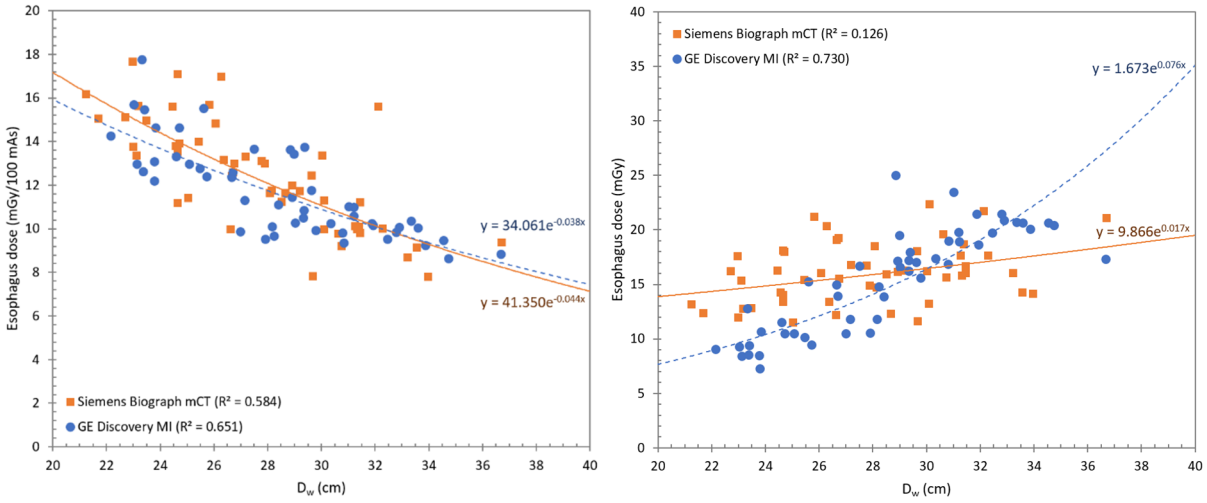

(a) Normalised dose (b) Absolute dose

Figure 25: Estimated (normalised) esophagus dose as a function of water equivalent diameter (D_w) for a diagnostic CT scan at 120 kV with tube current modulation as part of a whole-body PET/CT examination. Plot points are patient-specific organ doses for examinations on a Siemens Biograph mCT Flow (squares) and GE Discovery MI (circles). Associated exponential regression lines are visualised as a full and dashed line, respectively.

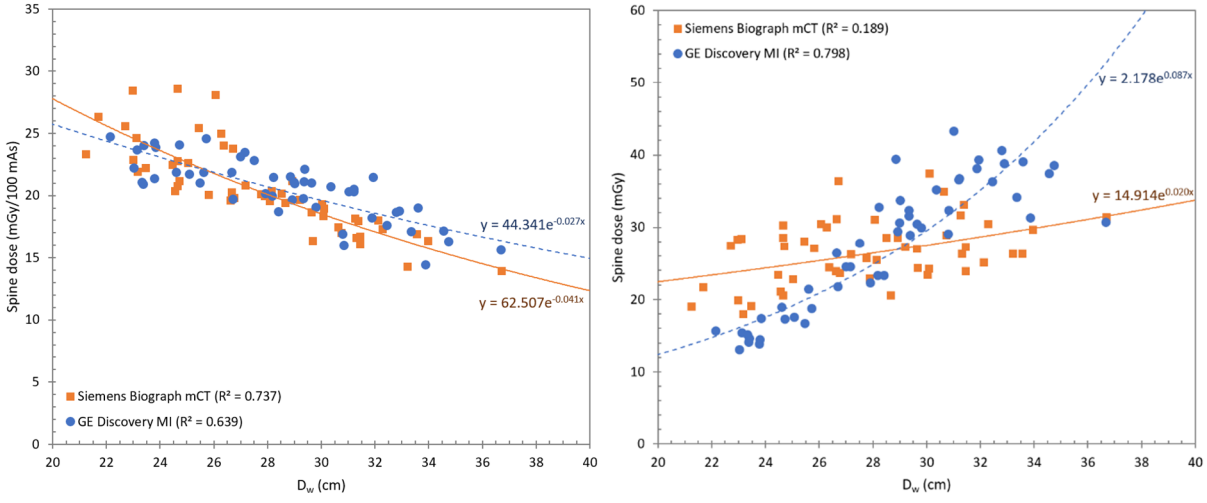

(a) Normalised dose (b) Absolute dose

Figure 26: Estimated (normalised) spine dose as a function of water equivalent diameter (D_w) for a diagnostic CT scan at 120 kV with tube current modulation as part of a whole-body PET/CT examination. Plot points are patient-specific organ doses for examinations on a Siemens Biograph mCT Flow (squares) and GE Discovery MI (circles). Associated exponential regression lines are visualised as a full and dashed line, respectively.

Monte Carlo dose computations were also performed for a diagnostic CT scan without tube current modulation. Figure 27 displays normalised estimated organ doses as a function of the water equivalent diameter (D_W) for the heart, lungs, esophagus and spine. For most organs a strong ($R^2 > 0.7$) to very strong ($R^2 > 0.8$) exponential correlation was found. Only for the regression analysis of the lung dose estimated for the Siemens PET/CT model the coefficient of determination is smaller than 0.5, namely 0.44 (Figure 27b).

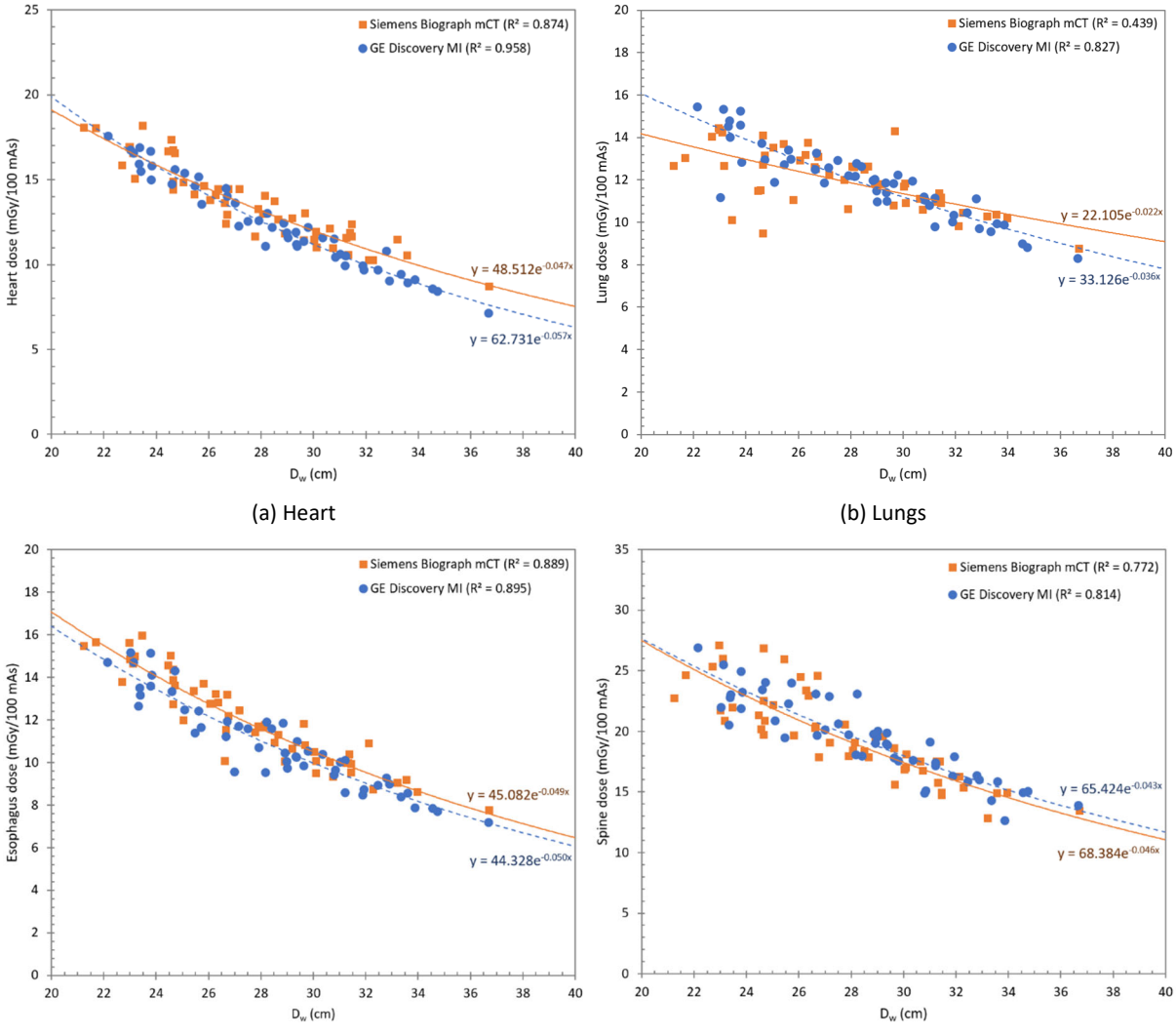

(a) Heart (b) Lungs

(c) Esophagus (d) Spine

Figure 27: Estimated normalised (a) heart, (b) lung, (c) esophagus and (d) spine dose as a function of water equivalent diameter (D_w) for a diagnostic CT scan at 120 kV with fixed tube current as part of a whole-body PET/CT examination. Plot points are patient-specific organ doses for examinations on a Siemens Biograph mCT Flow (squares) and GE Discovery MI (circles). Associated exponential regression lines are visualised as a full and dashed line, respectively.

The results of the regression analysis for breast, liver, kidney, rib and thyroid dose are displayed in 'Appendix A – Whole-body PET/CT organ dose correlations' for Monte Carlo dose simulations performed with and without tube current modulation.

5.2.2 Localisation CT scan

Figure 28 displays estimated organ doses as a function of the water equivalent diameter (D_W) for the heart, lungs, thyroid and spine of a whole-body localisation CT scan without tube current modulation. For each organ, the water equivalent diameter was correlated to the estimated dose values normalised to 100 mAs. The orange line corresponds to regression associated with dose values computed using the Siemens Biograph mCT Flow model while the dashed blue lines corresponds to the GE Discovery MI model. The lower organ doses for the GE PET/CT found earlier when looking at the organ dose distributions (Figure 22) are also reflected in these correlations. For both PET/CT models, a moderate correlation strength is found for the thyroid dose ($0.46 \leq R^2 < 0.6$). This is also the case for the lung dose of the Siemens PET/CT model. For all other organs, a strong ($R^2 > 0.7$) to very strong ($R^2 > 0.8$) correlation is found between the organ dose and the water equivalent diameter.

The results of the regression analysis for breast, liver, kidney, rib and esophagus dose are displayed in 'Appendix A – Whole-body PET/CT organ dose correlations'.

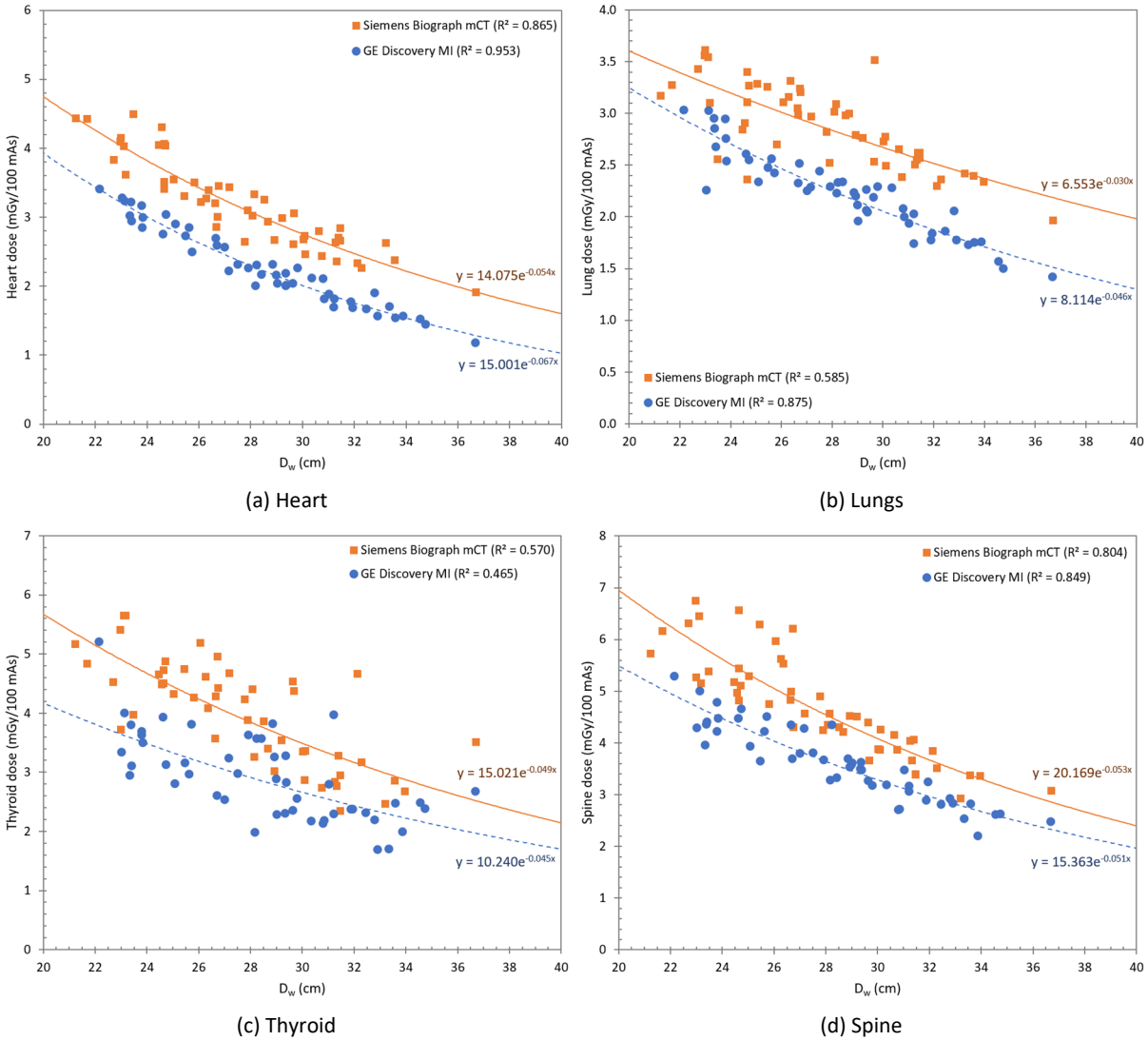

Figure 28: Estimated normalised (a) heart, (b) lung, (c) thyroid and (d) spine dose as a function of water equivalent diameter (D_w) for a localisation CT scan at 80 kV with fixed tube current as part of a whole-body PET/CT examination. Plot points are patient-specific organ doses for examinations on a Siemens Biograph mCT Flow (squares) and GE Discovery MI (circles). Associated exponential regression lines are visualised as a full and dashed line, respectively.

5.3 Correlation between organ dose and dose indicators

As described in section 2.7, the size-specific dose estimate (SSDE) was introduced to estimate patient doses more accurately. This metric takes into account both the size of the patient and the CT dose parameter $CTDI_{vol}$. The correlation between organ dose and SSDE was determined through regression analysis. The estimated regression function was of the linear form

$$y = a \cdot x \tag{10}$$

where the independent variable, x, corresponds to the size-specific dose estimate (SSDE) in mGy which is estimated per patient as described by equation 8 (see section 2.7). The dependent variable, y, corresponds to the organ dose expressed in mGy or mGy/100mAs (normalised dose unit).

The parameter a was estimated for each correlation between the Monte Carlo computed organ dose and patient-specific dose estimate. The coefficient of determination, R^2, was used as a measure to assess the strength of correlation between organ dose and D_W.

5.3.1 Diagnostic CT scan

Figure 29 - 32 display estimated organ doses as a function of the size-specific dose estimate (SSDE) for the heart, lungs, esophagus and thyroid of a whole-body diagnostic CT scan with tube current modulation. For each organ, the size-specific dose estimate was correlated to the estimated absolute dose values and to the dose values normalised to 100 mAs. The orange line corresponds to the linear regression associated with dose values computed using the Siemens Biograph mCT Flow model while the dashed blue lines corresponds to the GE Discovery MI model.

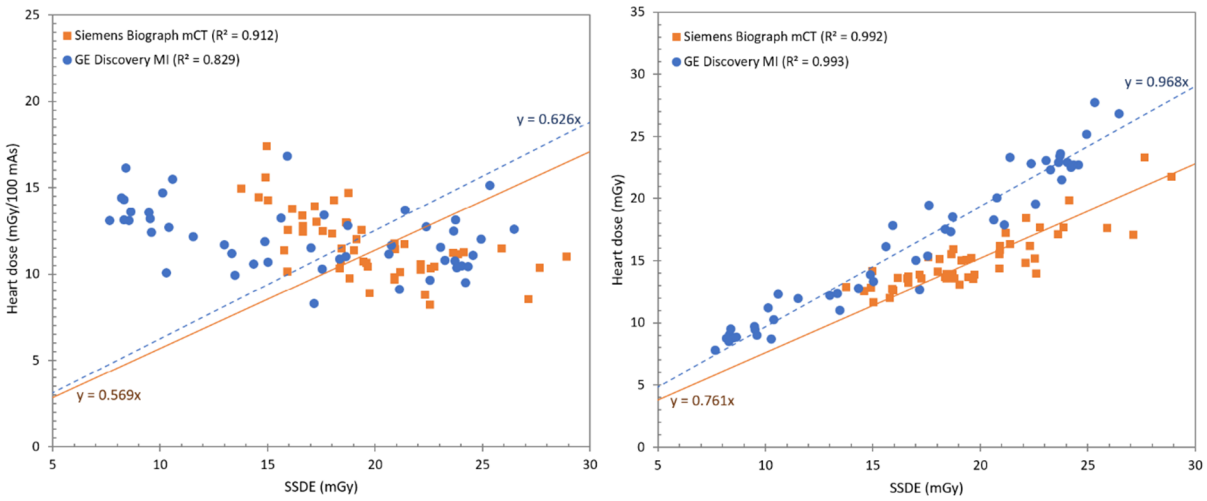

(a) Normalised dose (b) Absolute dose

Figure 29: Estimated (normalised) heart dose as a function of size-specific dose estimate (SSDE) for a diagnostic CT scan at 120 kV with tube current modulation as part of a whole-body PET/CT examination. Plot points are patient-specific organ doses for examinations on a Siemens Biograph mCT Flow (squares) and GE Discovery MI (circles). Associated linear regression lines are visualised as a full and dashed line, respectively.

For the regression of the normalised organ doses, very strong correlations ($R^2 > 0.8$) are found for all organs of the GE Discovery MI model except for the esophagus and thyroid. However, the observed correlations are still strong (coefficient of determination is equal or larger than 0.7). As can be seen, the data points are largely spread around the fitting model. Taking into account the patient-specific

tube current-time product gives a better model fit and even results into very strong linear correlations ($R^2 \geq 0.95$) for both PET/CT models.

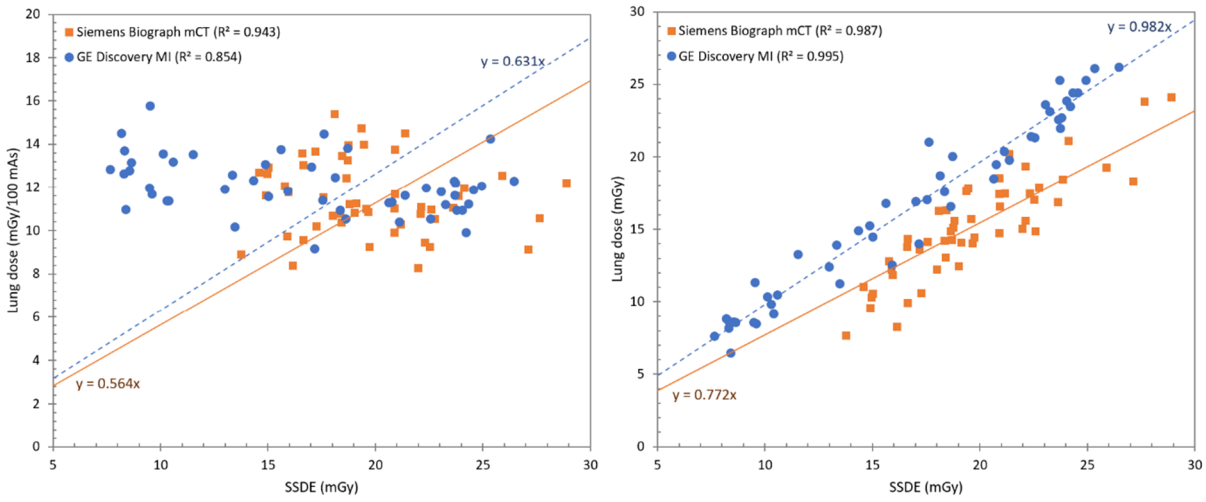

(a) Normalised dose (b) Absolute dose

Figure 30: Estimated (normalised) lung dose as a function of size-specific dose estimate (SSDE) for a diagnostic CT scan at 120 kV with tube current modulation as part of a whole-body PET/CT examination. Plot points are patient-specific organ doses for examinations on a Siemens Biograph mCT Flow (squares) and GE Discovery MI (circles). Associated linear regression lines are visualised as a full and dashed line, respectively.

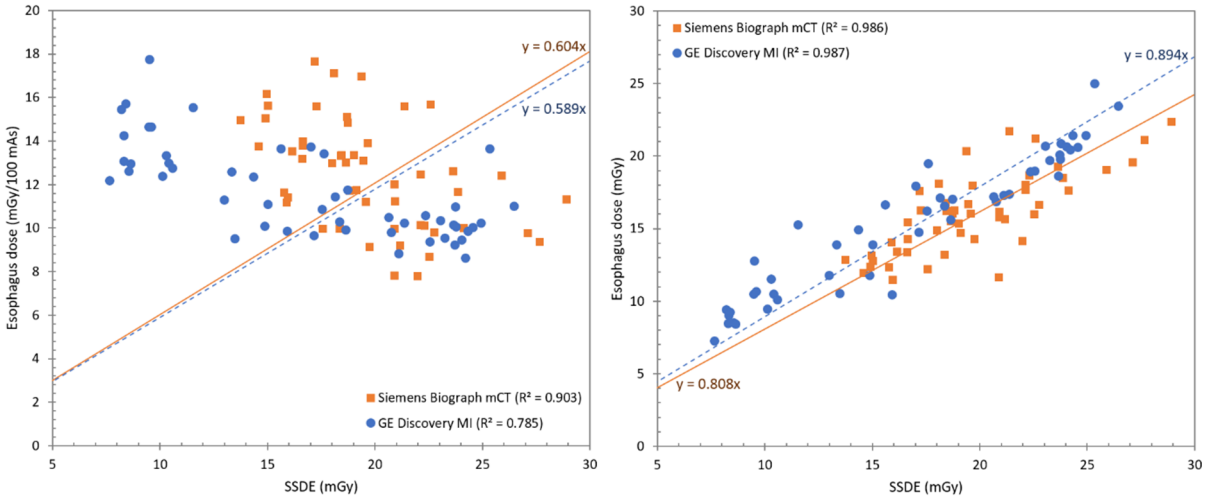

(a) Normalised dose (b) Absolute dose

Figure 31: Estimated (normalised) esophagus dose as a function of size-specific dose estimate (SSDE) for a diagnostic CT scan at 120 kV with tube current modulation as part of a whole-body PET/CT examination. Plot points are patient-specific organ doses for examinations on a Siemens Biograph mCT Flow (squares) and GE Discovery MI (circles). Associated linear regression lines are visualised as a full and dashed line, respectively.

For Monte Carlo dose computations performed without tube current modulation, very strong correlations ($R^2 > 0.97$) are even found for the normalised organ doses for both PET/CT models. Normalised estimated organ doses as a function of the size-specific dose estimate (SSDE) for the heart, lungs, esophagus and thyroid are shown in Figure 33. The linear fit model through the origin associates well with the spread in data points.

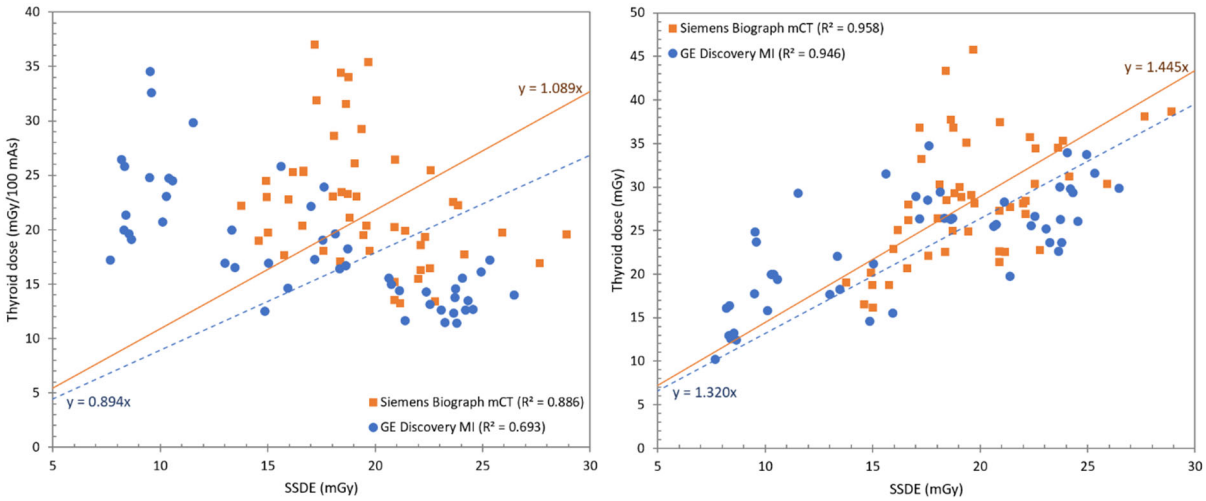

(a) Normalised dose (b) Absolute dose

Figure 32: Estimated (normalised) thyroid dose as a function of size-specific dose estimate (SSDE) for a diagnostic CT scan at 120 kV with tube current modulation as part of a whole-body PET/CT examination. Plot points are patient-specific organ doses for examinations on a Siemens Biograph mCT Flow (squares) and GE Discovery MI (circles). Associated linear regression lines are visualised as a full and dashed line, respectively.

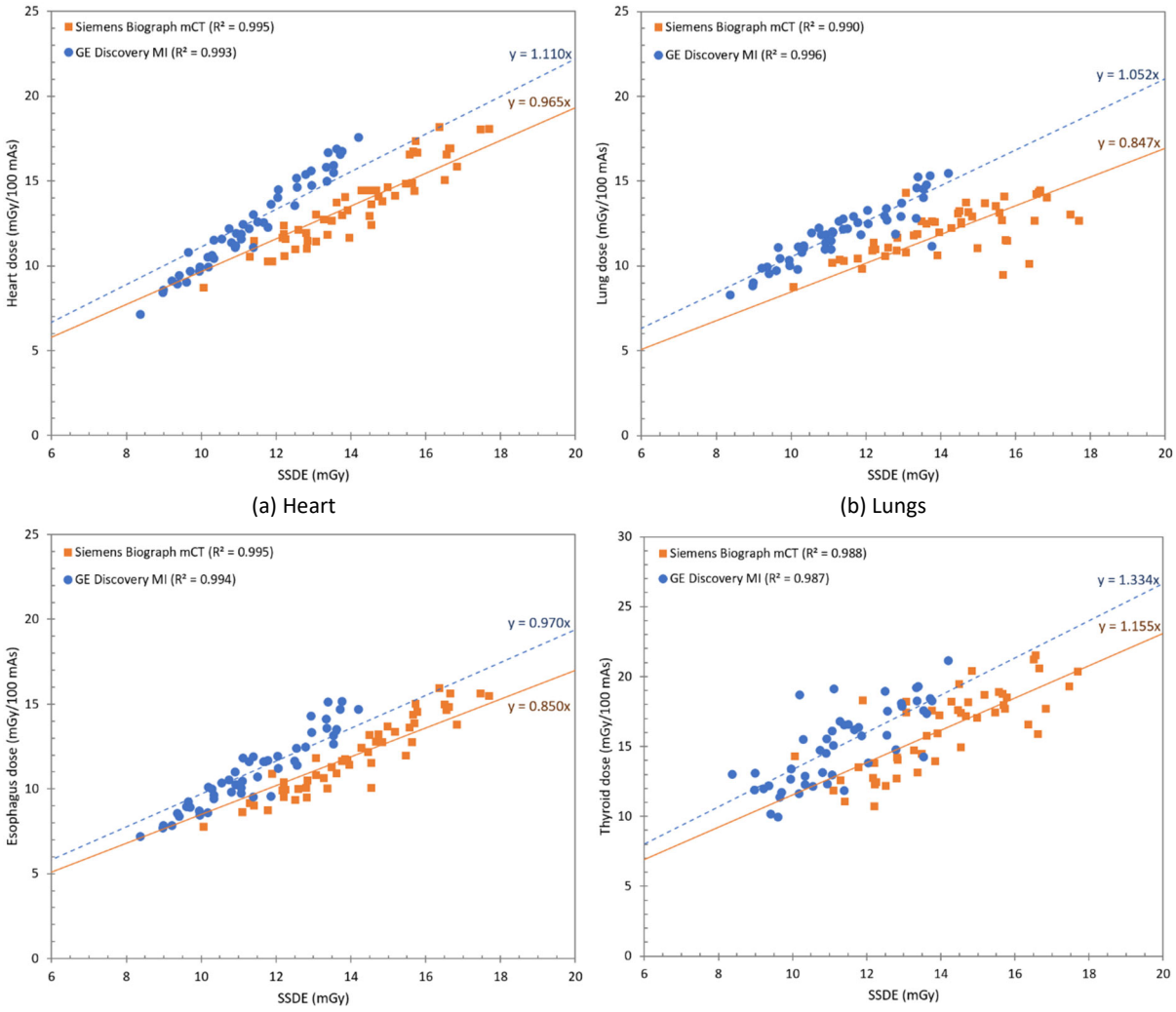

(a) Heart (b) Lungs

(c) Esophagus (d) Thyroid

Figure 33: Estimated normalised (a) heart, (b) lung, (c) esophagus and (d) thyroid dose as a function of size-specific dose estimate (SSDE) for a diagnostic CT scan at 120 kV with fixed tube current as part of a whole-body PET/CT examination. Plot points are patient-specific organ doses for examinations on a Siemens Biograph mCT Flow (squares) and GE Discovery MI (circles). Associated linear regression lines are visualised as a full and dashed line, respectively.

The results of the regression analysis for breast, liver, kidney, rib and spine dose are displayed in 'Appendix A – Whole-body PET/CT organ dose correlations' for Monte Carlo dose simulations performed with and without tube current modulation.

5.3.2 Localisation CT scan

Similar regression analysis was performed for the localisation CT of both models. For both systems, very strong correlations ($R^2 > 0.96$) between organ dose and size-specific dose estimate are found. Also here, the lower organ doses for the GE PET/CT found earlier when looking at the organ dose distributions (Figure 22) are reflected in the correlations. Figure 34 visualises the regression results for the heart and lung dose.

The results of the regression analysis for breast, liver, kidney, rib, thyroid, esophagus and spine dose are displayed in 'Appendix A – Whole-body PET/CT organ dose correlations'.

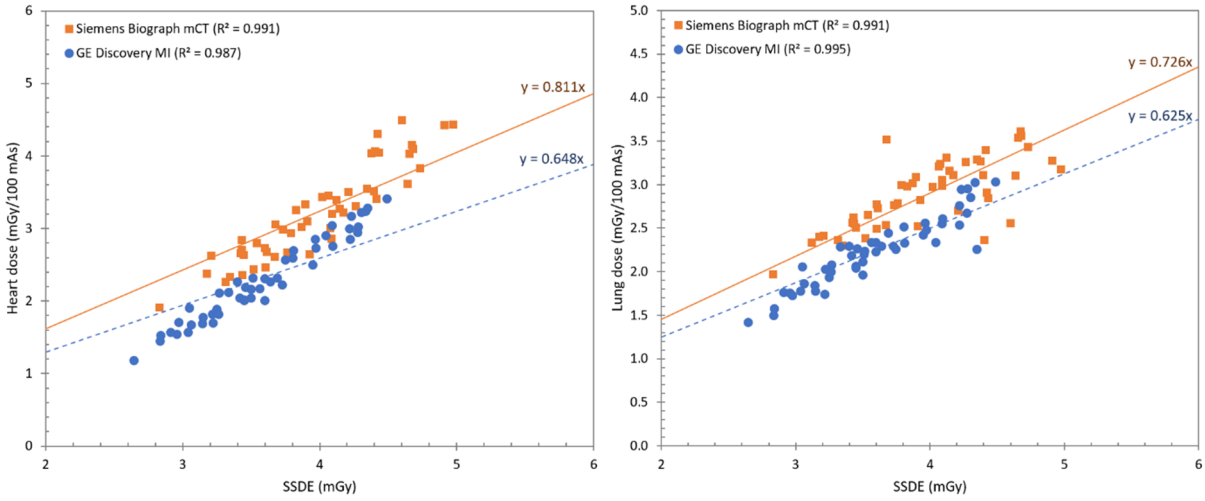

(a) Heart (b) Lungs

Figure 34: Estimated normalised (a) heart and (b) lung dose as a function of size-specific dose estimate (SSDE) for a localisation CT scan at 80 kV with fixed tube current as part of a whole-body PET/CT examination. Plot points are patient-specific organ doses for examinations on a Siemens Biograph mCT Flow (squares) and GE Discovery MI (circles). Associated linear regression lines are visualised as a full and dashed line, respectively.

6 CT organ doses in SPECT/CT

The most performed SPECT/CT examinations in the chest region are ventilation/perfusion lung scans and cardiac scans. Other frequently performed SPECT/CT studies near the thorax region are examinations of the cervical and lumbar spine. First, the organ doses and their correlation with the water equivalent diameter and size-specific dose estimate are discussed for the attenuation correction and localisation CT of ventilation/perfusion lung scans. Next, the results for the attenuation correction only and Ca-scoring CT of cardiac SPECT/CT examinations is discussed. Finally, CT organ doses and their correlations are studied for cervical and lumbar spine examinations with a diagnostic or localisation CT.

6.1 Ventilation/perfusion lung scan

The CT scan performed during a ventilation/perfusion lung SPECT/CT examination only serves attenuation correction and anatomical localisation purposes. The length of the CT scan corresponds with the SPECT field of the view. For a GE Discovery NM/CT 670 this examination is performed at a tube voltage of 100 kV. Monte Carlo simulations were performed for 30 patient models, 15 female and 15 male patients. A fixed tube current-time product of 100 mAs was applied.

6.1.1 Organ doses

Figure 35 shows the distribution of organ doses normalised to 100 mAs. As for whole-body PET/CT, the highest organ doses are found for the ribs and spine due to the higher attenuation coefficient of bone. In addition, here a wider spread in doses is observed for these structures. For soft tissues, organ doses are higher for the thyroid and breast because of their superficial position. The lowest dose is seen for the kidneys because they lie only partially in the field of view. Taking into account that these results are based on limited CT image data, doses of organs in the scan range are slightly underestimated while for organs lying more out the field of view the dose is somewhat overestimated (see chapter 4).

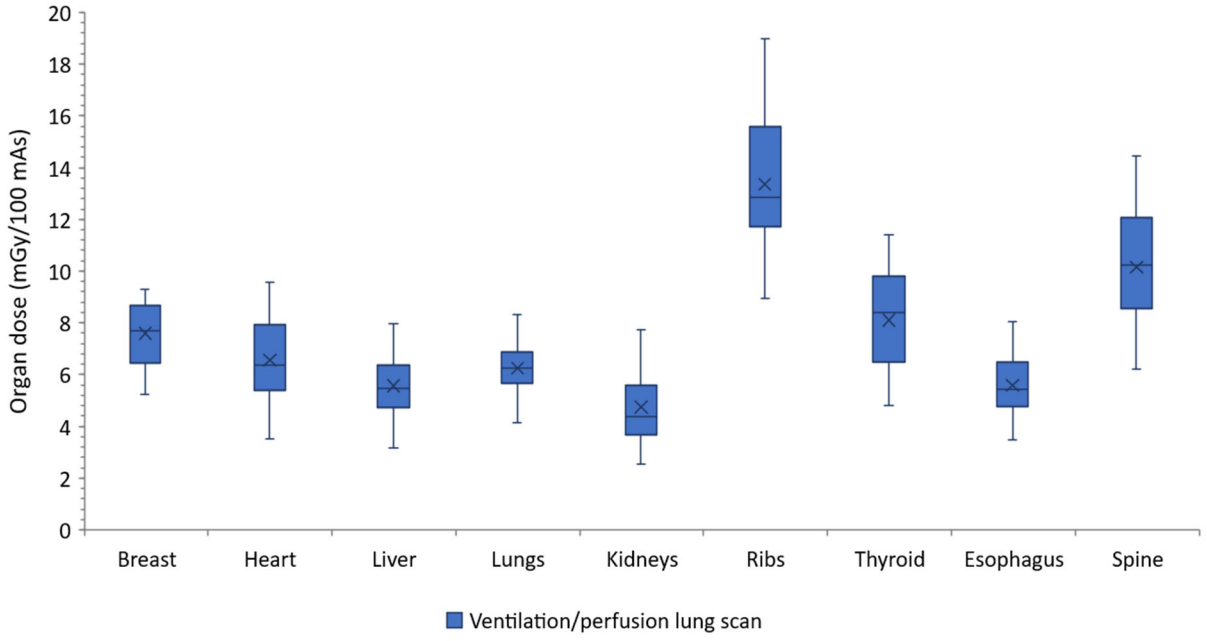

Figure 35: Distribution of the normalised organ doses for an attenuation correction and localisation CT at 100 kV with fixed tube current-time product as part of a ventilation/perfusion lung SPECT/CT examination on a GE Discovery NM/CT 670.

6.1.2 Correlation between organ doses and patient characteristics

As for CT scans as part of PET/CT examinations (section 5.2), the correlation between organ dose and the patient size metric water equivalent diameter was determined through regression analysis. The estimated regression function was of the exponential form as described by equation 9, with the water equivalent diameter (D_W) as independent variable and the organ dose as dependent variable. The water equivalent diameter was calculated as described by equation 7 considering the whole scan range.

The regression parameters a and b were estimated for each correlation between the Monte Carlo computed organ dose and patient-specific water equivalent diameter. The coefficient of determination, R^2, was used as a measure to assess the strength of correlation between organ dose and D_W.

Figure 36 displays estimated normalised organ doses as function of the water equivalent diameter (D_W) for the heart, lungs, kidneys and thyroid of an attenuation correction and localisation CT scan without tube current modulation at a GE Discovery NM/CT 670.

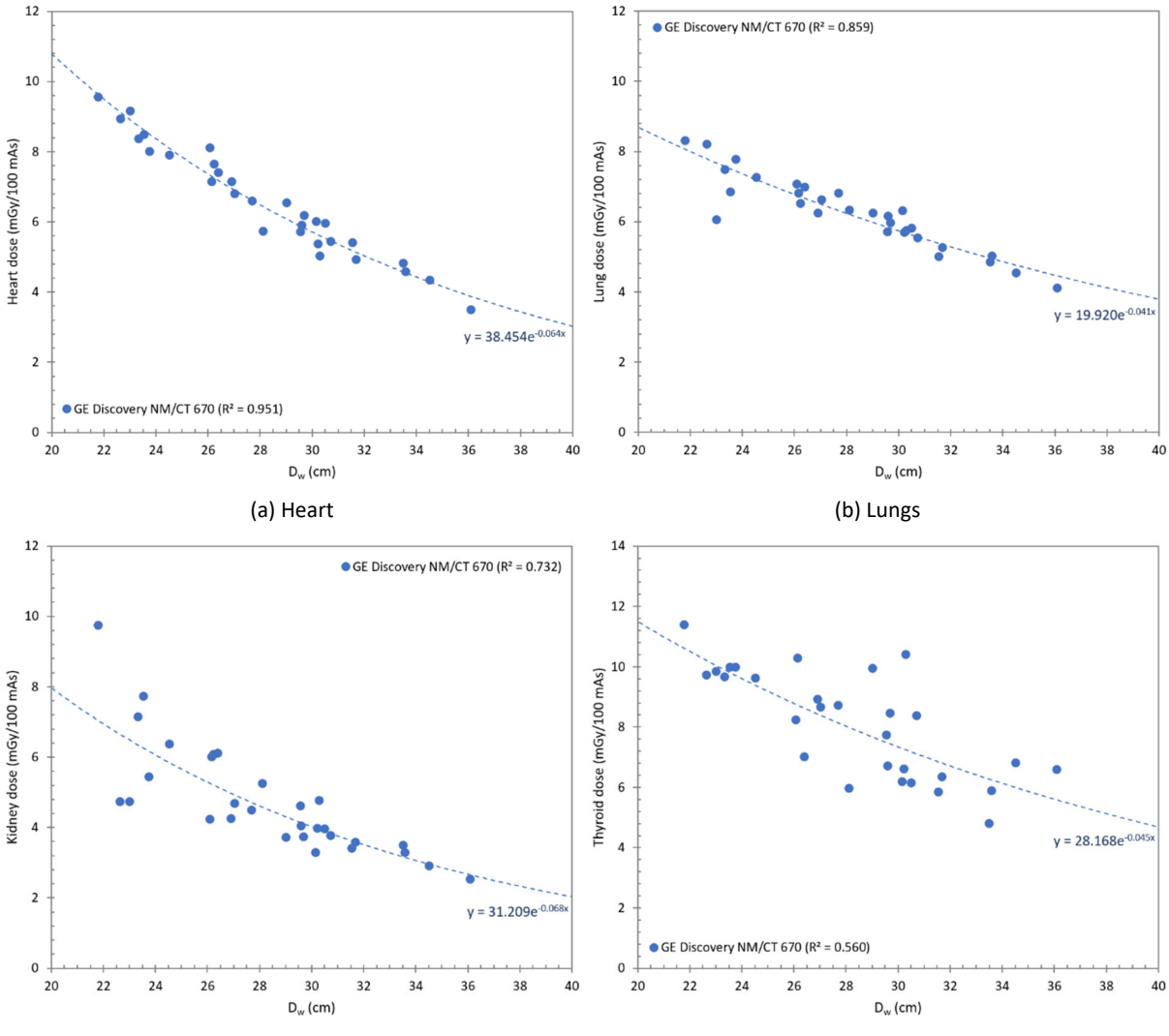

(a) Heart (b) Lungs

(c) Kidneys (d) Thyroid

Figure 36: Estimated normalised (a) heart, (b) lung, (c) kidney and (d) thyroid dose as a function of water equivalent diameter (D_W) for an attenuation correction and localisation CT scan at 100 kV with fixed tube current as part of a ventilation/perfusion SPECT/CT examination. Plot points are patient-specific organ doses for examinations on GE Discovery NM/CT 670 (circles). Associated exponential regression lines are visualised as a dashed line.

As can be seen, correlations are very strong for in-beam organs like the heart and lungs ($R^2 > 0.8$). For organs at the periphery of the scan range, a less strong correlation is found. Although the kidneys lie partially outside the scan range, the observed correlation is still strong ($R^2 \approx 0.73$). The superficial location, small size and the fact that the organ is located at the periphery of the scan range explains the moderate correlation for thyroid dose in comparison with other organs (Figure 36d).

The results of the regression analysis for breast, liver, rib, esophagus and spine dose are displayed in 'Appendix B – SPECT/CT organ dose correlations - Ventilation/perfusion lung scan'. Very strong correlations ($R^2 > 0.8$) were observed for all organs.

6.1.3 Correlation between organ dose and dose indicators

Regression analysis was also performed between organ dose and the size-specific dose estimate (SSDE) as described in section 5.3. The estimated normalised organ dose as a function of SSDE and associated linear regression functions (equation 10) are displayed in Figure 37 for the heart, lungs, kidneys and thyroid.

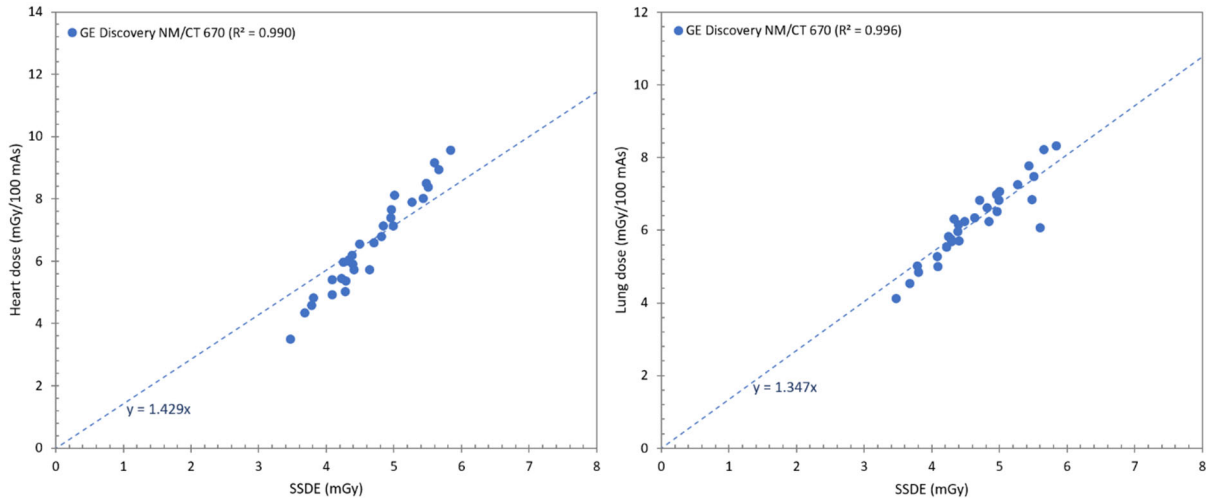

(a) Heart (b) Lungs

(c) Kidneys (d) Thyroid

Figure 37: Estimated normalised (a) heart, (b) lung, (c) kidney and (d) thyroid dose as a function of size-specific dose estimate (SSDE) for an attenuation correction and localisation CT scan at 100 kV with fixed tube current as part of a ventilation/perfusion SPECT/CT examination. Plot points are patient-specific organ doses for examinations on GE Discovery NM/CT 670 (circles). Associated linear regression lines are visualised as a dashed line.

For all organs, a very strong correlation ($R^2 > 0.98$) was found. The regression results of the breast, liver, rib, esophagus and spine dose are visualised in 'Appendix B – SPECT/CT organ dose correlations - Ventilation/perfusion lung scan'.

6.2 Cardiac SPECT/CT

Cardiac SPECT/CT examinations are composed of a rest and stress study performed mostly at two consecutive days. While the rest study is always performed with an attenuation correction (AC) only CT, the stress study may be a Calcium (Ca) scoring CT instead of a second AC CT. On a Siemens Symbia Intevo T16, both CT examinations are performed at a tube voltage of 130 kV. While the AC CT uses tube current modulation (reference tube current-time product of 18 mAs), a fixed tube current-time product of 75 mAs, smaller pitch and faster rotation time are applied for the Ca-scoring CT. Monte Carlo dose calculations of both CT examinations were performed for 32 patients, 17 female and 15 male patient models.

6.2.1 Organ doses

The distribution of organ doses normalised to 100 mAs for attenuation correction and Calcium scoring CT scans is visualised in Figure 38. As expected, organ doses are larger for a Ca-scoring CT. This is mainly because of the higher tube current. However, also the smaller pitch has an influence since the dose is inversely proportional to it. In terms of percentage difference, mean normalised organ doses are around 58% lower for the AC CT. Calculation of the absolute dose values even result in values that are around 91% lower for the attenuation correction CT than for the Ca-scoring CT.

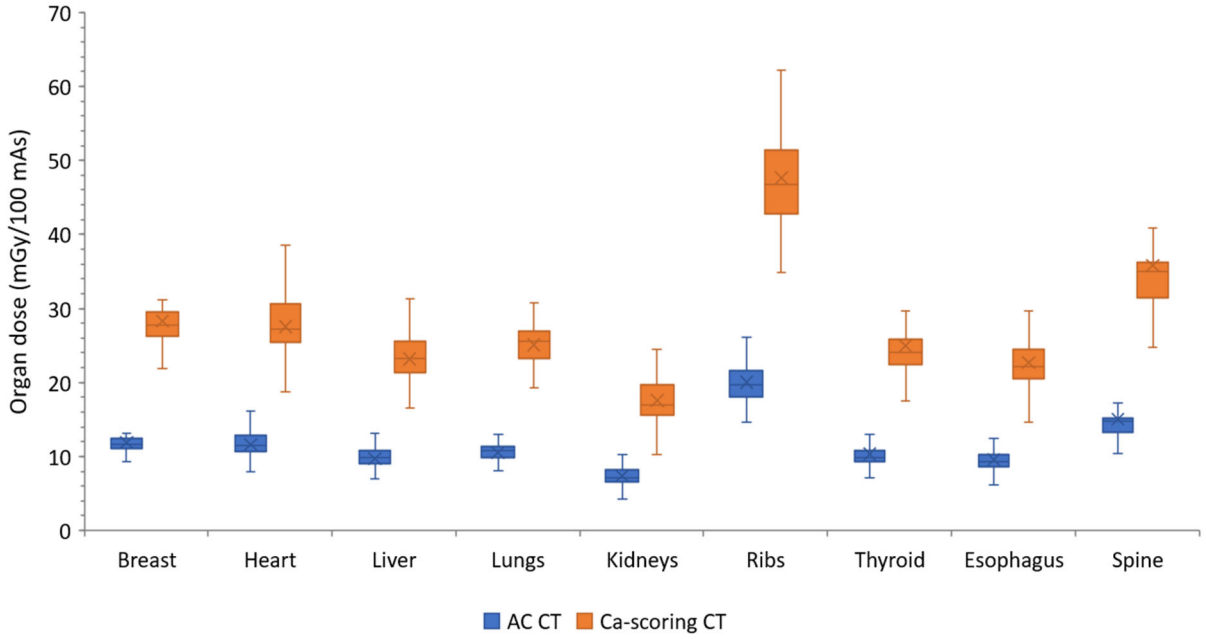

Figure 38: Distribution of the normalised organ doses for an attenuation correction (AC) and Calcium (Ca) scoring CT at 130 kV with and without tube current modulation, respectively, as part of a cardiac SPECT/CT examination on a Siemens Symbia Intevo T16.

As was the case in previous example, the highest organ doses are found for the ribs and bone due to their higher absorption coefficient . The lowest dose is again seen for the kidneys because they lie only partially in the field of view. Of course, these results are influenced by the limited CT image data. Doses

of organs in the scan range are slightly underestimated. However, this influence will be rather small for the AC CT because of the low tube current-time product that is used. For organs lying more out the field of view, the dose is slightly overestimated (see chapter 4).

The doses shown in Figure 38 are for a single CT examination, an attenuation correction or Ca-scoring CT. When calculating the organ doses of a patient undergoing a cardiac SPECT/CT examination two CT examinations need to be taken into account. This may be two attenuation correction CT scans or an attenuation correction and Ca-scoring CT.

6.2.2 Correlation between organ doses and patient characteristics

Figure 39 - 42 display estimated organ doses as a function of the water equivalent diameter (D_W) for the heart, lungs, spine and thyroid of attenuation correction and calcium (Ca) scoring CT scans with and without tube current modulation, respectively. For each organ, the water equivalent diameter was correlated to the estimated absolute dose values and to the dose values normalised to 100 mAs. The orange line corresponds to exponential regression (equation 9) associated with dose values of an attenuation correction CT while the dashed blue lines corresponds to Ca-scoring CT.

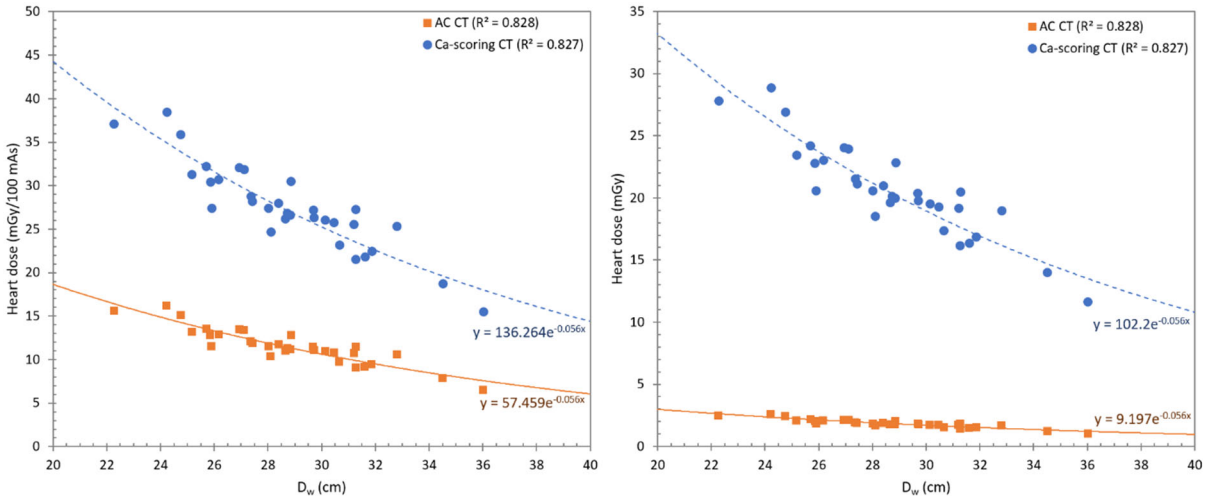

(a) Normalised dose (b) Absolute dose

Figure 39: Estimated (normalised) heart dose as a function of water equivalent diameter (D_W) for attenuation correction (AC) only and calcium (Ca) scoring CT scans at 130 kV with and without tube current modulation, respectively, as part of a cardiac SPECT/CT examination on a Siemens Symbia Intevo T16. Plot points are patient-specific organ doses for attenuation correction (squares) and Ca-scoring (circles) CT scans. Associated exponential regression lines are visualised as a full and dashed line, respectively.

As can be seen from Figure 39, the correlation between the heart dose and the water equivalent diameter is very strong ($R^2 > 0.8$) for both the normalised and absolute organ dose. This is also the case for the liver, kidneys, esophagus and breast. The resulting regression analyses can be found in 'Appendix B – SPECT/CT organ dose correlations - Cardiac SPECT/CT'. For the lungs, a weaker correlation is found (Figure 40). However, with an R^2 of 0.68 the observed correlation is still strong. On the other hand, the correlation of the dose with the water equivalent diameter is rather moderate for the spine (Figure 41) and ribs (Appendix B). For the thyroid, a weak correlation is found which can be explained by its superficial location, small size and the fact that the organ is located at the periphery of the scan range (Figure 42).

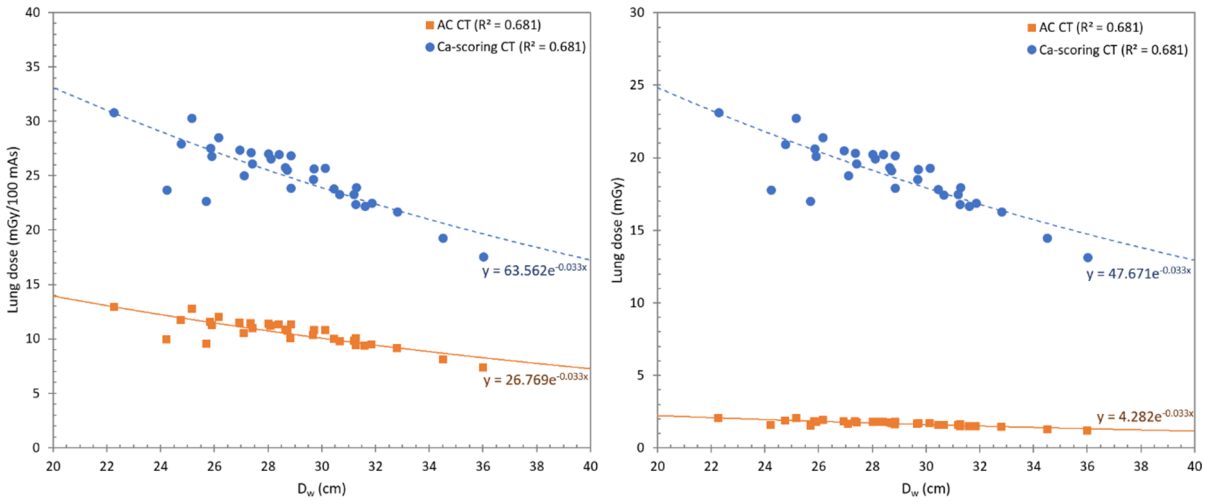

(a) Normalised dose (b) Absolute dose

Figure 40: Estimated (normalised) lung dose as a function of water equivalent diameter (D_W) for attenuation correction (AC) only and calcium (Ca) scoring CT scans at 130 kV with and without tube current modulation, respectively, as part of a cardiac SPECT/CT examination on a Siemens Symbia Intevo T16. Plot points are patient-specific organ doses for attenuation correction (squares) and Ca-scoring (circles) CT scans. Associated exponential regression lines are visualised as a full and dashed line, respectively.

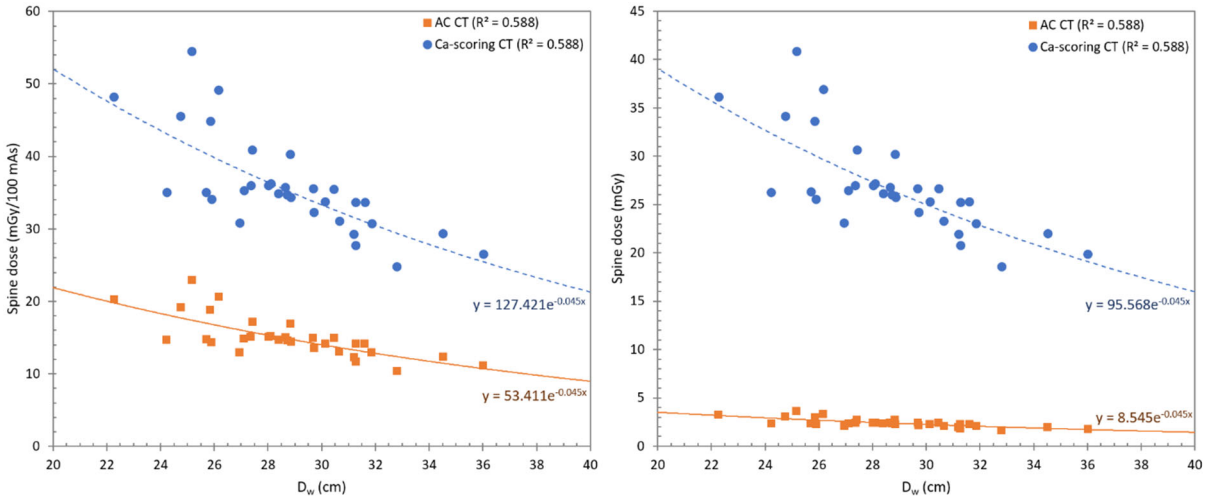

(a) Normalised dose (b) Absolute dose

Figure 41: Estimated (normalised) spine dose as a function of water equivalent diameter (D_W) for attenuation correction (AC) only and calcium (Ca) scoring CT scans at 130 kV with and without tube current modulation, respectively, as part of a cardiac SPECT/CT examination on a Siemens Symbia Intevo T16. Plot points are patient-specific organ doses for attenuation correction (squares) and Ca-scoring (circles) CT scans. Associated exponential regression lines are visualised as a full and dashed line, respectively.

Similar coefficients of determination are found for correlation of the normalised and absolute organ dose with the patient-specific water equivalent diameter. The lower organ doses for the attenuation correction CT found earlier when looking at the organ dose distributions (Figure 38Figure 22) are also reflected in these correlations.

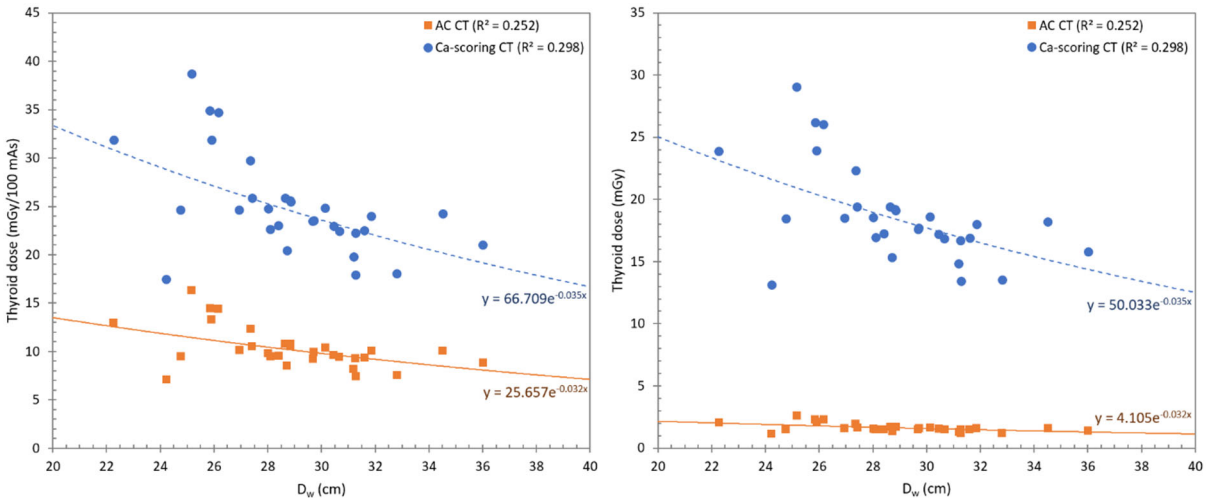

(a) Normalised dose (b) Absolute dose

Figure 42: Estimated (normalised) thyroid dose as a function of water equivalent diameter (D_W) for attenuation correction (AC) only and calcium (Ca) scoring CT scans at 130 kV with and without tube current modulation, respectively, as part of a cardiac SPECT/CT examination on a Siemens Symbia Intevo T16. Plot points are patient-specific organ doses for attenuation correction (squares) and Ca-scoring (circles) CT scans. Associated exponential regression lines are visualised as a full and dashed line, respectively.

6.2.3 Correlation between organ dose and dose indicators

Regression analysis for the heart, lung and thyroid dose as a function of size-specific dose estimate (SSDE) are shown in Figure 43, Figure 44 and Figure 45, respectively. For all organs, the regression was of the form $y = a \cdot x$ and the coefficient of determination (R^2) was larger than 0.97. There is thus a very strong correlation between the organ dose and size-specific dose estimate. This is seen for both the normalised and absolute dose. As was the case previously, the lower organ doses for the attenuation correction CT found earlier when looking at the organ dose distributions (Figure 38Figure 22) are also clearly reflected in the correlations of the organ doses. The regression analyses for the other organs can be found in 'Appendix B – SPECT/CT organ dose correlations - Cardiac SPECT/CT'.

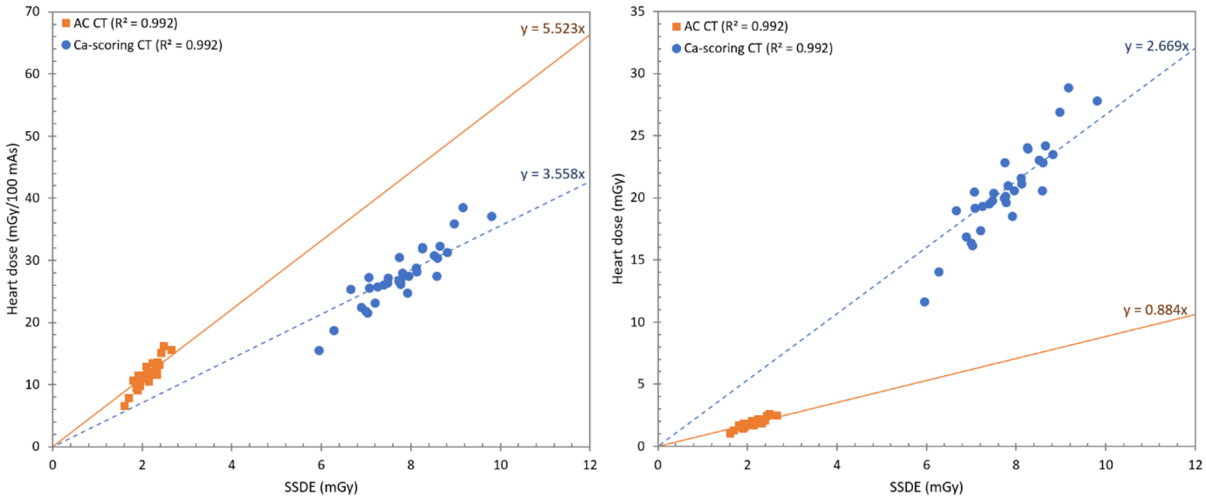

(a) Normalised dose (b) Absolute dose

Figure 43: Estimated (normalised) heart dose as a function of size-specific dose estimate (SSDE) for attenuation correction (AC) only and calcium (Ca) scoring CT scans at 130 kV with and without tube current modulation, respectively, as part of a cardiac SPECT/CT examination on a Siemens Symbia Intevo T16. Plot points are patient-specific organ doses for attenuation correction (squares) and Ca-scoring (circles) CT scans. Associated linear regression lines are visualised as a full and dashed line, respectively.

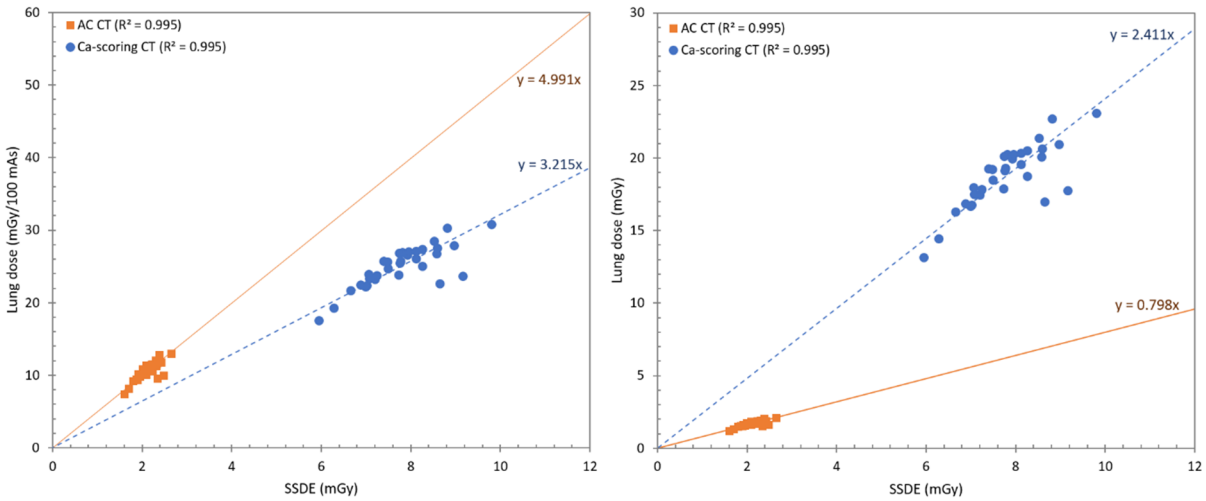

(a) Normalised dose (b) Absolute dose

Figure 44: Estimated (normalised) lung dose as a function of size-specific dose estimate (SSDE) for attenuation correction (AC) only and calcium (Ca) scoring CT scans at 130 kV with and without tube current modulation, respectively, as part of a cardiac SPECT/CT examination on a Siemens Symbia Intevo T16. Plot points are patient-specific organ doses for attenuation correction (squares) and Ca-scoring (circles) CT scans. Associated linear regression lines are visualised as a full and dashed line, respectively.

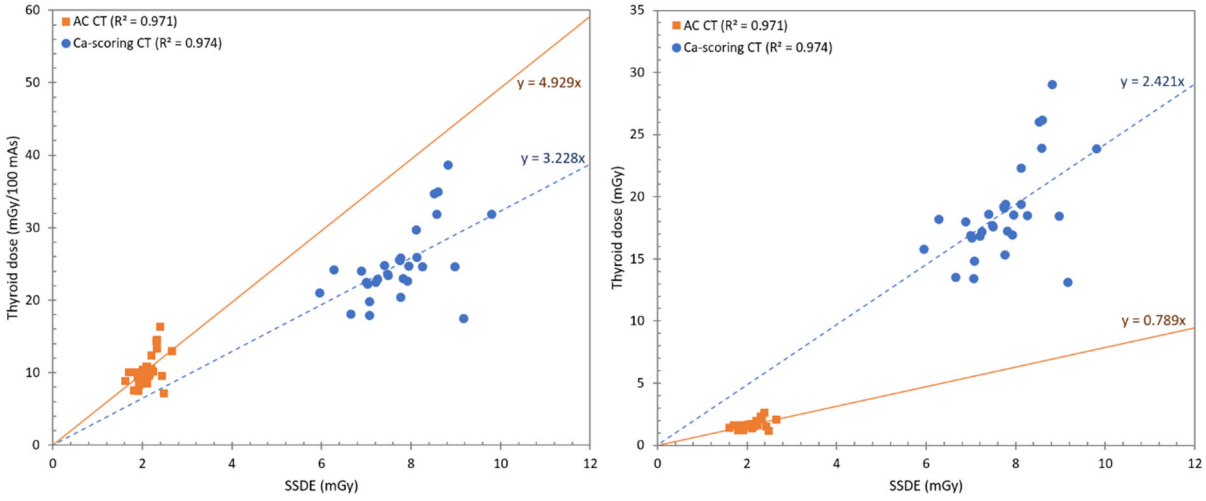

(a) Normalised dose (b) Absolute dose

Figure 45: Estimated (normalised) thyroid dose as a function of size-specific dose estimate (SSDE) for attenuation correction (AC) only and calcium (Ca) scoring CT scans at 130 kV with and without tube current modulation, respectively, as part of a cardiac SPECT/CT examination on a Siemens Symbia Intevo T16. Plot points are patient-specific organ doses for attenuation correction (squares) and Ca-scoring (circles) CT scans. Associated linear regression lines are visualised as a full and dashed line, respectively.

6.3 Cervical and lumbar spine SPECT/CT

Cervical and lumbar spine examinations are frequently performed SPECT/CT studies. Depending on the exact scan range, these studies may contain a part of the chest region. As for whole-body PET/CT examinations, cervical and lumbar spine SPECT/CT are performed with a diagnostic or localisation CT. Monte Carlo simulations of both a diagnostic and localisation CT were performed for 20 patients undergoing a CT scan of the cervical spine and for 20 patients undergoing a lumbar spine examination. This was done for similar protocols on a Siemens Symbia Intevo Bold and Siemens Symbia Intevo 6. All CT protocols use a tube voltage of 130 kV. For each SPECT/CT system, the scan parameters are the

same for a diagnostic CT scan of the cervical and lumbar spine. In clinical practice, a general protocol is used for localisation CT scans of the spine. Compared to the diagnostic CT a higher pitch and larger beam collimation is used for the localisation CT.

6.3.1 Organ doses

Figure 46 shows the distribution of organ doses normalised to 100 mAs for diagnostic and localisation CT scans of the cervical and lumbar spine aquired with a Siemens Symbia Intevo Bold and Intevo 6. As can be seen, there is no dose data available for the heart, liver and kidneys for a diagnostic CT of the cervical spine (Figure 46a). This is because neither of them are in the field of view of the diagnostic CT scan. The only dose contribution may come from scatter. However, these doses cannot be derived because the image data is limited to the diagnostic CT scan range. Due to the longer scan range of localisation CT scans of the cervical spine, organ doses are estimated for all organs of interest. This means that for the heart and the liver, respectively, all and almost all patients are included in the dose estimation. For the kidneys, the resulting mean organ dose is based on information of nine patients because no image data of the kidneys is included in the other patient models. For the breast, all ten female patients are now contributing to the dose distribution while there were only five patients for the diagnostic CT scan. Also diagnostic and localisation CT examinations of the lumbar spine differ in scan length. For both, the dose to the thyroid cannot be estimated because it lies far out of the field of view. The diagnostic CT doses shown in Figure 46b for the esophagus, heart, breast and lungs are based on 1, 2, 4 and 11 patient models, respectively while for the localisation CT, respectively, 14, 15, 6 and 17 patient models are included.

Independent of the CT protocol and hybrid imaging system used, the largest doses are found for the ribs and spine because of the higher attenuation coefficient of bone. For organs made up of soft tissue, superficial organs such as the thyroid and breast receive a higher dose.

As expected, organ doses are lower for localisation than for diagnostic CT scans. This is observed for both systems and is mainly caused by the larger pitch and resulting larger table feed of the localisation CT. For lumbar spine examinations, normalised mean organ doses are around 16% to 30% lower for the localisation CT at the Siemens Intevo Bold and around 57% to 64% lower for the localisation CT at the Siemens Intevo 6. For the cervical spine, decreases in normalised mean dose of around 4% to 35% and 45% to 68% are found for the localisation CT compared to the diagnostic CT on, respectively, the Siemens Intevo Bold and Intevo 6. The large variation in percentage dose difference between organs results from the difference in scan length of the localisation and diagnostic CT scan so that more or less of the organ volume is in the primary exposed volume.

Comparing the Siemens Symbia Intevo Bold with the Siemens Symbia Intevo 6 results in lower normalised mean organ doses for the localisation CT of the Intevo 6 SPECT/CT. Depending on the specific organ, normalised mean doses are around 31% to 42% lower. This may be induced by the applied pitch factor that is larger than one while all other scan parameters are practically the same. On the other hand, lower organ doses are observed for the diagnostic CT at the Siemens Intevo Bold. Normalised mean organ doses are around 22% to 32% higher at the Siemens Intevo 6. Because the Intevo 6 has a 6-slice CT instead of a 16-slice CT just as the Intevo Bold, different collimation settings are available. To achieve the same diagnostic CT quality, a smaller beam collimation was used for diagnostic CT scans of the cervical and lumbar spine at the Siemens Intevo 6 SPECT/CT. Due to similar pitch values this results in a smaller table increment and corresponding longer scan time. Because all other scan parameters are identical to those of the diagnostic CT at the Siemens Intevo Bold, the

smaller beam collimation may explain the larger organ doses found. Similar results are seen for cervical spine examinations as well as for studies of the lumbar spine.

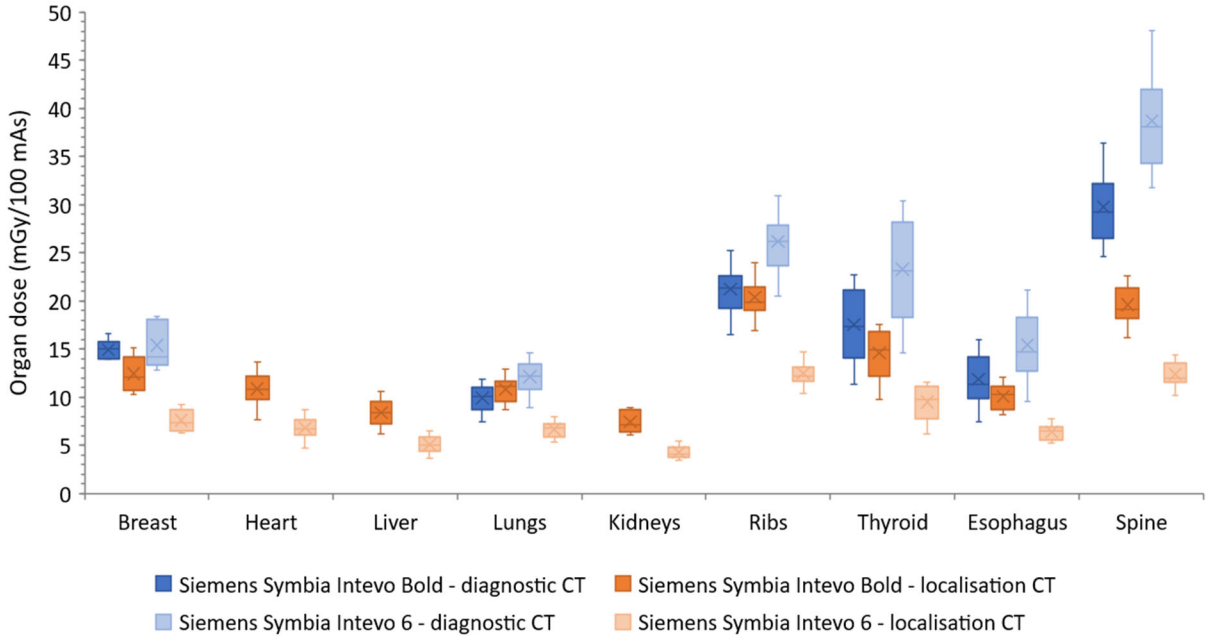

(a) Cervical spine SPECT/CT

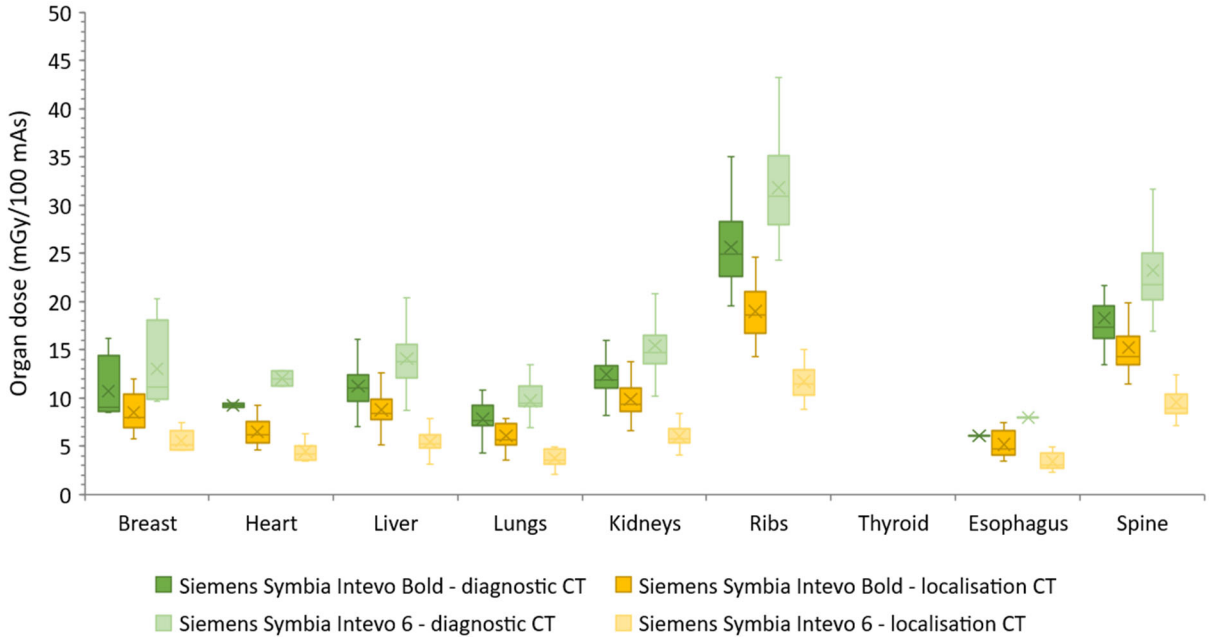

(b) Lumbar spine SPECT/CT

Figure 46: Distribution of the normalised organ doses for a diagnostic and localisation CT at 130 kV as part of a (a) cervical and (b) lumbar spine SPECT/CT examination on a Siemens Symbia Intevo Bold and Siemens Symbia Intevo 6.

6.3.2 Correlation between organ doses and patient characteristics

For both the cervical and lumbar spine SPECT/CT examinations, the correlation between organ dose and water equivalent diameter (D_W) was determined through regression analysis and an exponential relation was found as described by equation 9 (section 5.2). The coefficient of determination was used to assess the strength of the correlation.

Diagnostic or localisation CT of the cervical spine

Examples of regression analysis between organ dose and water equivalent diameter for cervical spine SPECT/CT studies are presented in Figure 47, Figure 48 and Figure 49 for the lungs, thyroid and spine, respectively. This is done for both the diagnostic and localisation CT scan. Because of the shorter scan length and the corresponding limited CT image data for diagnostic CT scans, no regression analysis could be performed for the heart, liver and kidney dose since they are located outside the field of view. For the localisation CT scans however, these organs could be included in the analysis as well. These graphs can be found in 'Appendix B – SPECT/CT organ dose correlations - Cervical and lumbar spine SPECT/CT'. For each organ, the water equivalent diameter was correlated to the estimated dose values normalised to 100 mAs. The orange line corresponds to regression associated with dose values computed using the Siemens Symbia Intevo Bold model while the dashed blue lines corresponds to the Siemens Symbia Intevo 6 model.

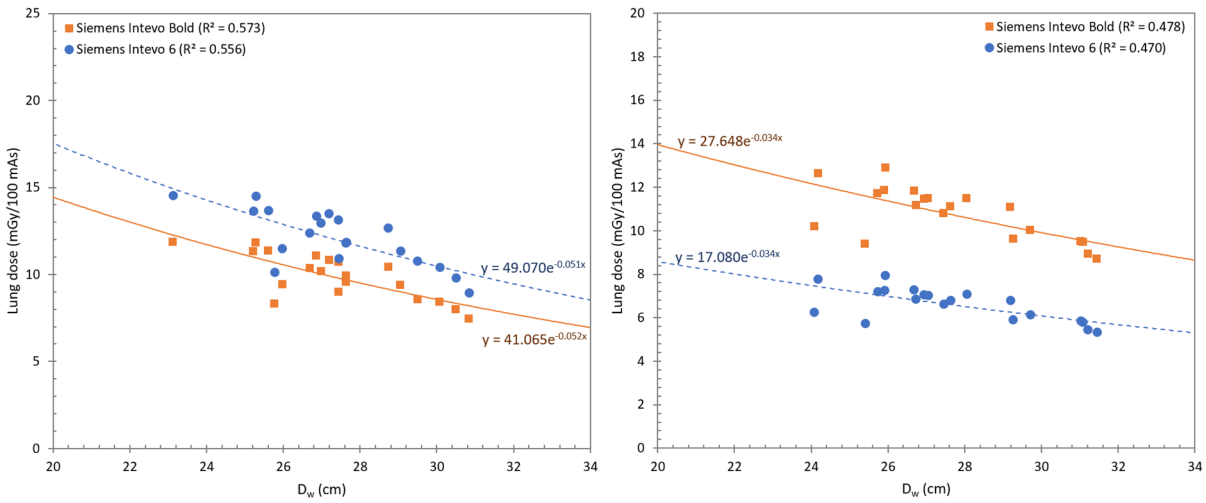

(a) Diagnostic CT (b) Localisation CT

Figure 47: Estimated normalised lung dose as a function of water equivalent diameter (D_w) for a (a) diagnostic and (b) localisation CT scan at 130 kV as part of a cervical spine SPECT/CT examination. Plot points are patient-specific organ doses for examinations on a Siemens Symbia Intevo Bold (squares) and Siemens Symbia Intevo 6 (circles). Associated exponential regression lines are visualised as a full and dashed line, respectively.

For all organs, similar strengths of correlation are found for both SPECT/CT systems. Next, a difference in correlation strength is found between the diagnostic CT scan and the localisation CT. Although the correlation for the lungs is moderate in both situations, the correlation is stronger for the diagnostic CT than for the localisation CT (Figure 47). For the thyroid and spine on the other hand, the correlation is weak ($R^2 \leq 0.4$) for the diagnostic CT while it is moderate to strong ($R^2 \approx 0.6$) for the localisation CT (Figure 48 and Figure 49). For the breast, heart, liver and esophagus, the correlation between the organ dose and water equivalent diameter is even strong ($R^2 \geq 0.7$) to very strong ($R^2 \geq 0.8$). This is explained by the contribution of more patient models to the analysis for the breast, heart and liver. For the esophagus, this may be because of the larger volume represented in the CT image data.

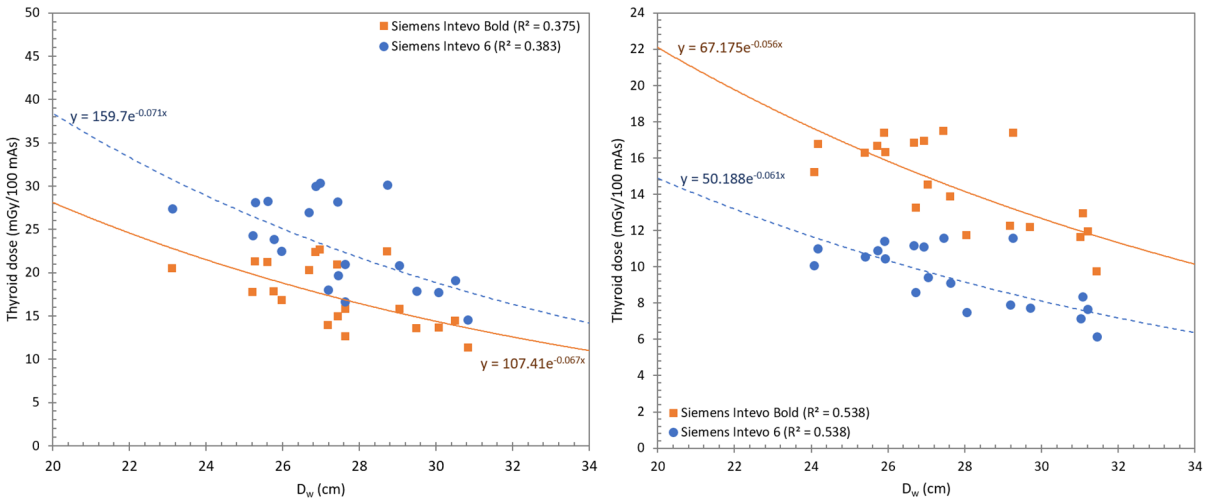

(a) Diagnostic CT (b) Localisation CT

Figure 48: Estimated normalised thyroid dose as a function of water equivalent diameter (D_w) for a (a) diagnostic and (b) localisation CT scan at 130 kV as part of a cervical spine SPECT/CT examination. Plot points are patient-specific organ doses for examinations on a Siemens Symbia Intevo Bold (squares) and Siemens Symbia Intevo 6 (circles). Associated exponential regression lines are visualised as a full and dashed line, respectively.

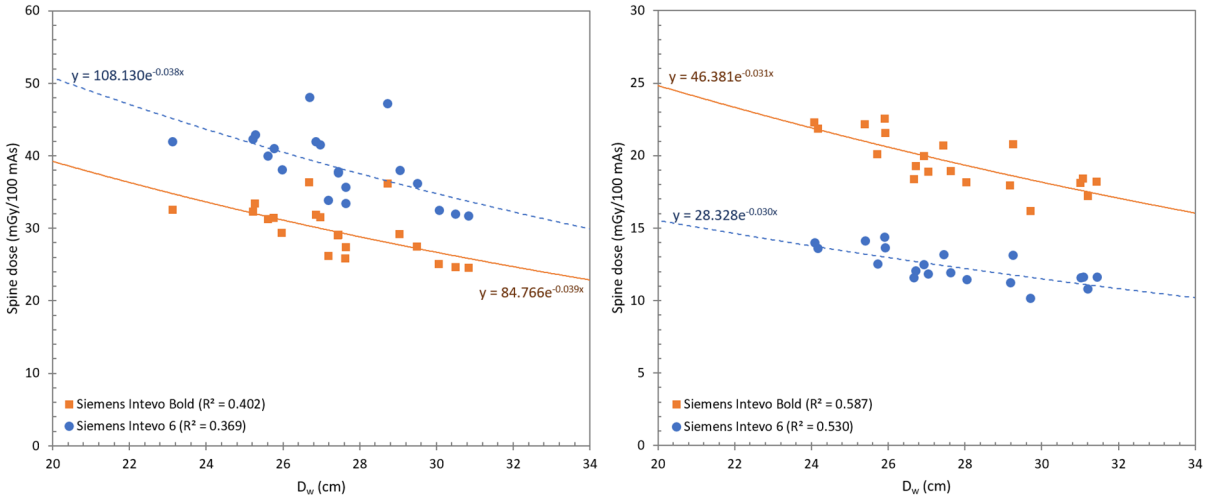

(a) Diagnostic CT (b) Localisation CT

Figure 49: Estimated normalised spine dose as a function of water equivalent diameter (D_w) for a (a) diagnostic and (b) localisation CT scan at 130 kV as part of a cervical spine SPECT/CT examination. Plot points are patient-specific organ doses for examinations on a Siemens Symbia Intevo Bold (squares) and Siemens Symbia Intevo 6 (circles). Associated exponential regression lines are visualised as a full and dashed line, respectively.

Diagnostic or localisation CT of the lumbar spine

The same was done for the diagnostic and localisation CT scan of lumbar spine SPECT/CT examinations. Again, similar correlation strengths were found for both systems. No regression analysis could be performed for the thyroid, esophagus, heart and breast dose of a diagnostic CT scan. The first, because the thyroid is located far outside the field of view which is also the case for the localisation CT. For the other three organs, this is due to the small number of patient models contributing to the analysis, ranging from one to four.

Figure 50 - 52 display estimated normalised organ doses as a function of water equivalent diameter for the lungs, kidneys and spine. For the lungs, the correlation is, although still moderate, stronger for

the diagnostic CT than for the localisation CT (Figure 50). The kidney and spine dose on the other hand correlate strong ($R^2 \geq 0.7$) with the patient-specific water equivalent diameter. This is explained by the fact that the kidneys and spine are in the field of view while the lungs are located in the periphery.

For the other organs, correlations are similar or stronger for the localisation CT than for the diagnostic CT. As for the kidneys and spine, a strong correlation is found for the breast, heart and liver dose of a diagnostic CT examination. A weak correlation is seen for the esophagus dose resulting from the location of the organ on the periphery of the scan range. These graphs are presented in 'Appendix B – SPECT/CT organ dose correlations - Cervical and lumbar spine SPECT/CT'.

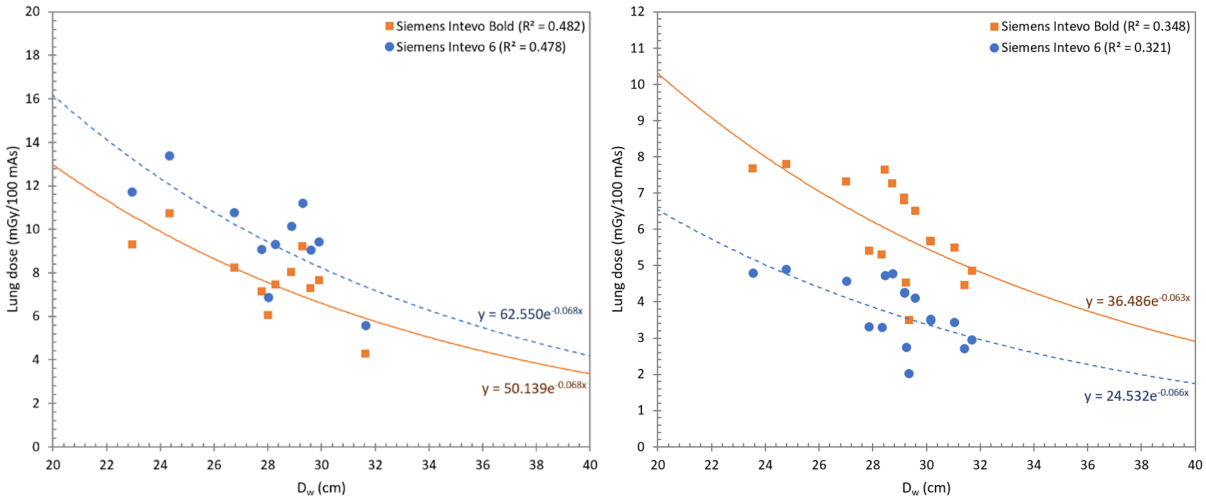

(a) Diagnostic CT (b) Localisation CT

Figure 50: Estimated normalised lung dose as a function of water equivalent diameter (D_w) for a (a) diagnostic and (b) localisation CT scan at 130 kV as part of a lumbar spine SPECT/CT examination. Plot points are patient-specific organ doses for examinations on a Siemens Symbia Intevo Bold (squares) and Siemens Symbia Intevo 6 (circles). Associated exponential regression lines are visualised as a full and dashed line, respectively.

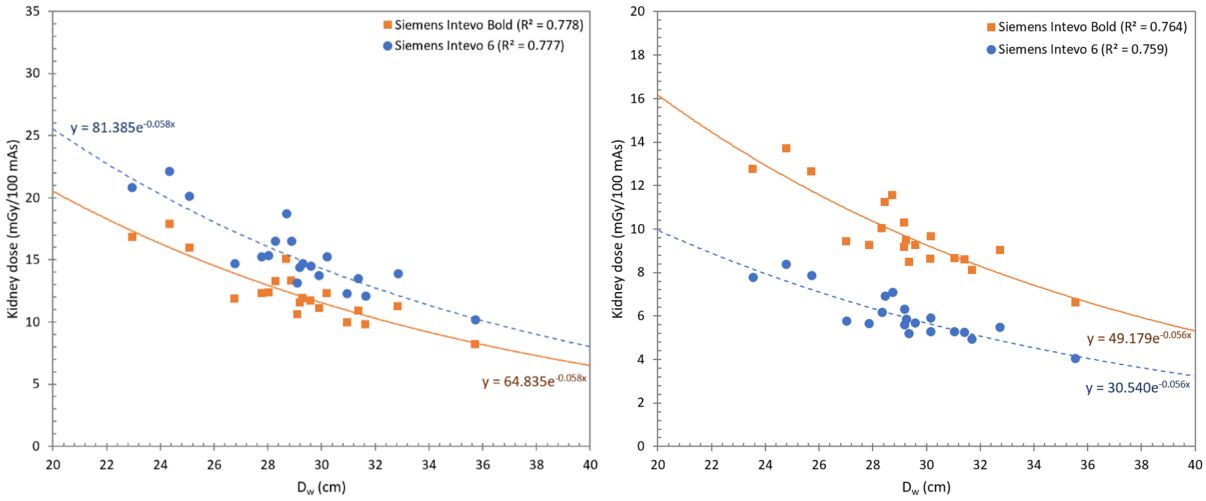

(a) Diagnostic CT (b) Localisation CT

Figure 51: Estimated normalised kidney dose as a function of water equivalent diameter (D_w) for a (a) diagnostic and (b) localisation CT scan at 130 kV as part of a lumbar spine SPECT/CT examination. Plot points are patient-specific organ doses for examinations on a Siemens Symbia Intevo Bold (squares) and Siemens Symbia Intevo 6 (circles). Associated exponential regression lines are visualised as a full and dashed line, respectively.

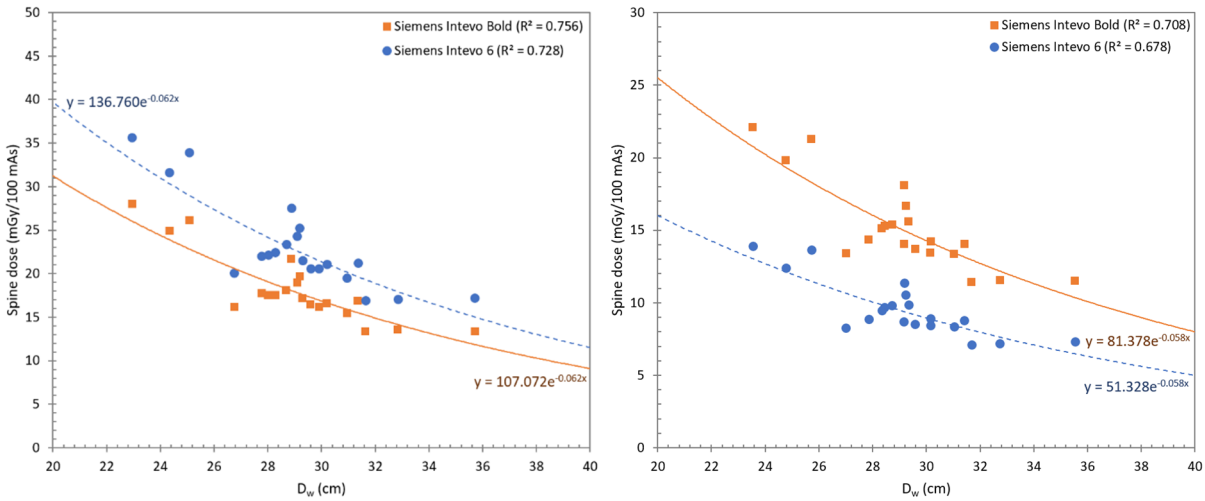

(a) Diagnostic CT (b) Localisation CT

Figure 52: Estimated normalised spine dose as a function of water equivalent diameter (D_w) for a (a) diagnostic and (b) localisation CT scan at 130 kV as part of a lumbar spine SPECT/CT examination. Plot points are patient-specific organ doses for examinations on a Siemens Symbia Intevo Bold (squares) and Siemens Symbia Intevo 6 (circles). Associated exponential regression lines are visualised as a full and dashed line, respectively.

6.3.3 Correlation between organ dose and dose indicators

At last, the correlation between organ dose and size-specific dose estimate (SSDE) was studied. This was done for both SPECT/CT systems and for the diagnostic and localisation CT scans of the cervical and lumbar spine. Examples of the resulting linear regression fits and their coefficients of determination are displayed in Figure 53 - 55 for the cervical spine and in Figure 56 - 57 for the lumbar spine. In all cases, a very strong correlation was found ($R^2 > 0.96$). The regression curves for the other organs are found in 'Appendix B – SPECT/CT organ dose correlations - Cervical and lumbar spine SPECT/CT'.

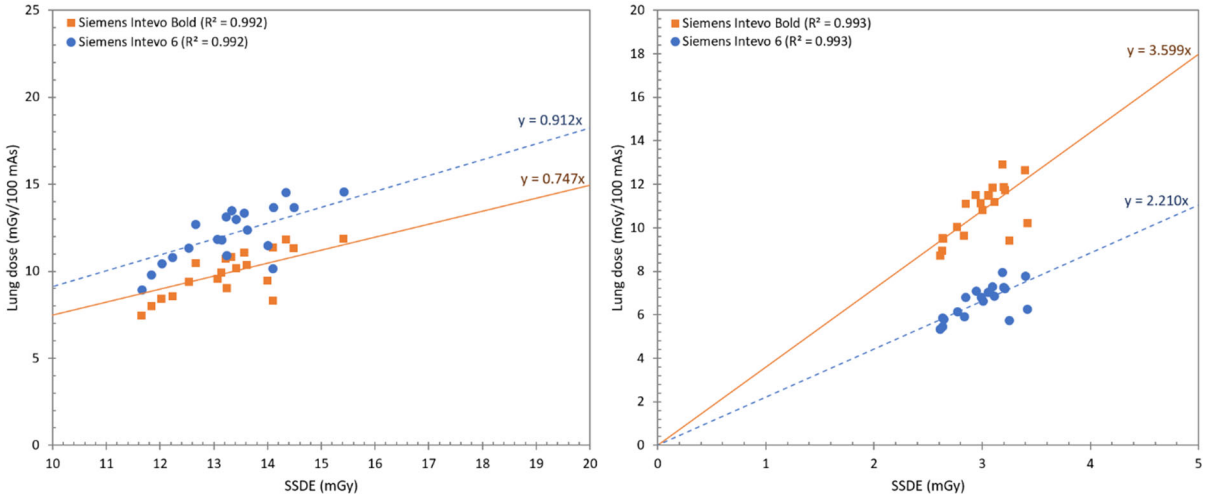

(a) Diagnostic CT (b) Localisation CT

Figure 53: Estimated normalised lung dose as a function of size-specific dose estimate (SSDE) for a (a) diagnostic and (b) localisation CT scan at 130 kV as part of a cervical spine SPECT/CT examination. Plot points are patient-specific organ doses for examinations on a Siemens Symbia Intevo Bold (squares) and Siemens Symbia Intevo 6 (circles). Associated linear regression lines are visualised as a full and dashed line, respectively.

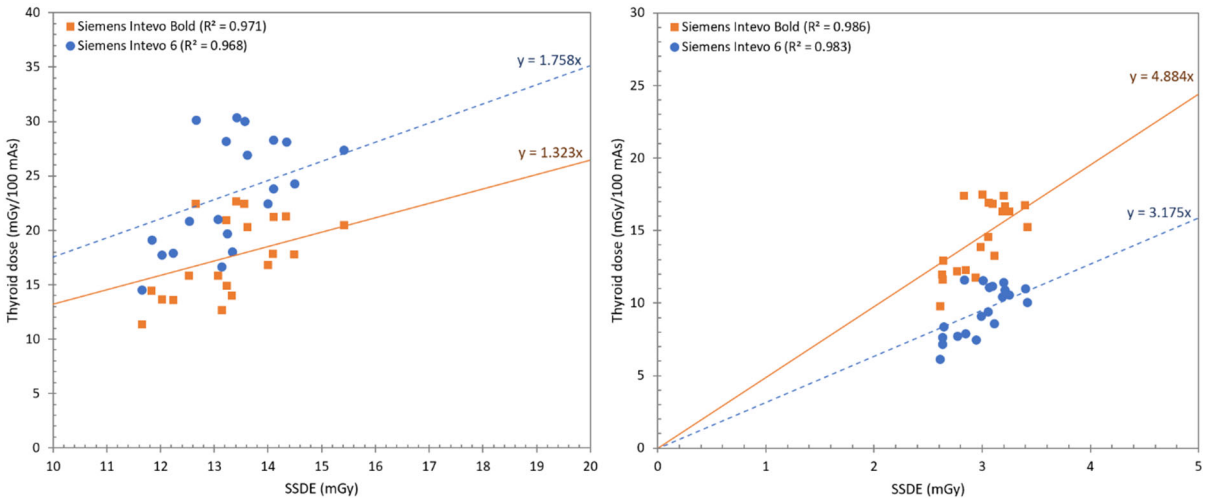

(a) Diagnostic CT (b) Localisation CT

Figure 54: Estimated normalised thyroid dose as a function of size-specific dose estimate (SSDE) for a (a) diagnostic and (b) localisation CT scan at 130 kV as part of a cervical spine SPECT/CT examination. Plot points are patient-specific organ doses for examinations on a Siemens Symbia Intevo Bold (squares) and Siemens Symbia Intevo 6 (circles). Associated linear regression lines are visualised as a full and dashed line, respectively.

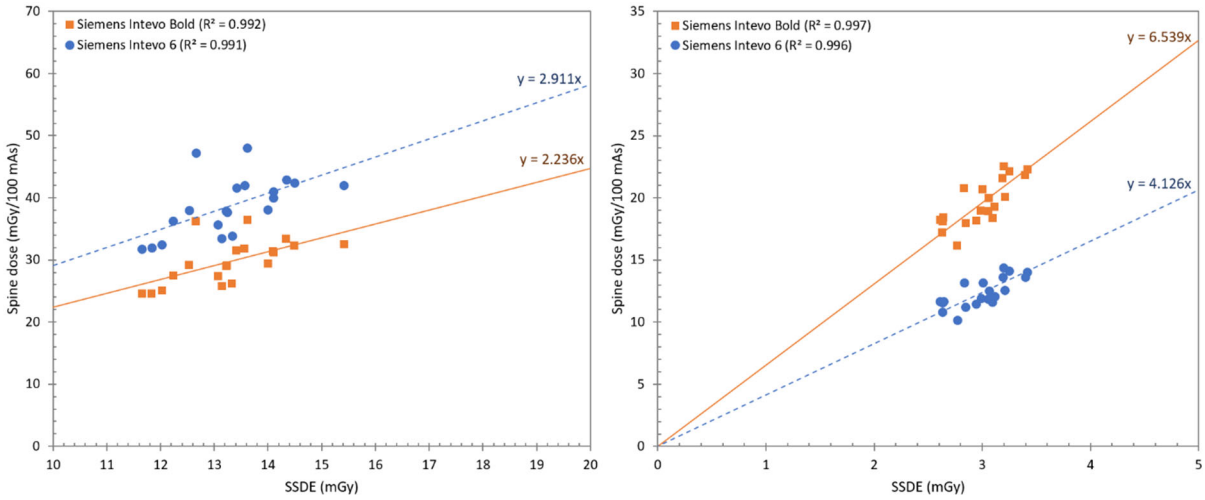

(a) Diagnostic CT (b) Localisation CT

Figure 55: Estimated normalised spine dose as a function of size-specific dose estimate (SSDE) for a (a) diagnostic and (b) localisation CT scan at 130 kV as part of a cervical spine SPECT/CT examination. Plot points are patient-specific organ doses for examinations on a Siemens Symbia Intevo Bold (squares) and Siemens Symbia Intevo 6 (circles). Associated linear regression lines are visualised as a full and dashed line, respectively.

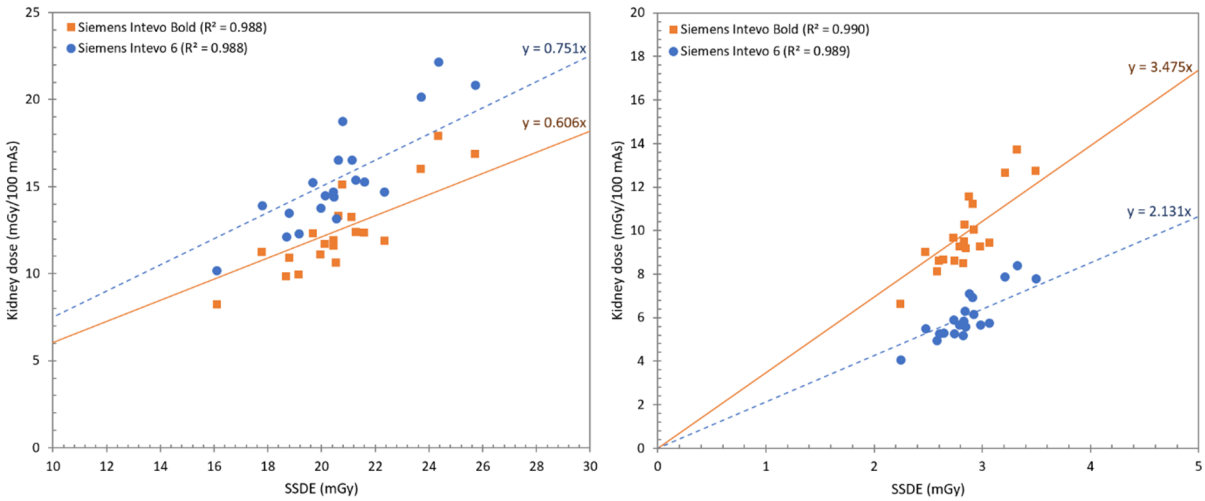

(a) Diagnostic CT (b) Localisation CT

Figure 56: Estimated normalised kidney dose as a function of size-specific dose estimate (SSDE) for a (a) diagnostic and (b) localisation CT scan at 130 kV as part of a lumbar spine SPECT/CT examination. Plot points are patient-specific organ doses for examinations on a Siemens Symbia Intevo Bold (squares) and Siemens Symbia Intevo 6 (circles). Associated linear regression lines are visualised as a full and dashed line, respectively.

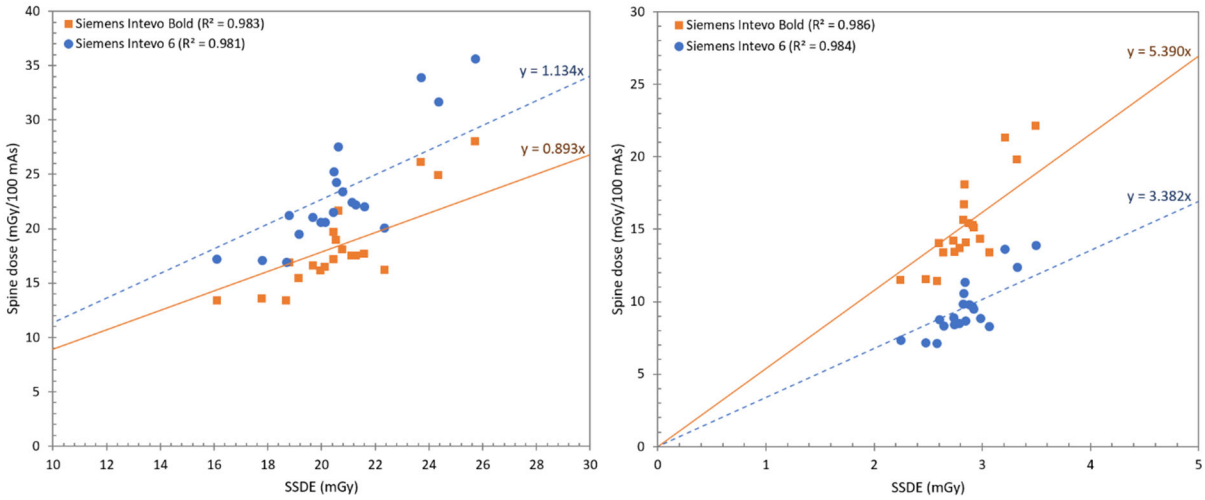

(a) Diagnostic CT (b) Localisation CT

Figure 57: Estimated normalised spine dose as a function of size-specific dose estimate (SSDE) for a (a) diagnostic and (b) localisation CT scan at 130 kV as part of a lumbar spine SPECT/CT examination. Plot points are patient-specific organ doses for examinations on a Siemens Symbia Intevo Bold (squares) and Siemens Symbia Intevo 6 (circles). Associated linear regression lines are visualised as a full and dashed line, respectively.

7 Conclusion

Today, Monte Carlo methods are the golden standard to perform patient-specific dosimetry because they allow both an accurate description of the X-ray modalities and the implementation of anatomical models. The method used in this study combines Monte Carlo computational techniques with patient CT scans. To estimate absorbed doses to irradiated organs and tissues accurately, the reconstructed field of view of the CT scans must include the entire cross-section of the patient. Suitable patient CT scans were collected for whole-body PET/CT, ventilation/perfusion lung SPECT/CT, cardiac SPECT/CT and cervical and lumbar spine SPECT/CT examinations in nuclear medicine. These CT images were then used as input volume for patient-specific dose simulations. Next, each CT scanner had to be characterised which includes information on the geometric, spectral and shaped filter characteristics. For each CT examination, where applicable, tube current modulation was considered in the simulation as well. In order to calculate organ doses, organ structures were segmented with image analysis software using (semi-)automated and freehand techniques.

Several methodologies exist to determine X-ray beam spectra and model the shaped filter of a CT scanner. To obtain the best results, quantitative spectral information and information on the bowtie filter material and shape is provided by the manufacturer. However, manufacturer's data is not always available. Artificial X-ray beam spectra can be created with the help of spectrum generators such as SpekCalc. Therefore, information on the anode angle and amount of filtration (materials and thicknesses) is needed. If this information is not known, the methodology as described by Turner *et al.* [16] for equivalent energy spectra in CT can be used which only requires physical half-value layer measurements. The bowtie filter on the other hand can also be characterised based on measured dose values. All of this may have an influence on the estimated organ doses resulting from the Monte Carlo dose computations. From this study follows that the impact of X-ray spectra determination and bowtie filter modelling is rather small. Modelling the bowtie filter based on dose measurements leads to CT organ doses that are maximum 1% higher, independent of the X-ray spectrum determination method. For all X-ray spectrum determination methods used, organ doses are within 6% from those resulting from simulations with the spectrum provided by the manufacturer. Half-value layer and dose measurements are thus good alternative methods to obtain equivalent X-ray spectra and bowtie filter profiles, respectively, when no data from the manufacturer is available.

In conventional CT, the available image data are limited to the patient's scan range, and no information exists regarding the rest of the body. The same limitation occurs in SPECT/CT imaging where the scan range of the CT examination is limited to the field of view of the SPECT exam or shorter depending on the clinical indication. This influences the accurate incorporation of scatter in the dose calculation and the calculation of organ doses out of the field of view. Having whole-body patient CT images from whole-body PET/CT examinations available has the potential to study this influence. From this study follows that limitation of the patient model to the scan range results in a small underestimation of the absorbed dose for organs located in the field of view of the CT scan because scatter from the rest of the body is excluded. For organs located at the periphery or outside the field of view, organ doses are overestimated. This overestimation is rather small for organs located almost completely in the scan range. A larger dose overestimation is found for organs that in percentage terms lie more out of the field of view than within because the entire organ volume cannot be taken into account in the dose calculation.

The derived absolute and normalised organ doses were correlated with the patient-specific water equivalent diameter, which is a size-specific metric. Therefore, exponential regression analysis was applied. For diagnostic CT scans with tube current modulation as part of whole-body PET/CT examinations, normalised organ dose correlations range from weak ($R^2 < 0.4$) to strong ($R^2 = 0.6 - 0.75$)

while stronger correlations are found when looking to the absolute organ doses. Moderate ($R^2 \approx 0.6$) to very strong ($R^2 > 0.8$) correlations between organ dose and water equivalent diameter are seen when a fixed tube current is used instead. For the localisation CT of a whole-body PET/CT study strong ($R^2 = 0.6 - 0.8$) to very strong ($R^2 > 0.8$) correlations are found for all organs except the thyroid. The latter may be explained by its superficial location and small size. For most of the organs, good correlations with the water equivalent diameter are also found for ventilation/perfusion lung and cardiac SPECT/CT studies ($R^2 > 0.7$). The weaker correlation for the thyroid dose may again be explained by the superficial location and small size of the organ. For cervical and lumbar spine SPECT/CT examinations, correlations are good ($R^2 > 0.7$) for organs in the field of view. Organs located at the periphery of the scan range show weaker correlations between organ dose and water equivalent diameter.

Finally, the derived absolute and normalised organ doses were correlated with the size-specific dose estimate using linear regression analysis. This metric takes into account both the size of the patient and the CT dose parameter $CTDI_{vol}$. For all organs and all CT examinations studied, very good correlations are found between (normalised) organ dose and size-specific dose estimate ($R^2 > 0.8$ for PET/CT studies and $R^2 > 0.95$ for SPECT/CT studies).

The proposed method has thus several advantages. First, patient models are used instead of phantoms resulting into patient-specific organ dosimetry. Secondly, the method of X-ray beam determination and bowtie filter modelling in order to characterise the CT scanner has only a small influence on the estimated organ doses. Next, good correlations between normalised organ dose and water equivalent diameter are found for organs in the field of view of SPECT/CT examinations and for whole-body PET/CT examinations with fixed tube current. Finally, very good correlations are found between organ dose and size-specific dose estimate.

8 References

1. Lee, T.C., et al., *Morphology supporting function: attenuation correction for SPECT/CT, PET/CT, and PET/MR imaging.* Quarterly Journal of Nuclear Medicine and Molecular Imaging, 2016. **60**(1): p. 25-39.
2. Bockisch, A., et al., *Hybrid Imaging by SPECT/CT and PET/CT: Proven Outcomes in Cancer Imaging.* Seminars in Nuclear Medicine, 2009. **39**(4): p. 276-289.
3. Tonkopi, E. and A.A. Ross, *Assessment of Effective Dose from Cone Beam Ct Imaging in Spect/Ct Examination in Comparison with Other Modalities.* Radiation Protection Dosimetry, 2016. **172**(4): p. 438-442.
4. Salvatori, M., et al., *Radiation dose in nuclear medicine: the hybrid imaging.* La Radiologia medica, 2019.
5. Etard, C., et al., *National survey of patient doses from whole-body FDG PET-CT examinations in France in 2011.* Radiation Protection Dosimetry, 2012. **152**(4): p. 334-338.
6. Avramova-Cholakova, S., et al., *Patient Doses from Pet-Ct Procedures.* Radiation Protection Dosimetry, 2015. **165**(1-4): p. 430-433.
7. Brix, G., et al., *Radiation exposure of patients undergoing whole-body dual-modality 18F-FDG PET/CT examinations.* Journal of nuclear medicine : official publication, Society of Nuclear Medicine, 2005. **46**(4): p. 608-13.
8. Iball, G.R., et al., *A national survey of computed tomography doses in hybrid PET-CT and SPECT-CT examinations in the UK.* Nuclear Medicine Communications, 2017. **38**(6): p. 459-470.
9. Tonkopi, E., A.A. Ross, and A. MacDonald, *JOURNAL CLUB: CT Dose Optimization for Whole-Body PET/CT Examinations.* American Journal of Roentgenology, 2013. **201**(2): p. 257-263.
10. Myronakis, M., J. Stratakis, and J. Damilakis, *Deliverable D2.14: Report on a) the organ dose data representation and b) collected organ doses*. 2020.
11. Chen, W., et al., *Fast on-site Monte Carlo tool for dose calculations in CT applications.* Medical Physics, 2012. **39**(6): p. 2985-2996.
12. Deak, P., et al., *Validation of a Monte Carlo tool for patient-specific dose simulations in multi-slice computed tomography.* European Radiology, 2008. **18**(4): p. 759-772.
13. Schmidt, B. and W.A. Kalender, *A fast voxel-based Monte Carlo method for scanner- and patient-specific dose calculations in computed tomography.* Physica Medica-European Journal of Medical Physics, 2002. **18**(2): p. 43-53.
14. Tucker, D.M., G.T. Barnes, and D.P. Chakraborty, *Semiempirical model for generating tungsten target x-ray spectra.* Medical physics, 1991. **18**(2): p. 211-8.
15. Poludniowski, G., et al., *SpekCalc: a program to calculate photon spectra from tungsten anode x-ray tubes.* Physics in Medicine and Biology, 2009. **54**(19): p. N433-N438.
16. Turner, A.C., et al., *A method to generate equivalent energy spectra and filtration models based on measurement for multidetector CT Monte Carlo dosimetry simulations.* Medical physics, 2009. **36**(6): p. 2154-64.
17. Siewerdsen, J.H., et al., *Spektr: a computational tool for x-ray spectral analysis and imaging system optimization.* Medical physics, 2004. **31**(11): p. 3057-67.
18. AAPM, *Size-Specific Dose Estimates (SSDE) in pediatric and adult body ct examinations (Task Group 204)*. 2011, American Association of Physicists in Medicine.
19. AAPM, *Use of water equivalent diameter for calculating patient size and Size-Specific Dose Estimate (SSDE) in CT (Task Group 220)*. 2014, American Association of Physicists in Medicine.
20. Yang, K., et al., *Direct and fast measurement of CT beam filter profiles with simultaneous geometrical calibration.* Medical Physics, 2017. **44**(1): p. 57-70.

9 Appendix A – Whole-body PET/CT organ dose correlations

This appendix lists the regression analyses that are not presented in Chapter 5 - CT organ doses in PET/CT. In the first part, the correlation between the organ dose and water equivalent diameter or size-specific dose estimate can be found for a diagnostic CT scan with tube current modulation. Secondly, the results for a diagnostic CT with fixed tube current are presented. At last, the results for the localisation CT with fixed tube current are shown.

9.1 Diagnostic CT with automatic tube current modulation

A. Correlation between organ doses and water equivalent diameter

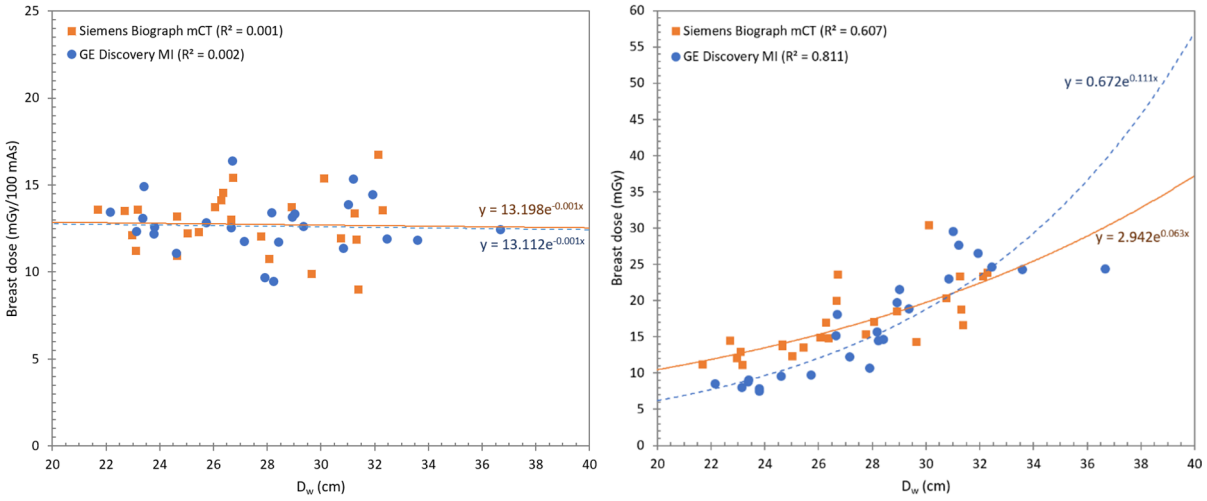

(a) Normalised dose (b) Absolute dose

Figure 58: Estimated (normalised) breast dose as a function of water equivalent diameter (D_w) for a diagnostic CT scan at 120 kV with tube current modulation as part of a whole-body PET/CT examination. Plot points are patient-specific organ doses for examinations on a Siemens Biograph mCT Flow (circles) and GE Discovery MI (squares). Associated exponential regression lines are visualised as a full and dashed line, respectively.

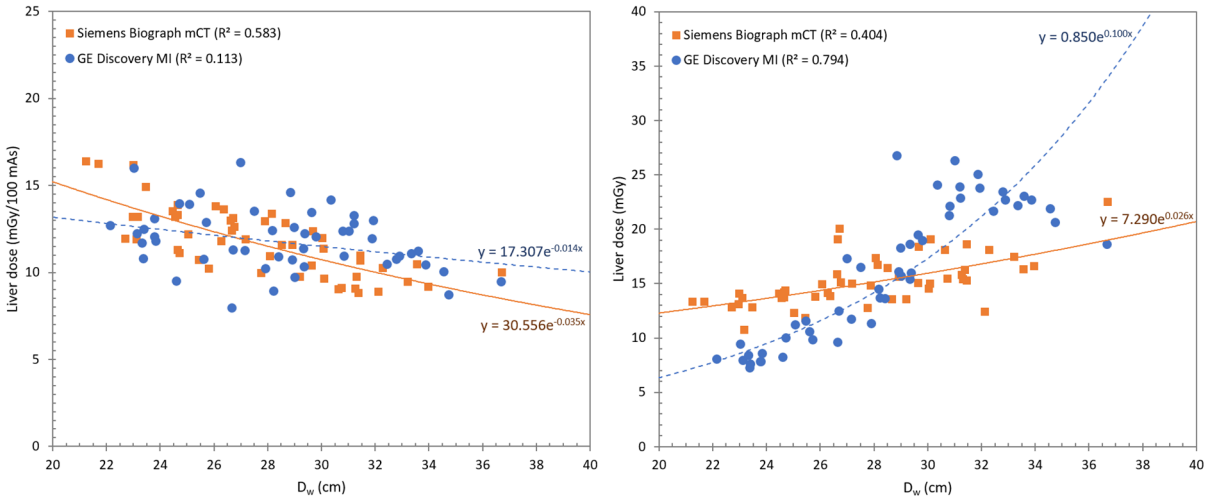

(a) Normalised dose (b) Absolute dose

Figure 59: Estimated (normalised) liver dose as a function of water equivalent diameter (D_w) for a diagnostic CT scan at 120 kV with tube current modulation as part of a whole-body PET/CT examination. Plot points are patient-specific organ doses for examinations on a Siemens Biograph mCT Flow (circles) and GE Discovery MI (squares). Associated exponential regression lines are visualised as a full and dashed line, respectively.

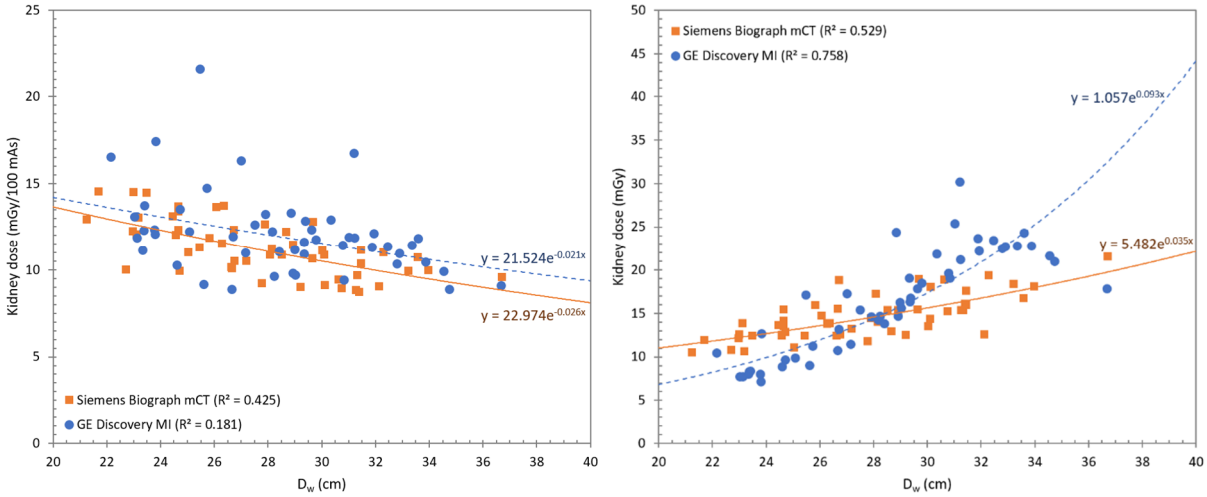

(a) Normalised dose (b) Absolute dose

Figure 60: Estimated (normalised) kidney dose as a function of water equivalent diameter (D_w) for a diagnostic CT scan at 120 kV with tube current modulation as part of a whole-body PET/CT examination. Plot points are patient-specific organ doses for examinations on a Siemens Biograph mCT Flow (circles) and GE Discovery MI (squares). Associated exponential regression lines are visualised as a full and dashed line, respectively.

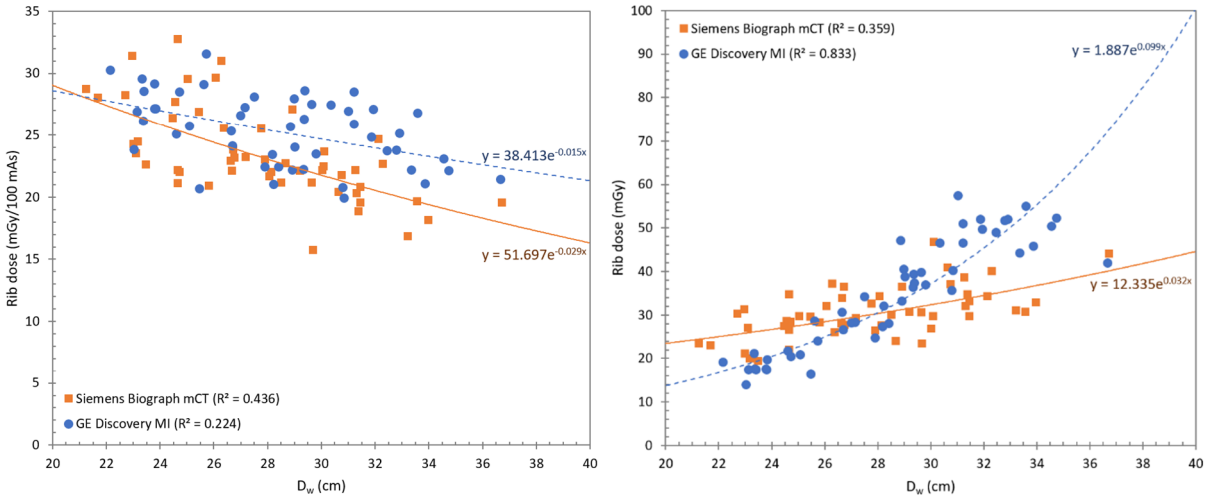

(a) Normalised dose (b) Absolute dose

Figure 61: Estimated (normalised) rib dose as a function of water equivalent diameter (D_w) for a diagnostic CT scan at 120 kV with tube current modulation as part of a whole-body PET/CT examination. Plot points are patient-specific organ doses for examinations on a Siemens Biograph mCT Flow (circles) and GE Discovery MI (squares). Associated exponential regression lines are visualised as a full and dashed line, respectively.

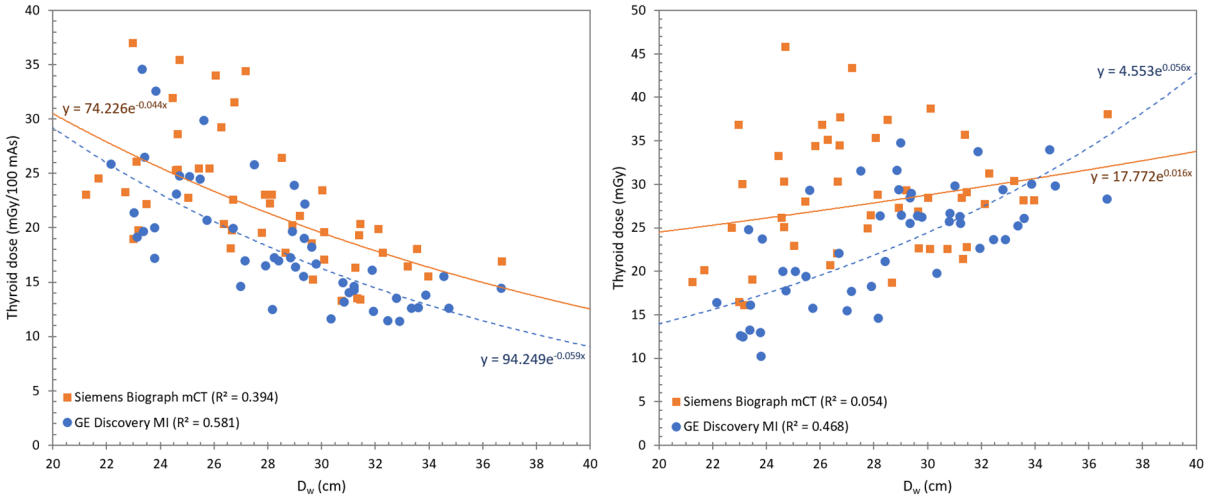

(a) Normalised dose (b) Absolute dose

Figure 62: Estimated (normalised) thyroid dose as a function of water equivalent diameter (D_w) for a diagnostic CT scan at 120 kV with tube current modulation as part of a whole-body PET/CT examination. Plot points are patient-specific organ doses for examinations on a Siemens Biograph mCT Flow (circles) and GE Discovery MI (squares). Associated exponential regression lines are visualised as a full and dashed line, respectively.

B. Correlation between organ doses and size-specific dose estimate

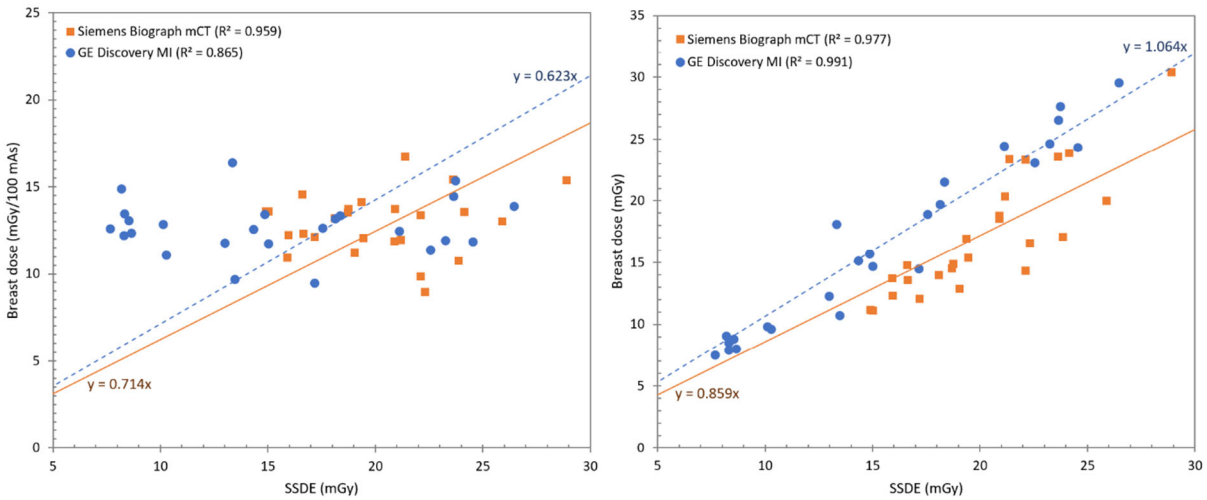

(a) Normalised dose (b) Absolute dose

Figure 63: Estimated (normalised) breast dose as a function of size-specific dose estimate (SSDE) for a diagnostic CT scan at 120 kV with tube current modulation as part of a whole-body PET/CT examination. Plot points are patient-specific organ doses for examinations on a Siemens Biograph mCT Flow (squares) and GE Discovery MI (circles). Associated linear regression lines are visualised as a full and dashed line, respectively.

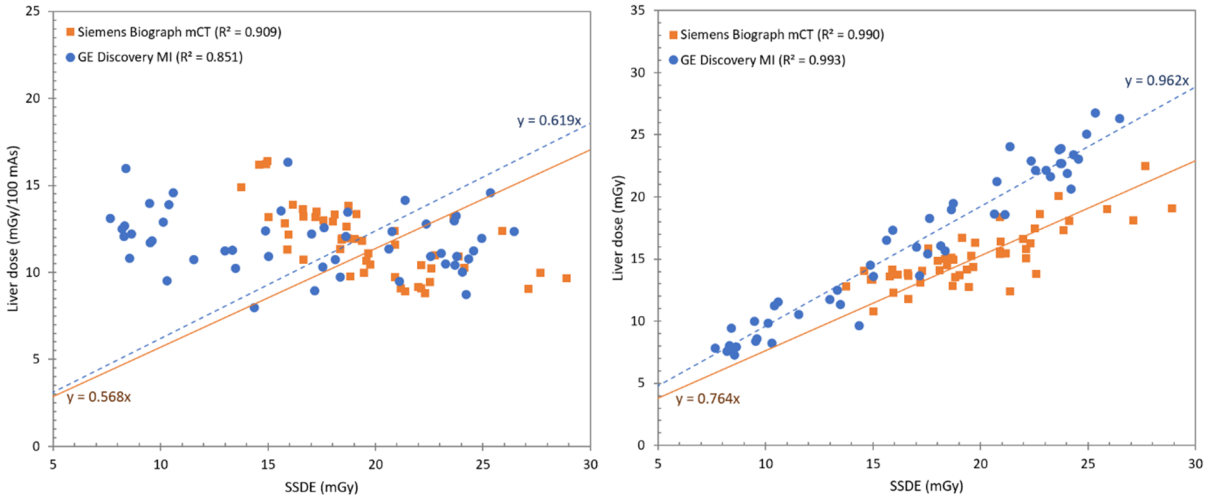

(a) Normalised dose (b) Absolute dose

Figure 64: Estimated (normalised) liver dose as a function of size-specific dose estimate (SSDE) for a diagnostic CT scan at 120 kV with tube current modulation as part of a whole-body PET/CT examination. Plot points are patient-specific organ doses for examinations on a Siemens Biograph mCT Flow (squares) and GE Discovery MI (circles). Associated linear regression lines are visualised as a full and dashed line, respectively.

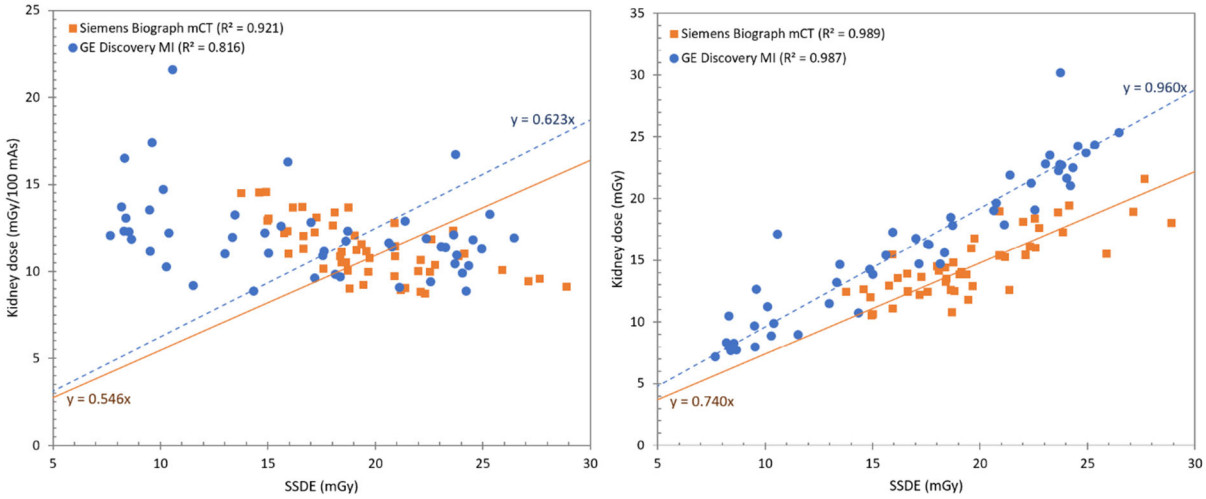

(a) Normalised dose (b) Absolute dose

Figure 65: Estimated (normalised) kidney dose as a function of size-specific dose estimate (SSDE) for a diagnostic CT scan at 120 kV with tube current modulation as part of a whole-body PET/CT examination. Plot points are patient-specific organ doses for examinations on a Siemens Biograph mCT Flow (squares) and GE Discovery MI (circles). Associated linear regression lines are visualised as a full and dashed line, respectively.

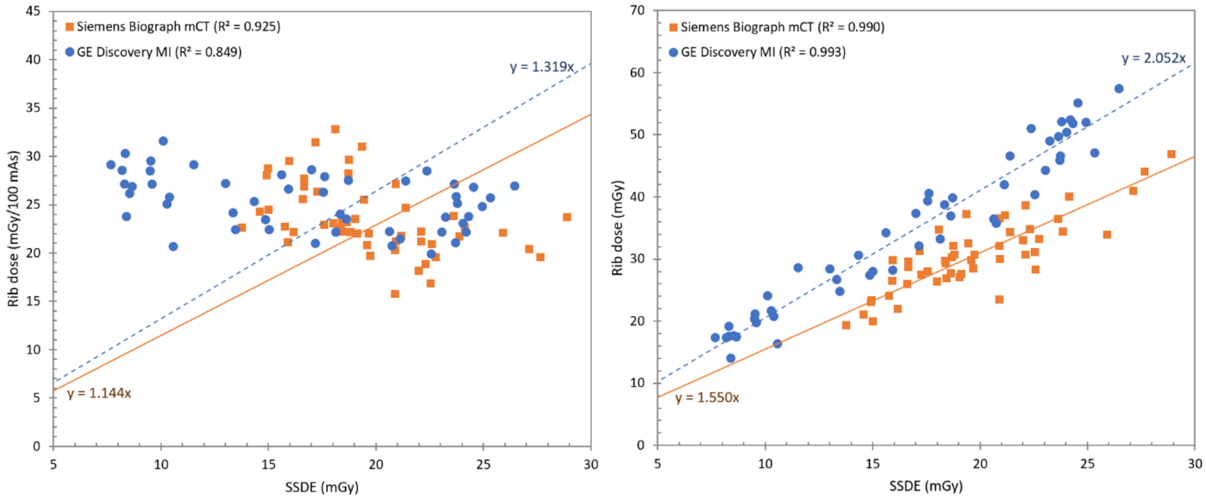

(a) Normalised dose (b) Absolute dose

Figure 66: Estimated (normalised) rib dose as a function of size-specific dose estimate (SSDE) for a diagnostic CT scan at 120 kV with tube current modulation as part of a whole-body PET/CT examination. Plot points are patient-specific organ doses for examinations on a Siemens Biograph mCT Flow (squares) and GE Discovery MI (circles). Associated linear regression lines are visualised as a full and dashed line, respectively.

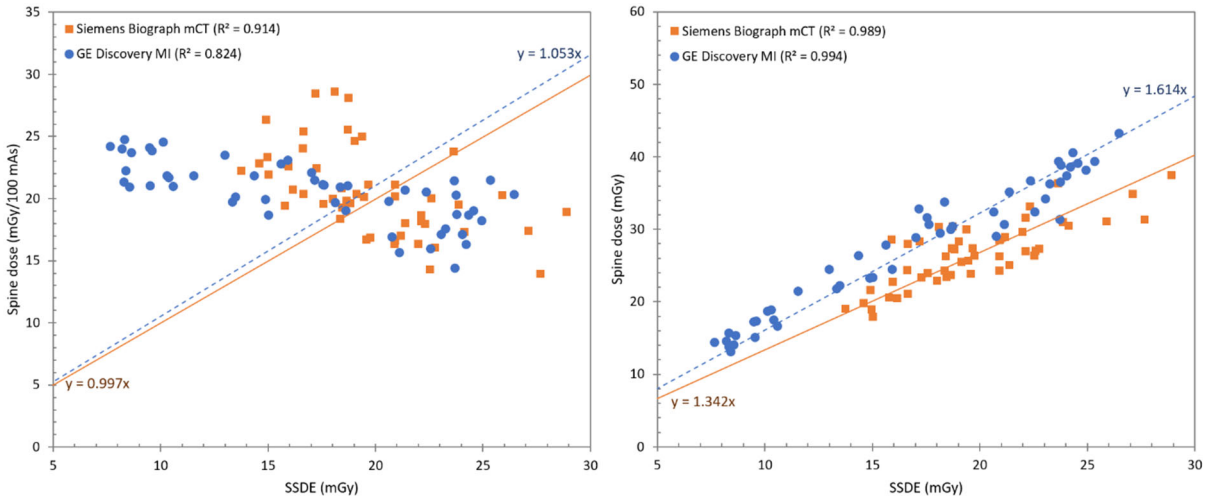

(a) Normalised dose (b) Absolute dose

Figure 67: Estimated (normalised) spine dose as a function of size-specific dose estimate (SSDE) for a diagnostic CT scan at 120 kV with tube current modulation as part of a whole-body PET/CT examination. Plot points are patient-specific organ doses for examinations on a Siemens Biograph mCT Flow (squares) and GE Discovery MI (circles). Associated linear regression lines are visualised as a full and dashed line, respectively.

9.2 Diagnostic CT with fixed mAs

A. Correlation between organ doses and water equivalent diameter

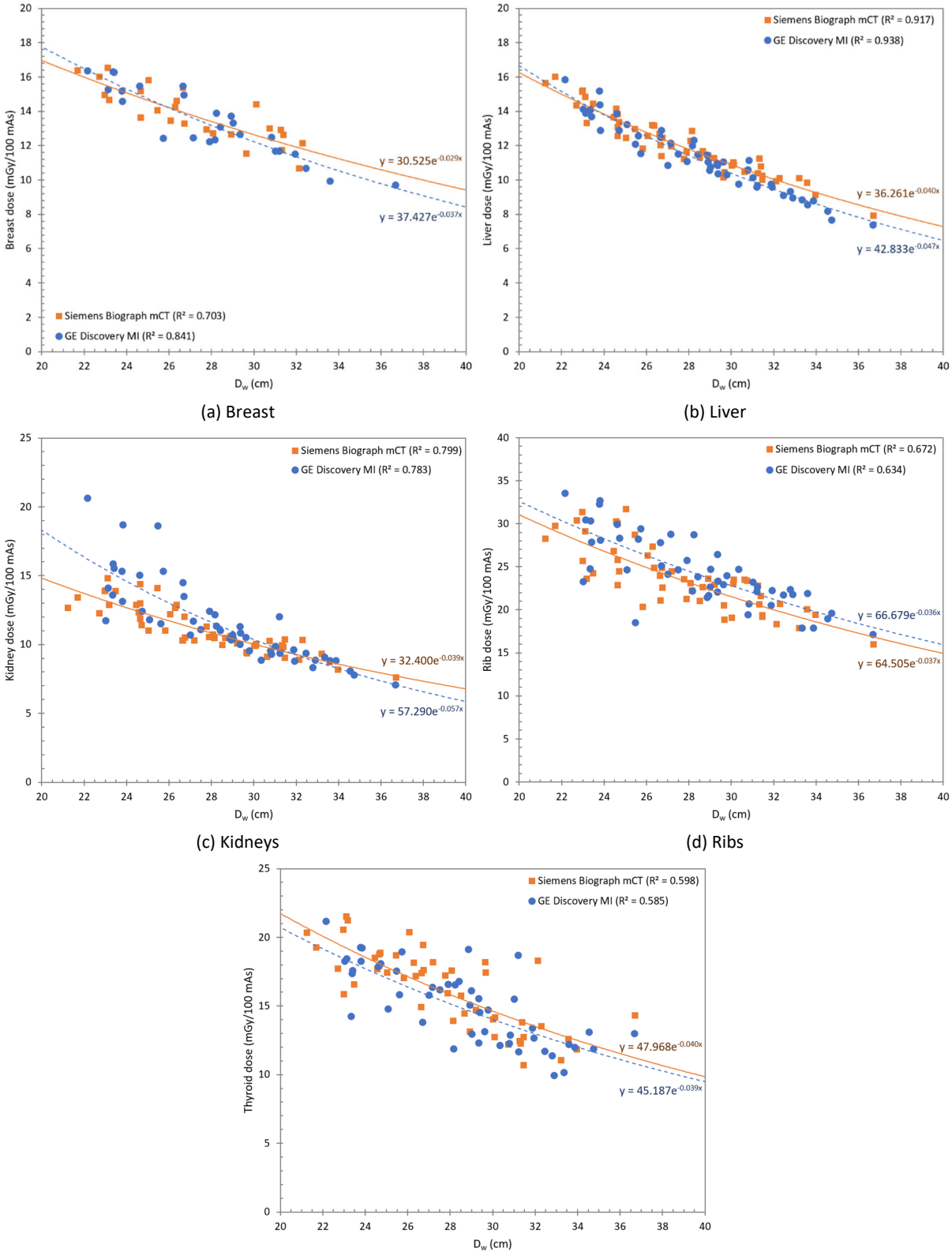

(a) Breast (b) Liver

(c) Kidneys (d) Ribs

(e) Thyroid

Figure 68: Estimated normalised (a) breast, (b) liver, (c) kidney, (d) rib and (e) thyroid dose as a function of water equivalent diameter (D_w) for a diagnostic CT scan at 120 kV with fixed tube current as part of a whole-body PET/CT examination. Plot points are patient-specific organ doses for examinations on a Siemens Biograph mCT Flow (squares) and GE Discovery MI (circles). Associated exponential regression lines are visualised as a full and dashed line, respectively.

B. Correlation between organ doses and size-specific dose estimate

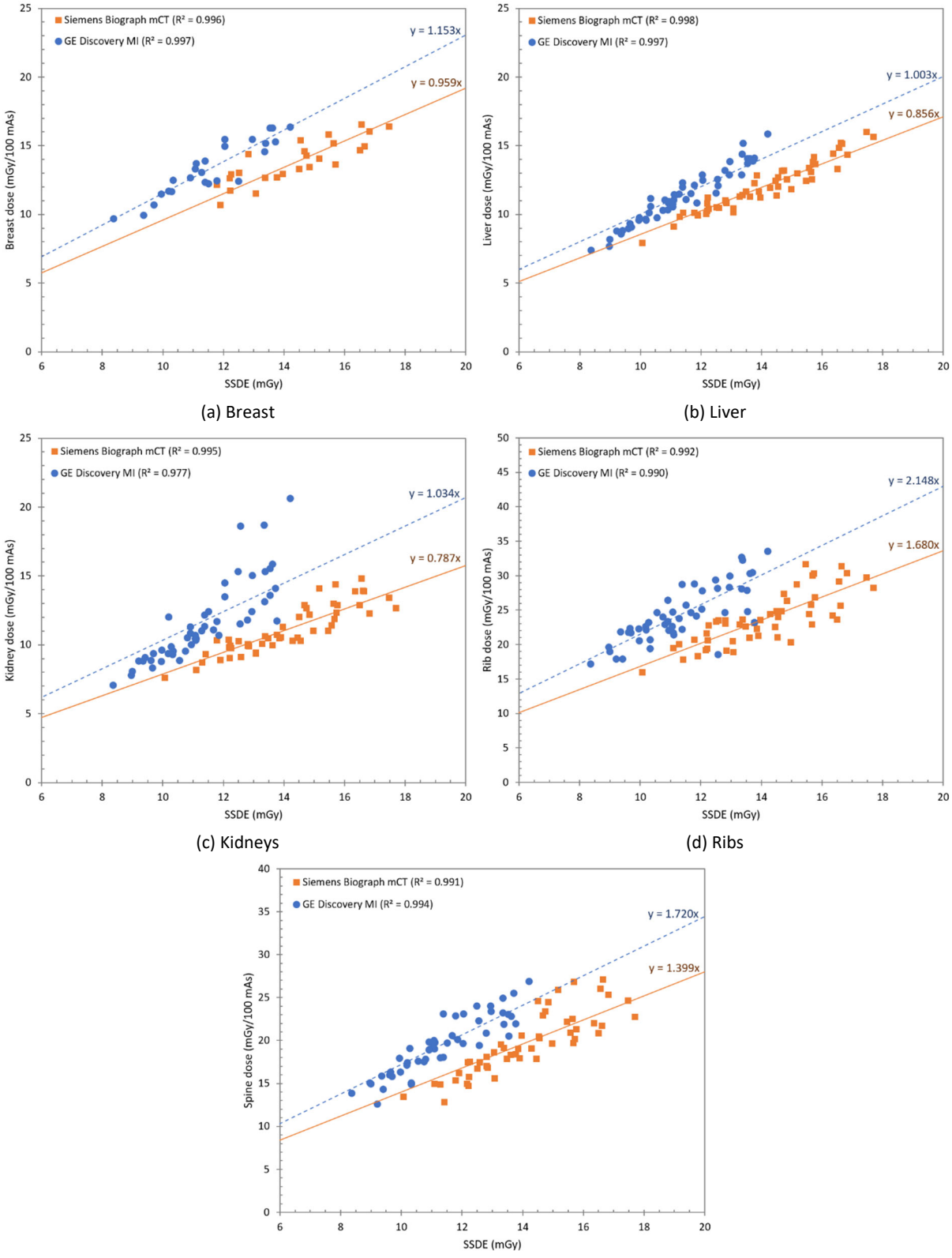

Figure 69: Estimated normalised (a) breast, (b) liver, (c) kidney, (d) rib and (e) spine dose as a function of size-specific dose estimate (SSDE) for a diagnostic CT scan at 120 kV with fixed tube current as part of a whole-body PET/CT examination. Plot points are patient-specific organ doses for examinations on a Siemens Biograph mCT Flow (squares) and GE Discovery MI (circles). Associated linear regression lines are visualised as a full and dashed line, respectively.

9.3 Localisation CT with fixed mAs

A. Correlation between organ doses and water equivalent diameter

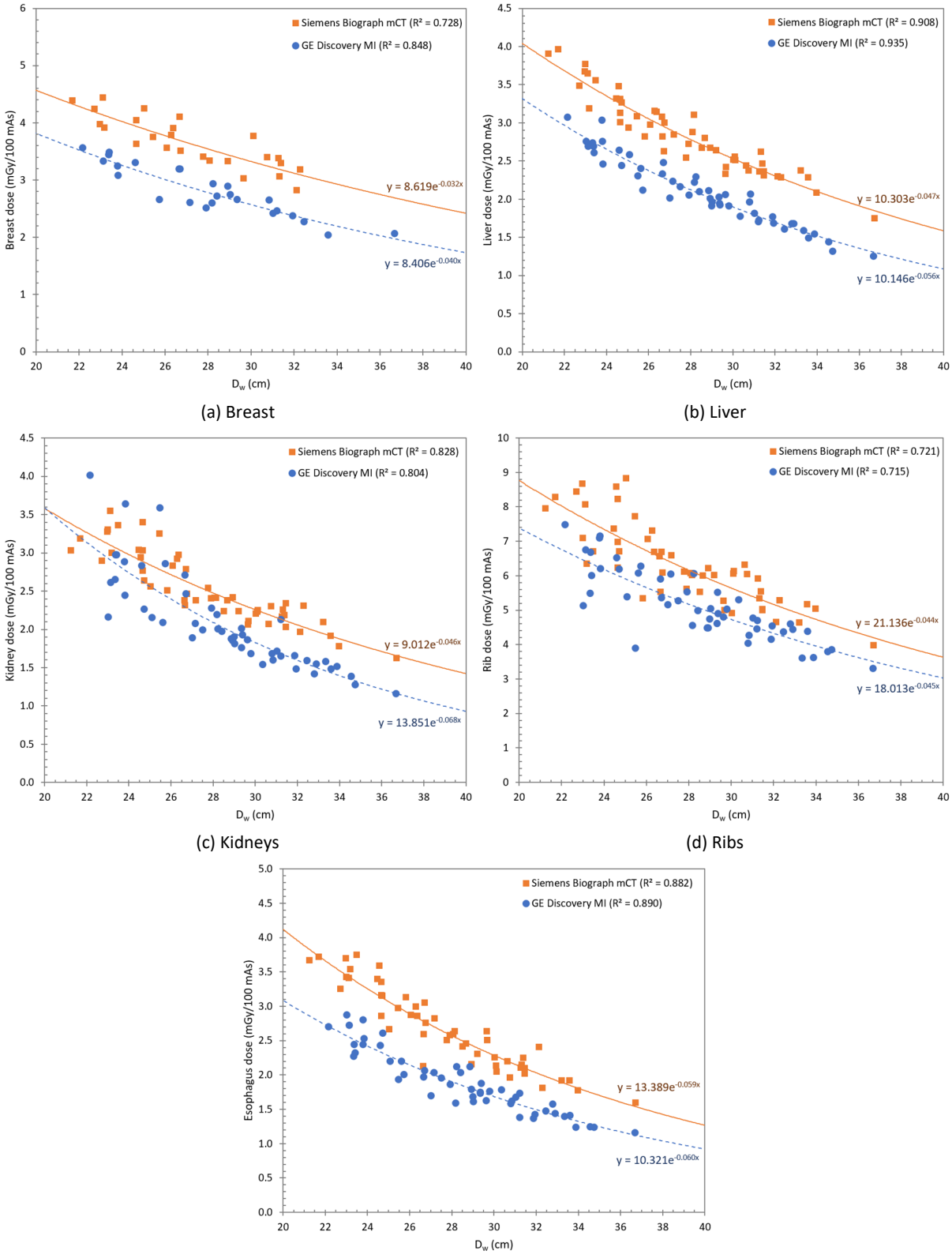

Figure 70: Estimated normalised (a) breast, (b) liver, (c) kidney, (d) rib and (e) esophagus dose as a function of water equivalent diameter (D_w) for a localisation CT scan at 80 kV with fixed tube current as part of a whole-body PET/CT examination. Plot points are patient-specific organ doses for examinations on a Siemens Biograph mCT Flow (squares) and GE Discovery MI (circles). Associated exponential regression lines are visualised as a full and dashed line, respectively.

B. Correlation between organ doses and size-specific dose estimate

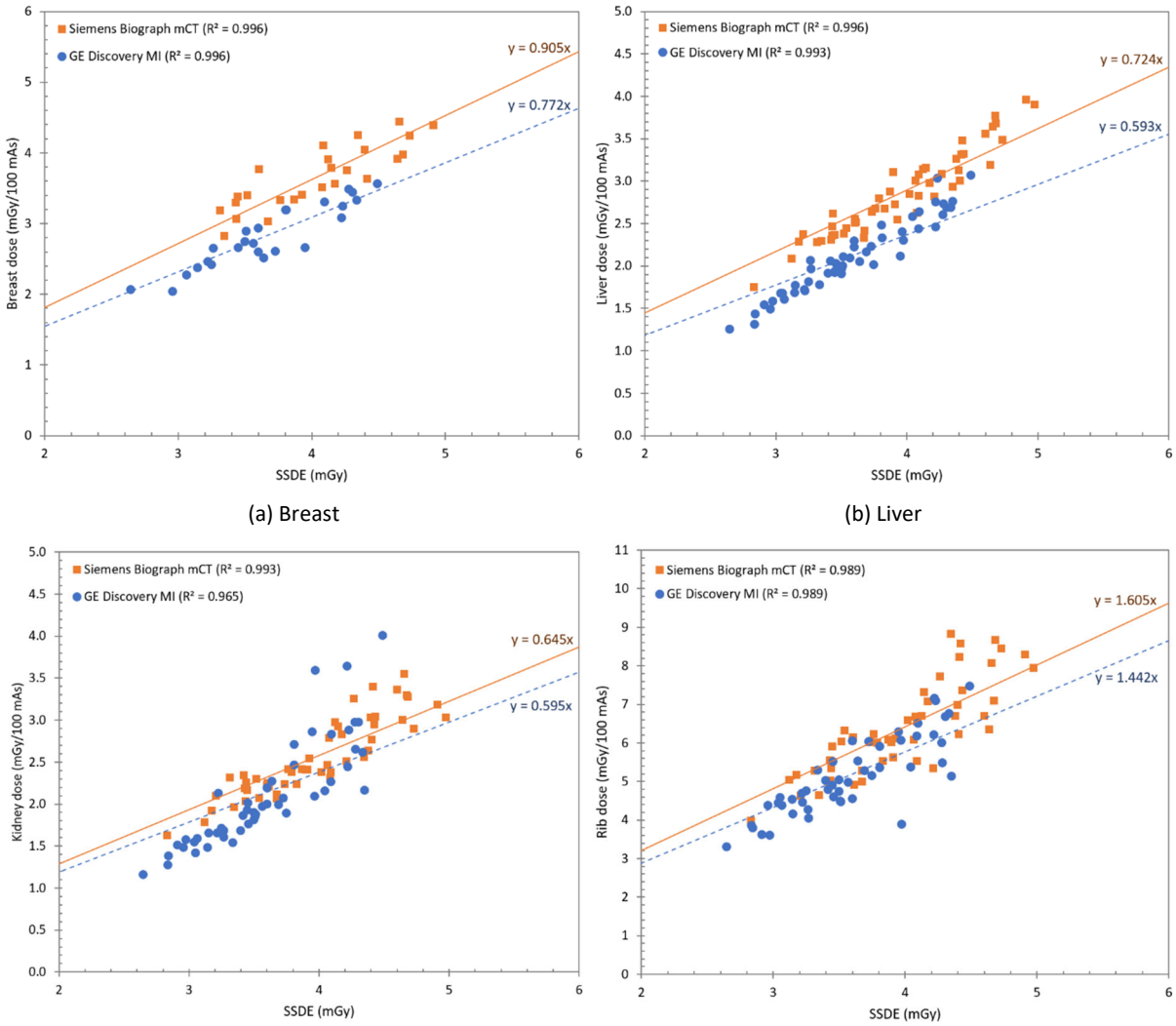

(a) Breast (b) Liver

(c) Kidneys (d) Ribs

Figure 71: Estimated normalised (a) breast, (b) liver, (c) kidney and (d) rib dose as a function of size-specific dose estimate (SSDE) for a localisation CT scan at 80 kV with fixed tube current as part of a whole-body PET/CT examination. Plot points are patient-specific organ doses for examinations on a Siemens Biograph mCT Flow (squares) and GE Discovery MI (circles). Associated linear regression lines are visualised as a full and dashed line, respectively.

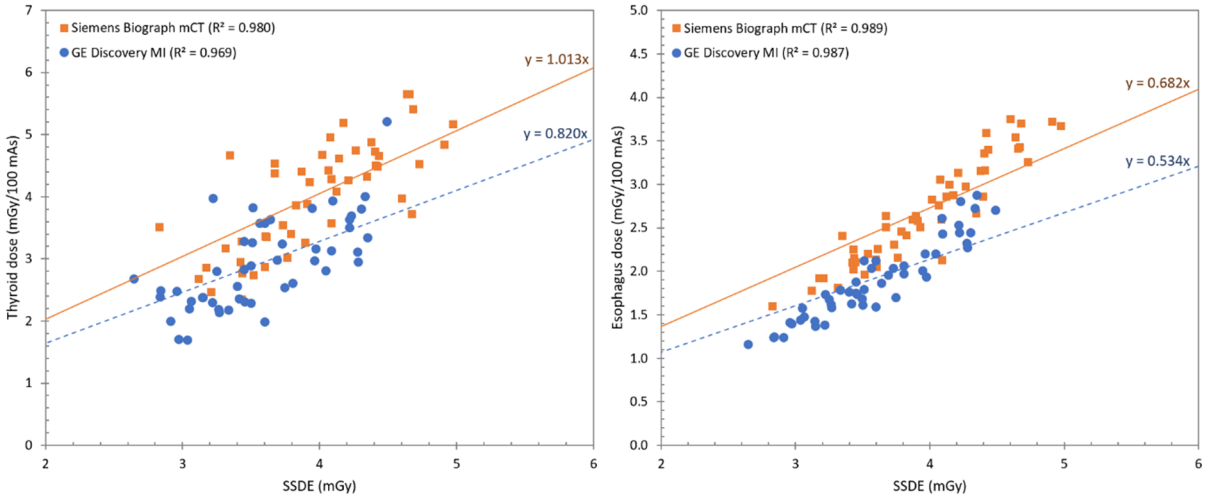

(a) Thyroid (b) Esophagus

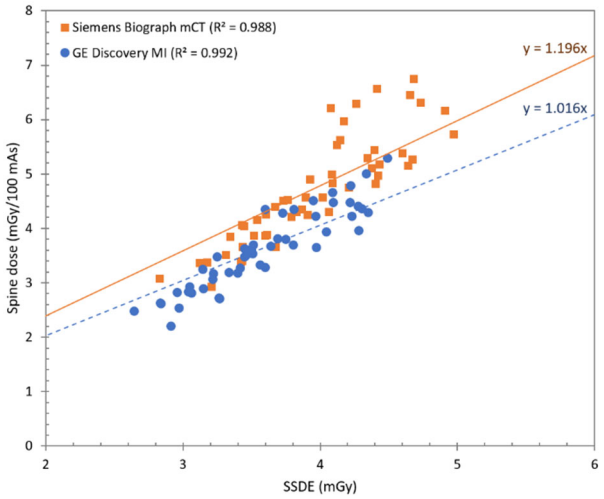

(c) Spine

Figure 72: Estimated normalised (a) thyroid, (b) esophagus and (c) spine dose as a function of size-specific dose estimate (SSDE) for a localisation CT scan at 80 kV with fixed tube current as part of a whole-body PET/CT examination. Plot points are patient-specific organ doses for examinations on a Siemens Biograph mCT Flow (squares) and GE Discovery MI (circles). Associated linear regression lines are visualised as a full and dashed line, respectively.

10 Appendix B – SPECT/CT organ dose correlations

This appendix lists the regression analyses that are not presented in Chapter 6 - CT organ doses in SPECT/CT. In the first part, the correlation between the organ dose and water equivalent diameter or size-specific dose estimate can be found for the attenuation correction and localisation CT of ventilation/perfusion lung scans. Secondly, the results for an attenuation correction and calcium scoring CT of cardiac SPECT/CT studies are shown. At last, the results for the diagnostic and localisation CT of cervical and lumbar spine SPECT/CT examinations are presented.

10.1 Ventilation/perfusion lung scan

A. Correlation between organ doses and water equivalent diameter

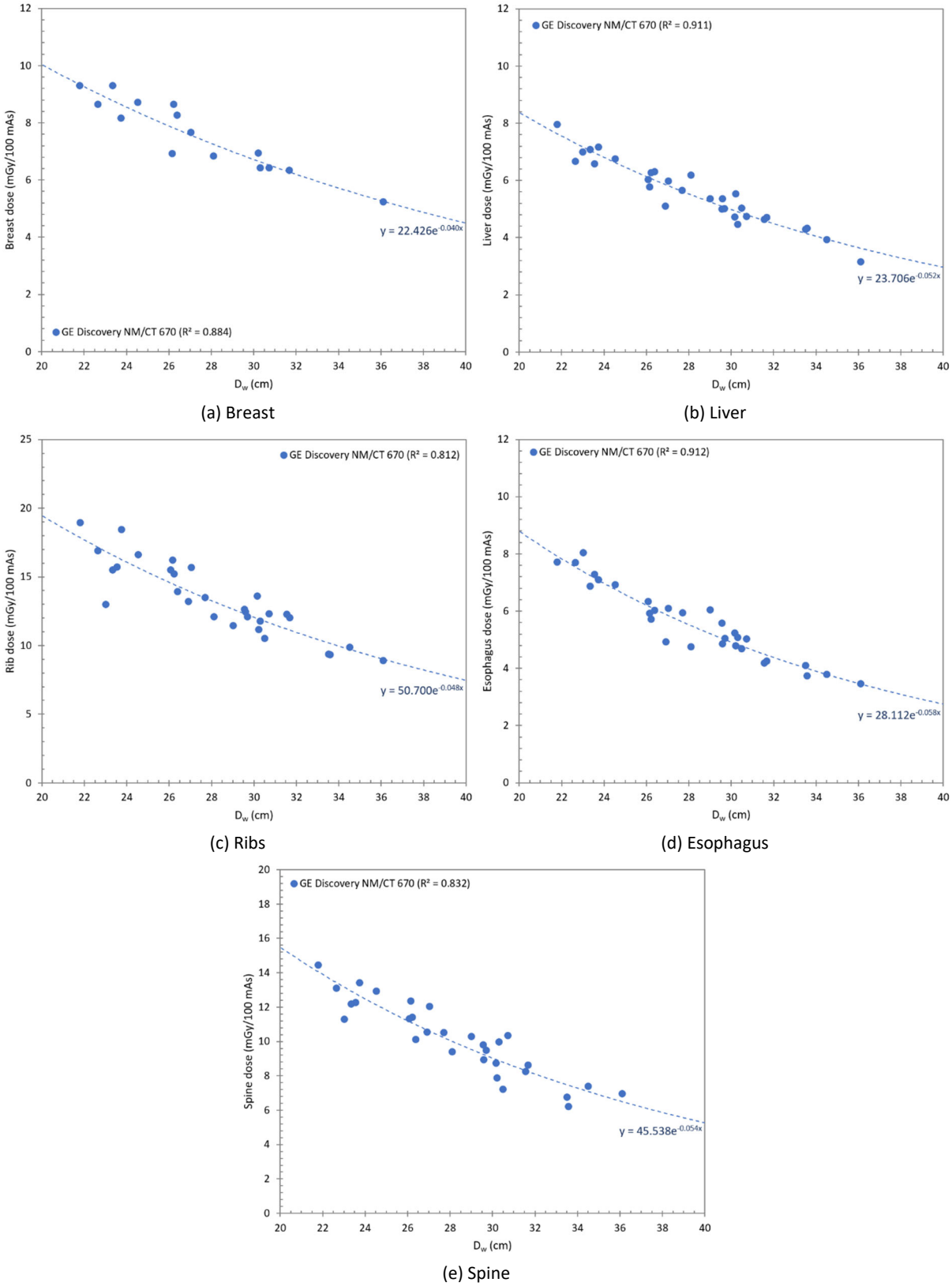

Figure 73: Estimated normalised (a) breast, (b) liver, (c) rib, (d) esophagus and (e) spine dose as a function of water equivalent diameter (D_W) for an attenuation correction and localisation CT scan at 100 kV with fixed tube current as part of a ventilation/perfusion SPECT/CT examination. Plot points are patient-specific organ doses for examinations on GE Discovery NM/CT 670 (circles). Associated exponential regression lines are visualised as a dashed line.

B. Correlation between organ doses and size-specific dose estimate

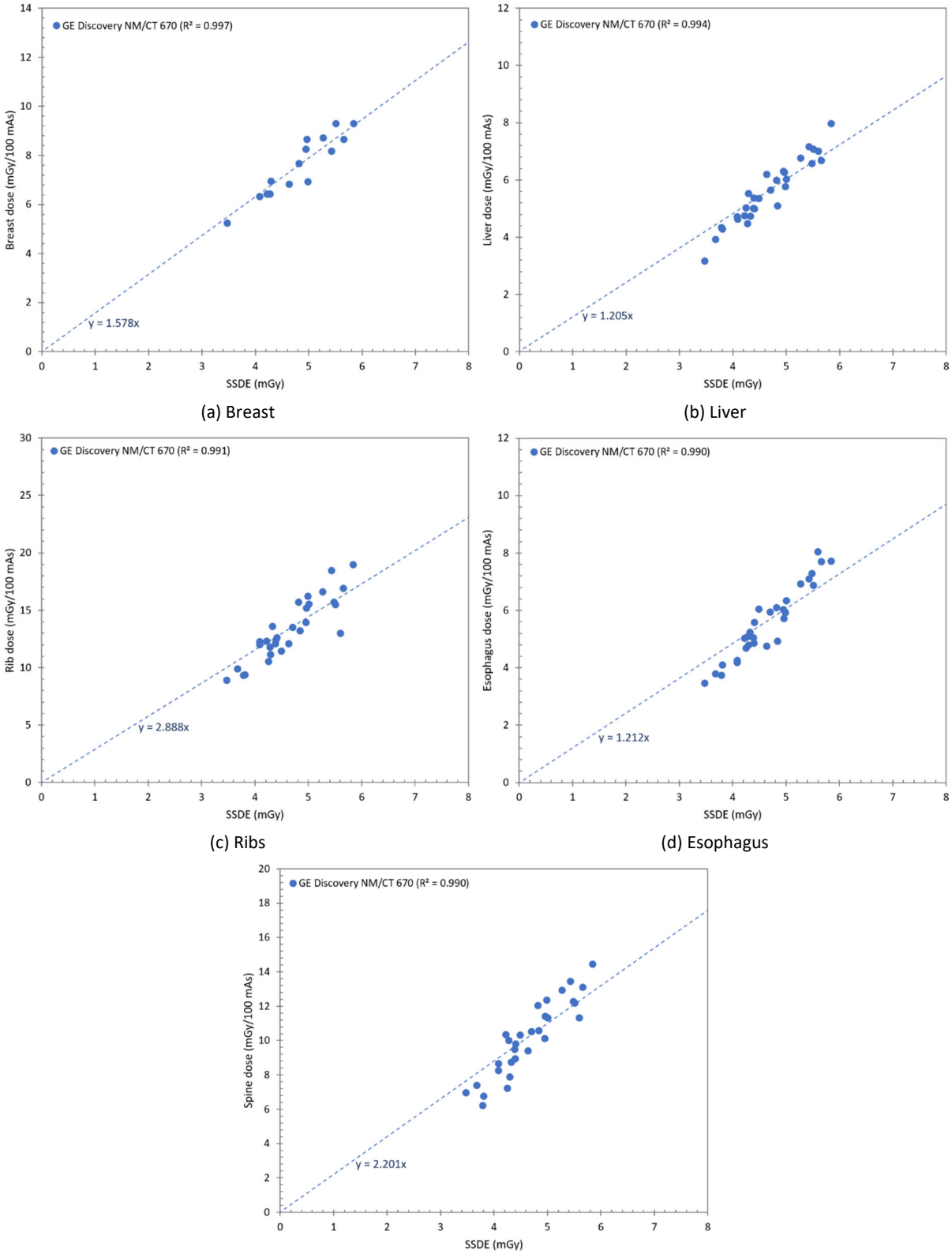

Figure 74: Estimated normalised (a) breast, (b) liver, (c) rib, (d) esophagus and (e) spine dose as a function of size-specific dose estimate (SSDE) for an attenuation correction and localisation CT scan at 100 kV with fixed tube current as part of a ventilation/perfusion SPECT/CT examination. Plot points are patient-specific organ doses for examinations on GE Discovery NM/CT 670 (circles). Associated linear regression lines are visualised as a dashed line.

10.2 Cardiac SPECT/CT

A. Correlation between organ doses and water equivalent diameter

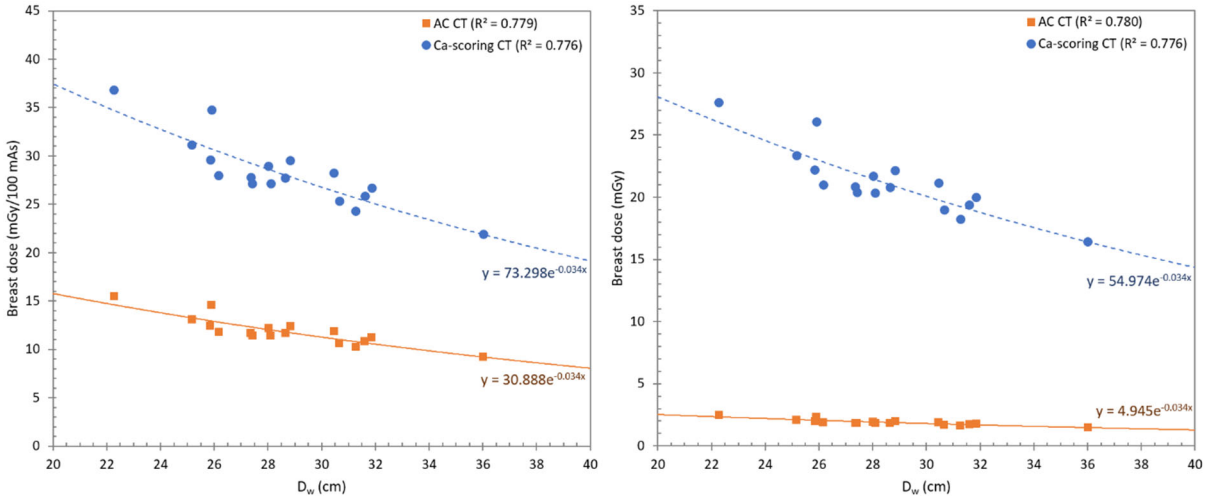

(a) Normalised dose (b) Absolute dose

Figure 75: Estimated (normalised) breast dose as a function of water equivalent diameter (D_W) for attenuation correction (AC) only and calcium (Ca) scoring CT scans at 130 kV with and without tube current modulation, respectively, as part of a cardiac SPECT/CT examination on a Siemens Symbia Intevo T16. Plot points are patient-specific organ doses for attenuation correction (squares) and Ca-scoring (circles) CT scans. Associated exponential regression lines are visualised as a full and dashed line, respectively.

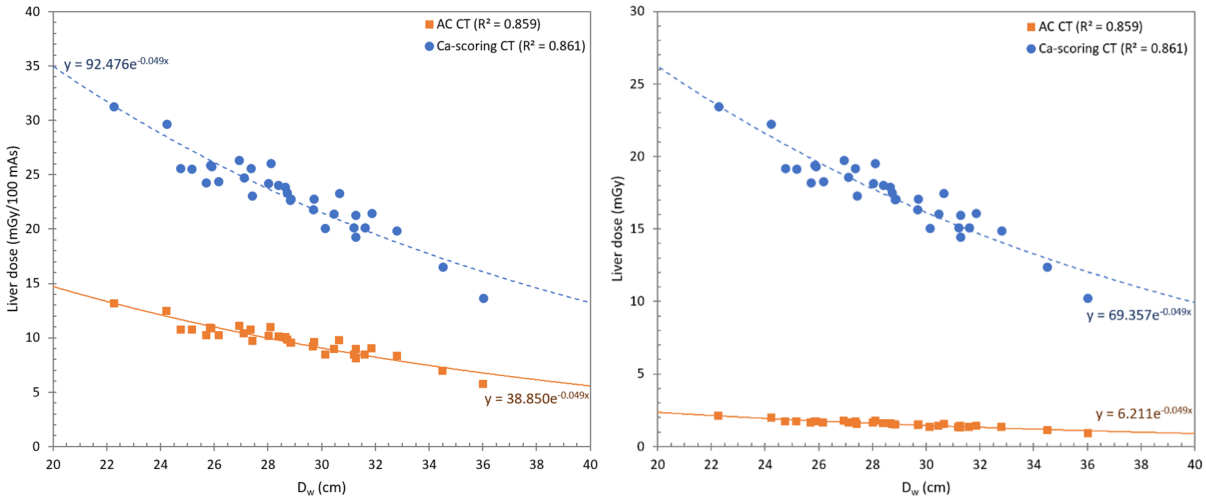

(a) Normalised dose (b) Absolute dose

Figure 76: Estimated (normalised) liver dose as a function of water equivalent diameter (D_W) for attenuation correction (AC) only and calcium (Ca) scoring CT scans at 130 kV with and without tube current modulation, respectively, as part of a cardiac SPECT/CT examination on a Siemens Symbia Intevo T16. Plot points are patient-specific organ doses for attenuation correction (squares) and Ca-scoring (circles) CT scans. Associated exponential regression lines are visualised as a full and dashed line, respectively.

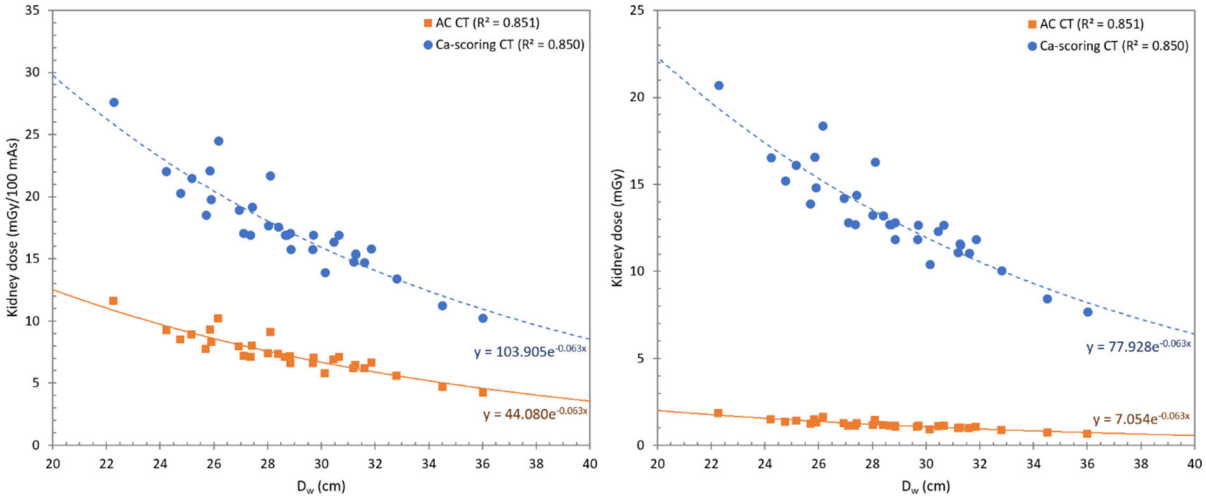

(a) Normalised dose (b) Absolute dose

Figure 77: Estimated (normalised) kidney dose as a function of water equivalent diameter (D_W) for attenuation correction (AC) only and calcium (Ca) scoring CT scans at 130 kV with and without tube current modulation, respectively, as part of a cardiac SPECT/CT examination on a Siemens Symbia Intevo T16. Plot points are patient-specific organ doses for attenuation correction (squares) and Ca-scoring (circles) CT scans. Associated exponential regression lines are visualised as a full and dashed line, respectively.

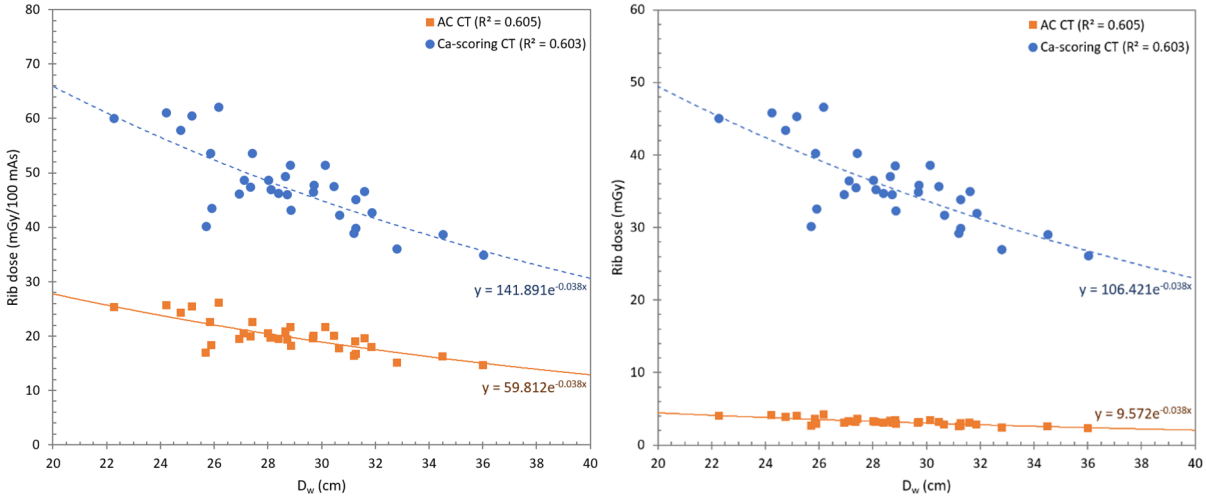

(a) Normalised dose (b) Absolute dose

Figure 78: Estimated (normalised) rib dose as a function of water equivalent diameter (D_W) for attenuation correction (AC) only and calcium (Ca) scoring CT scans at 130 kV with and without tube current modulation, respectively, as part of a cardiac SPECT/CT examination on a Siemens Symbia Intevo T16. Plot points are patient-specific organ doses for attenuation correction (squares) and Ca-scoring (circles) CT scans. Associated exponential regression lines are visualised as a full and dashed line, respectively.

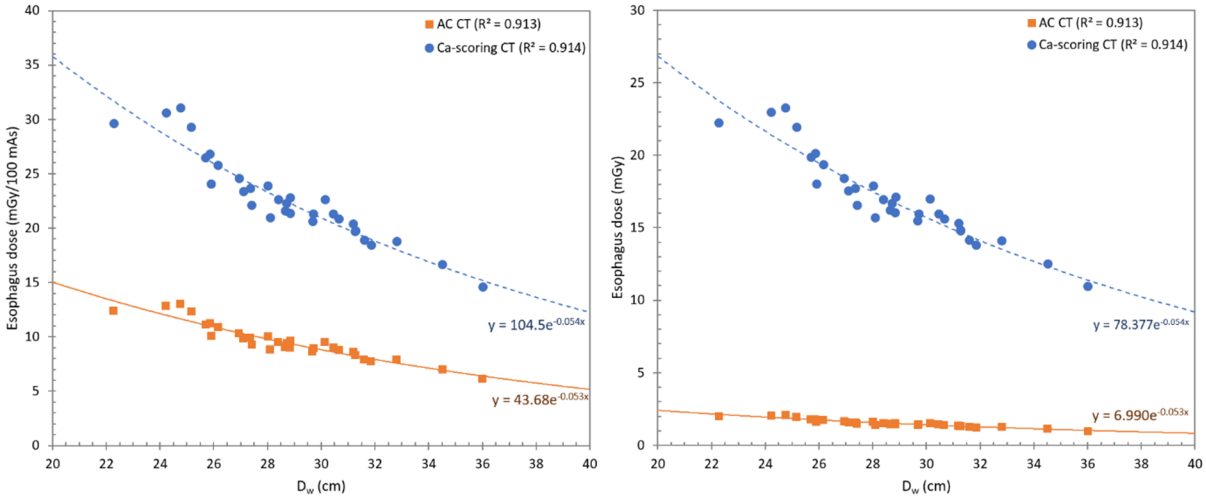

(a) Normalised dose (b) Absolute dose

Figure 79: Estimated (normalised) esophagus dose as a function of water equivalent diameter (D_W) for attenuation correction (AC) only and calcium (Ca) scoring CT scans at 130 kV with and without tube current modulation, respectively, as part of a cardiac SPECT/CT examination on a Siemens Symbia Intevo T16. Plot points are patient-specific organ doses for attenuation correction (squares) and Ca-scoring (circles) CT scans. Associated exponential regression lines are visualised as a full and dashed line, respectively.

B. Correlation between organ doses and size-specific dose estimate

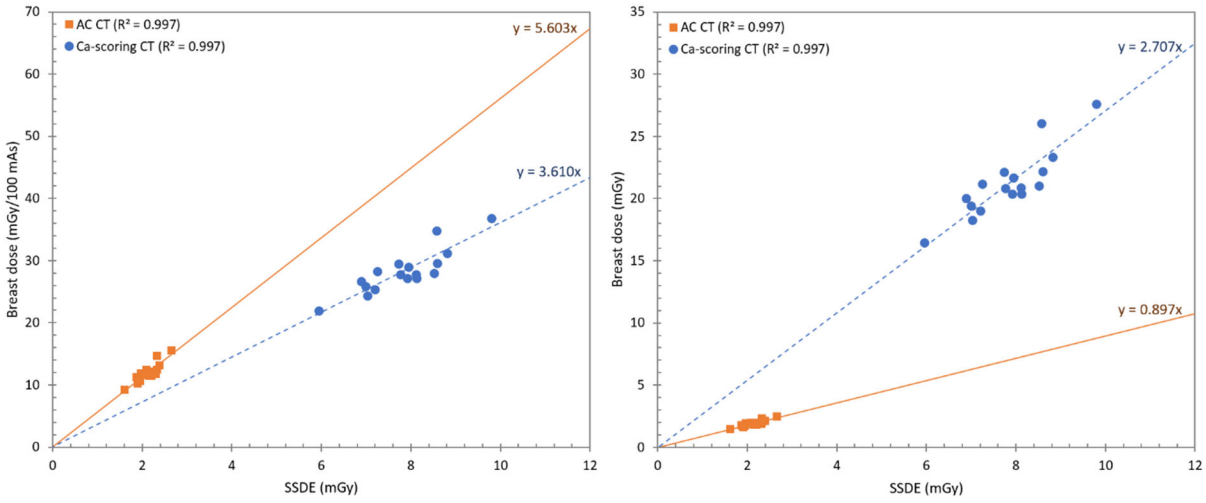

(a) Normalised dose (b) Absolute dose

Figure 80: Estimated (normalised) breast dose as a function of size-specific dose estimate (SSDE) for attenuation correction (AC) only and calcium (Ca) scoring CT scans at 130 kV with and without tube current modulation, respectively, as part of a cardiac SPECT/CT examination on a Siemens Symbia Intevo T16. Plot points are patient-specific organ doses for attenuation correction (squares) and Ca-scoring (circles) CT scans. Associated linear regression lines are visualised as a full and dashed line, respectively.

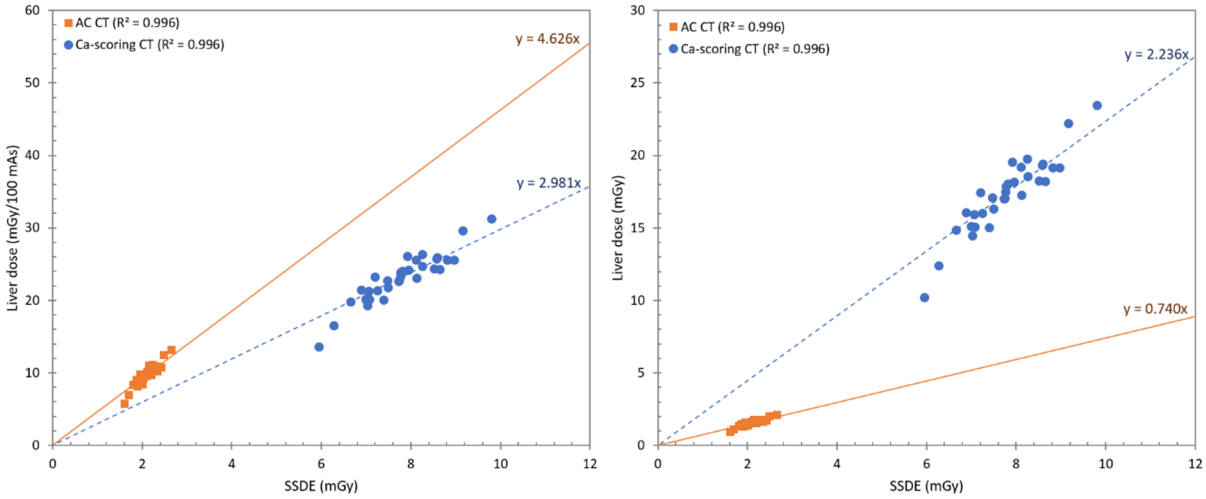

(a) Normalised dose (b) Absolute dose

Figure 81: Estimated (normalised) liver dose as a function of size-specific dose estimate (SSDE) for attenuation correction (AC) only and calcium (Ca) scoring CT scans at 130 kV with and without tube current modulation, respectively, as part of a cardiac SPECT/CT examination on a Siemens Symbia Intevo T16. Plot points are patient-specific organ doses for attenuation correction (squares) and Ca-scoring (circles) CT scans. Associated linear regression lines are visualised as a full and dashed line, respectively.

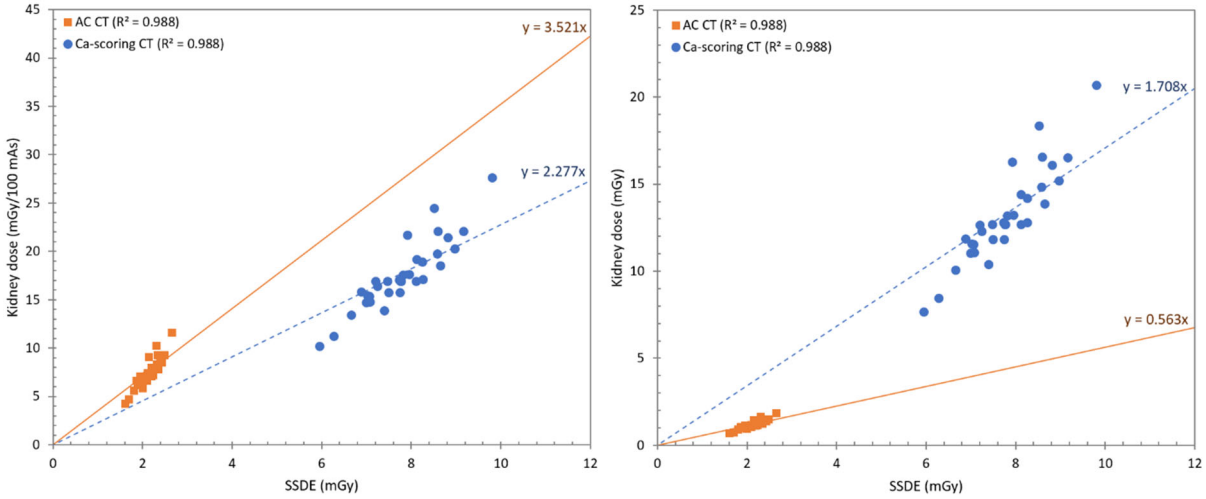

(a) Normalised dose (b) Absolute dose

Figure 82: Estimated (normalised) kidney dose as a function of size-specific dose estimate (SSDE) for attenuation correction (AC) only and calcium (Ca) scoring CT scans at 130 kV with and without tube current modulation, respectively, as part of a cardiac SPECT/CT examination on a Siemens Symbia Intevo T16. Plot points are patient-specific organ doses for attenuation correction (squares) and Ca-scoring (circles) CT scans. Associated linear regression lines are visualised as a full and dashed line, respectively.

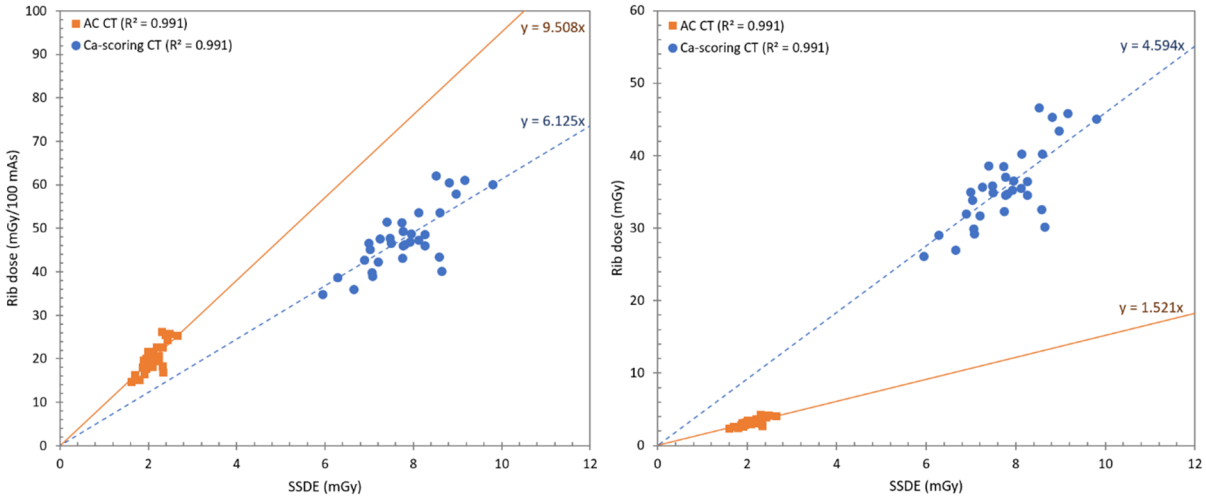

(a) Normalised dose (b) Absolute dose

Figure 83: Estimated (normalised) rib dose as a function of size-specific dose estimate (SSDE) for attenuation correction (AC) only and calcium (Ca) scoring CT scans at 130 kV with and without tube current modulation, respectively, as part of a cardiac SPECT/CT examination on a Siemens Symbia Intevo T16. Plot points are patient-specific organ doses for attenuation correction (squares) and Ca-scoring (circles) CT scans. Associated linear regression lines are visualised as a full and dashed line, respectively.

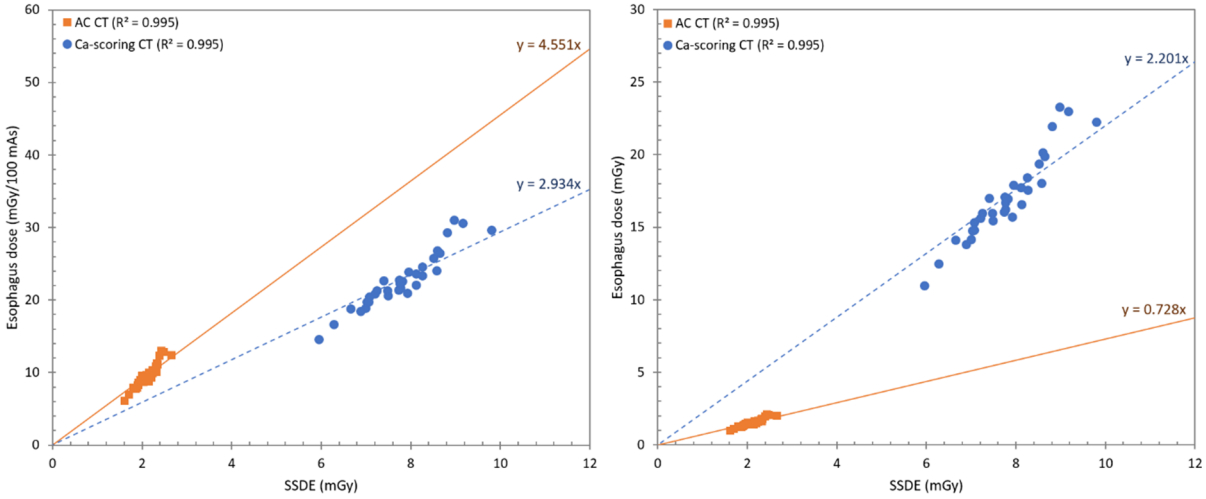

(a) Normalised dose (b) Absolute dose

Figure 84: Estimated (normalised) esophagus dose as a function of size-specific dose estimate (SSDE) for attenuation correction (AC) only and calcium (Ca) scoring CT scans at 130 kV with and without tube current modulation, respectively, as part of a cardiac SPECT/CT examination on a Siemens Symbia Intevo T16. Plot points are patient-specific organ doses for attenuation correction (squares) and Ca-scoring (circles) CT scans. Associated linear regression lines are visualised as a full and dashed line, respectively.

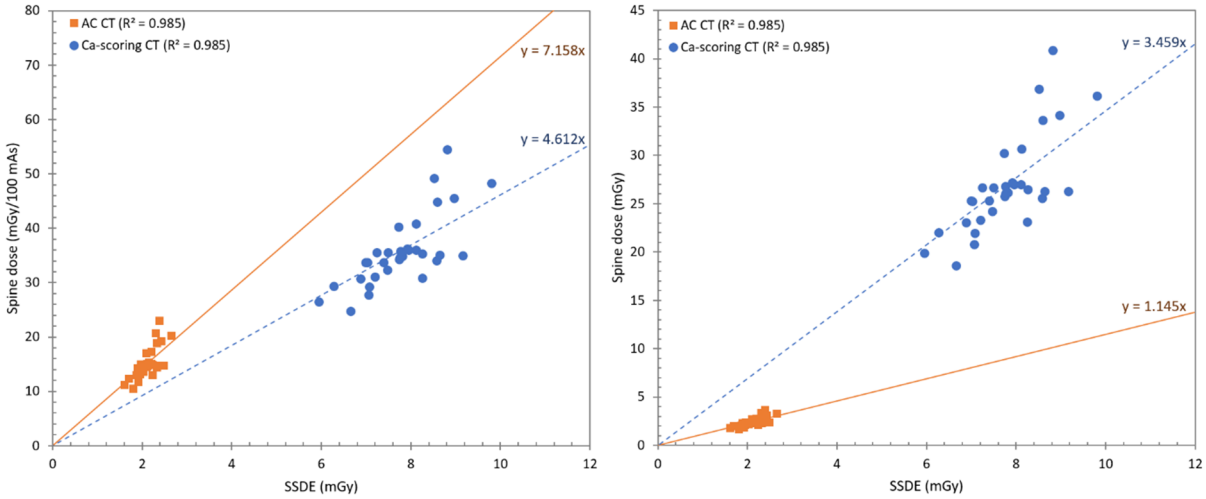

(a) Normalised dose (b) Absolute dose

Figure 85: Estimated (normalised) spine dose as a function of size-specific dose estimate (SSDE) for attenuation correction (AC) only and calcium (Ca) scoring CT scans at 130 kV with and without tube current modulation, respectively, as part of a cardiac SPECT/CT examination on a Siemens Symbia Intevo T16. Plot points are patient-specific organ doses for attenuation correction (squares) and Ca-scoring (circles) CT scans. Associated linear regression lines are visualised as a full and dashed line, respectively.

10.3 Cervical and lumbar spine SPECT/CT

A. Diagnostic CT of the cervical spine

Correlation between organ doses and water equivalent diameter

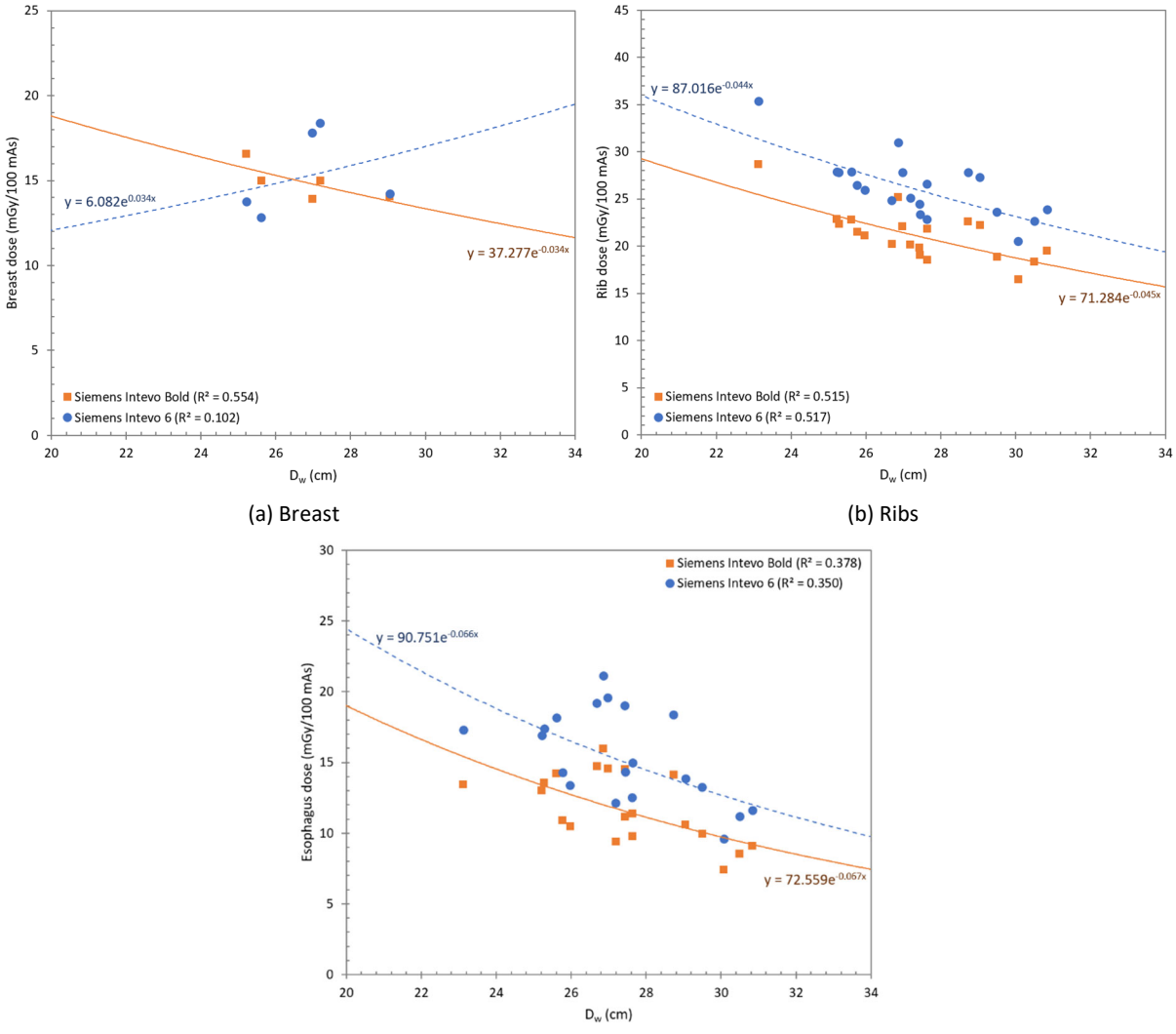

(a) Breast (b) Ribs

(c) Esophagus

Figure 86: Estimated normalised (a) breast, (b) rib and (c) esophagus dose as a function of water equivalent diameter (D_w) for a diagnostic CT scan at 130 kV as part of a cervical spine SPECT/CT examination. Plot points are patient-specific organ doses for examinations on a Siemens Symbia Intevo Bold (squares) and Siemens Symbia Intevo 6 (circles). Associated exponential regression lines are visualised as a full and dashed line, respectively.

Correlation between organ doses and size-specific dose estimate

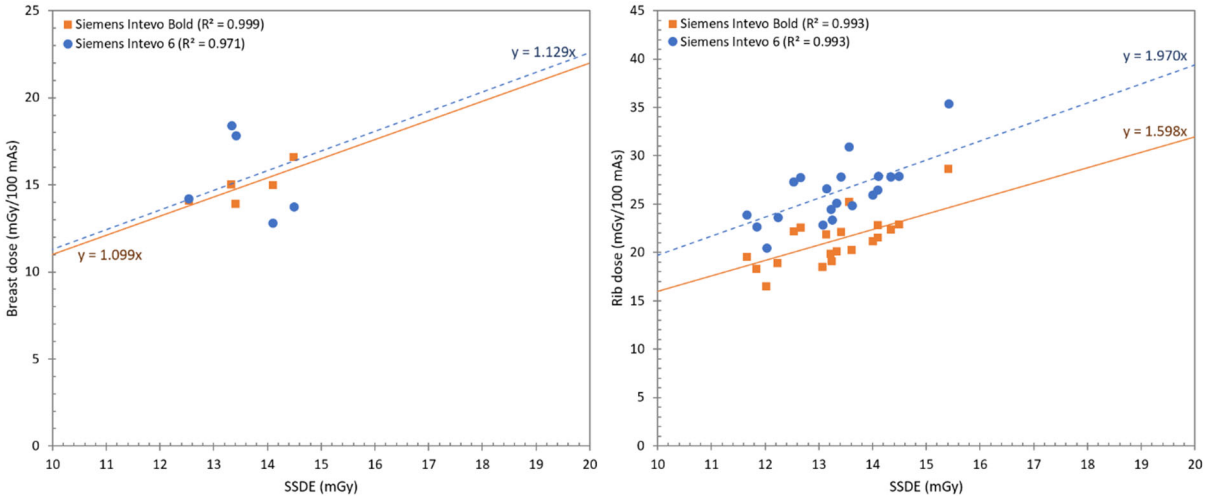

(a) Breast (b) Ribs

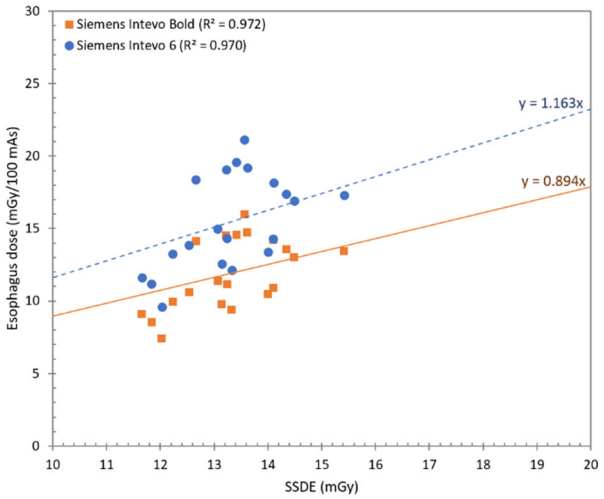

(c) Esophagus

Figure 87: Estimated normalised (a) breast, (b) rib and (c) esophagus dose as a function of size-specific dose estimate (SSDE) for a diagnostic CT scan at 130 kV as part of a cervical spine SPECT/CT examination. Plot points are patient-specific organ doses for examinations on a Siemens Symbia Intevo Bold (squares) and Siemens Symbia Intevo 6 (circles). Associated exponential regression lines are visualised as a full and dashed line, respectively.

B. Localisation CT of the cervical spine

Correlation between organ doses and water equivalent diameter

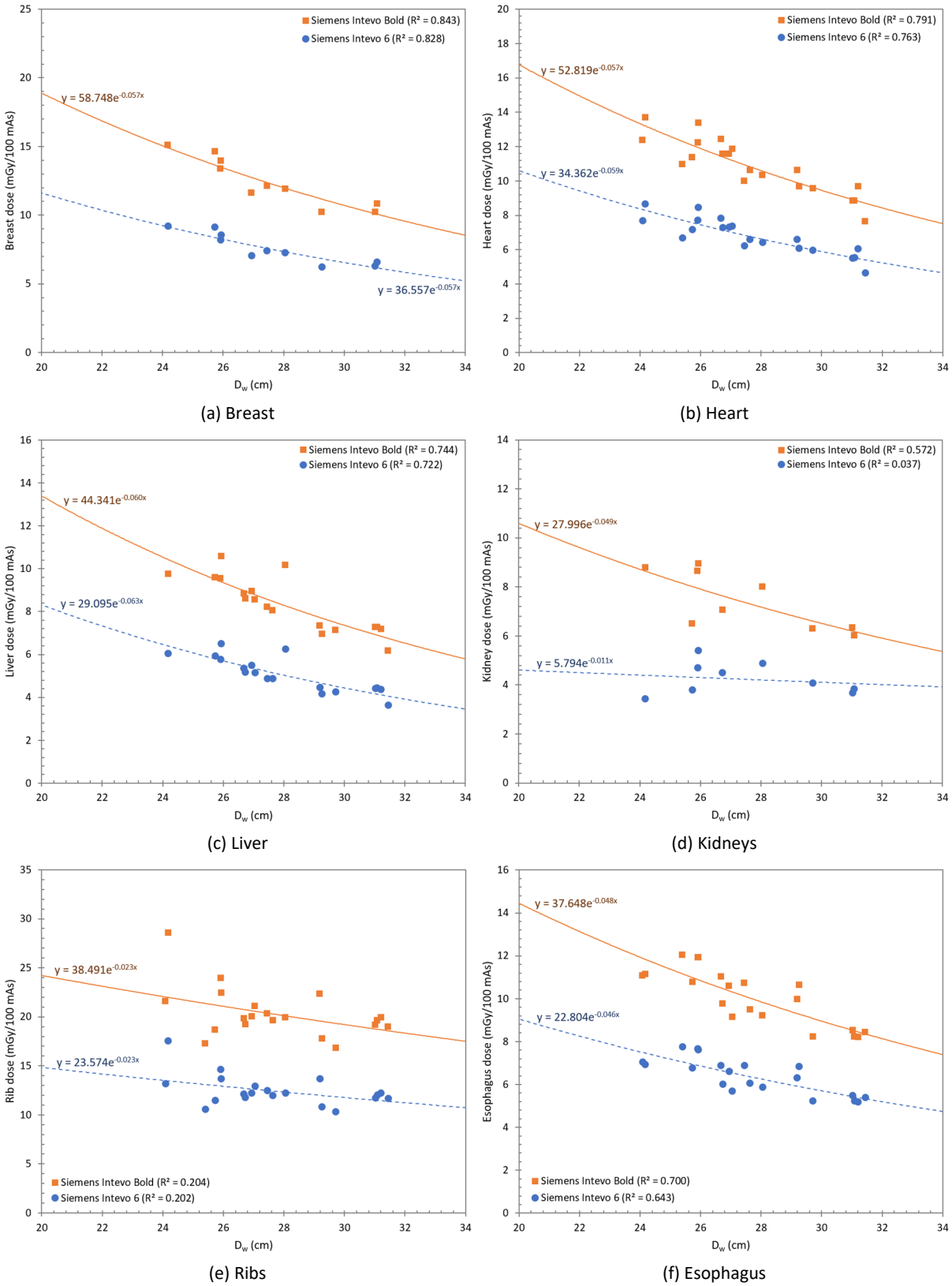

Figure 88: Estimated normalised (a) breast, (b) heart, (c) liver, (d) kidney, (e) rib and (f) esophagus dose as a function of water equivalent diameter (D_w) for a localisation CT scan at 130 kV as part of a cervical spine SPECT/CT examination. Plot points are patient-specific organ doses for examinations on a Siemens Symbia Intevo Bold (squares) and Siemens Symbia Intevo 6 (circles). Associated exponential regression lines are visualised as a full and dashed line, respectively.

Correlation between organ doses and size-specific dose estimate

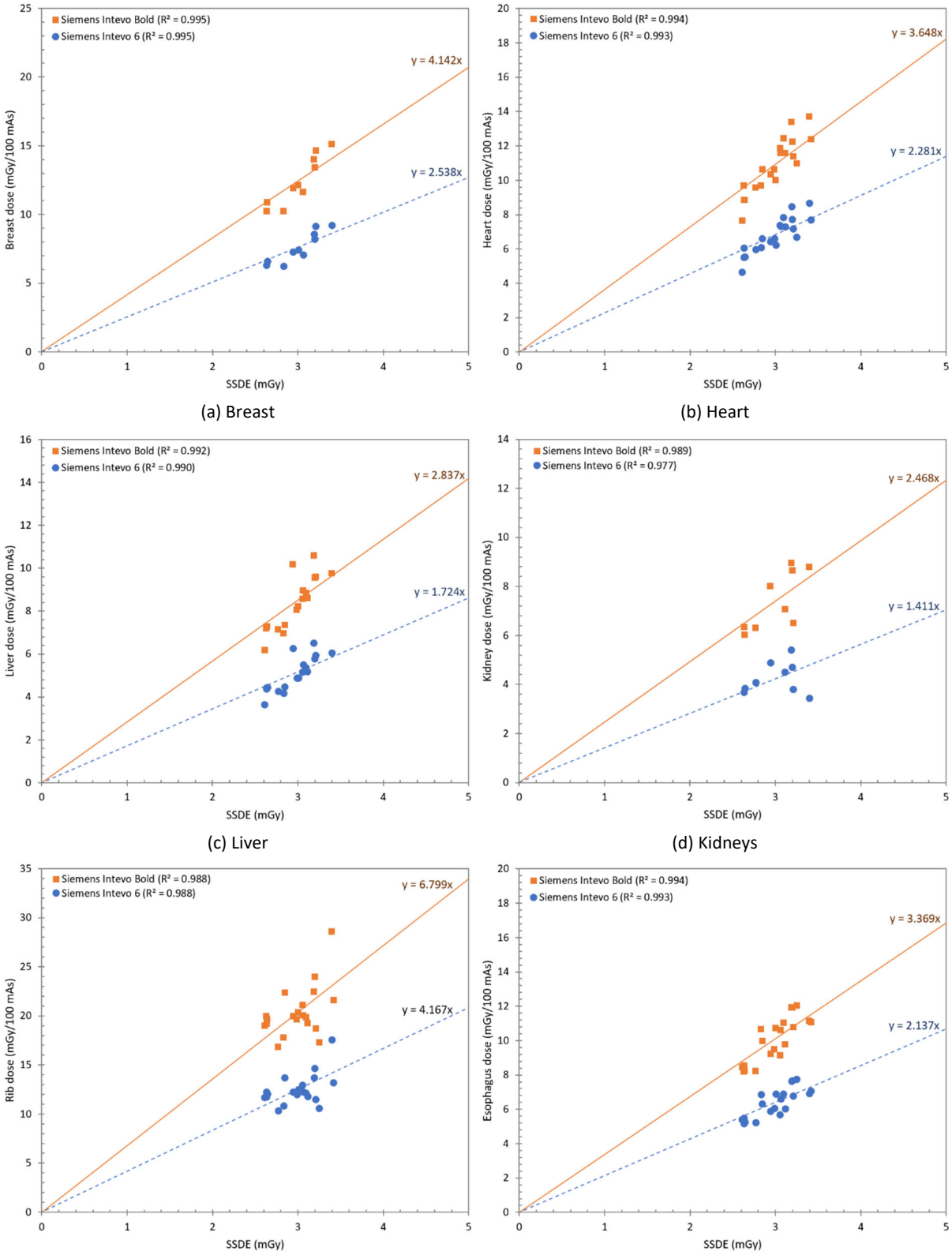

Figure 89: Estimated normalised (a) breast, (b) heart, (c) liver, (d) kidney, (e) rib and (f) esophagus dose as a function of size-specific dose estimate (SSDE) for a localisation CT scan at 130 kV as part of a cervical spine SPECT/CT examination. Plot points are patient-specific organ doses for examinations on a Siemens Symbia Intevo Bold (squares) and Siemens Symbia Intevo 6 (circles). Associated exponential regression lines are visualised as a full and dashed line, respectively.

C. Diagnostic CT of the lumbar spine

Correlation between organ doses and water equivalent diameter

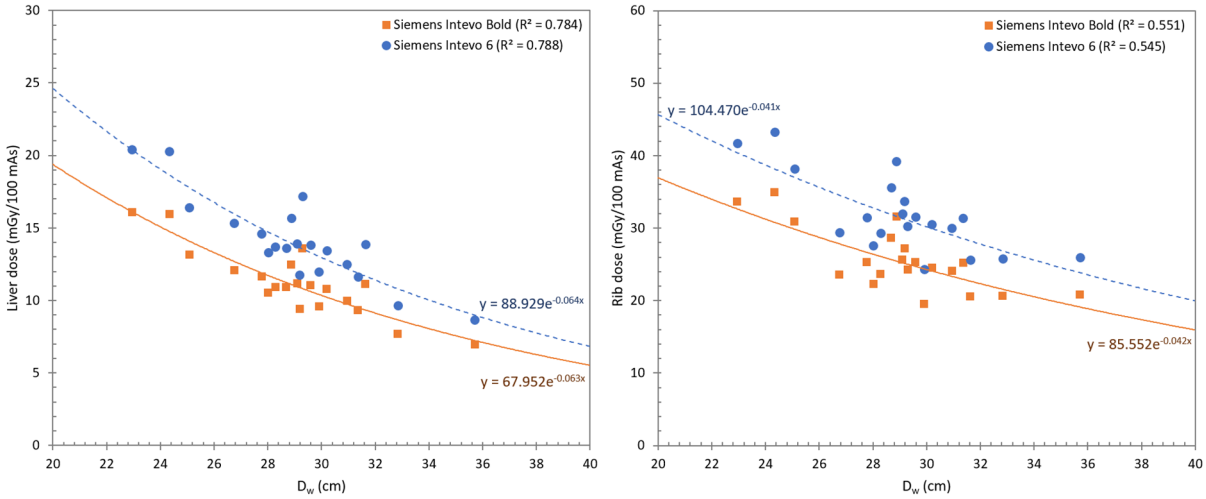

(a) Liver (b) Ribs

Figure 90: Estimated normalised (a) liver and (b) rib dose as a function of water equivalent diameter (D_w) for a diagnostic CT scan at 130 kV as part of a lumbar spine SPECT/CT examination. Plot points are patient-specific organ doses for examinations on a Siemens Symbia Intevo Bold (squares) and Siemens Symbia Intevo 6 (circles). Associated exponential regression lines are visualised as a full and dashed line, respectively.

Correlation between organ doses and size-specific dose estimate

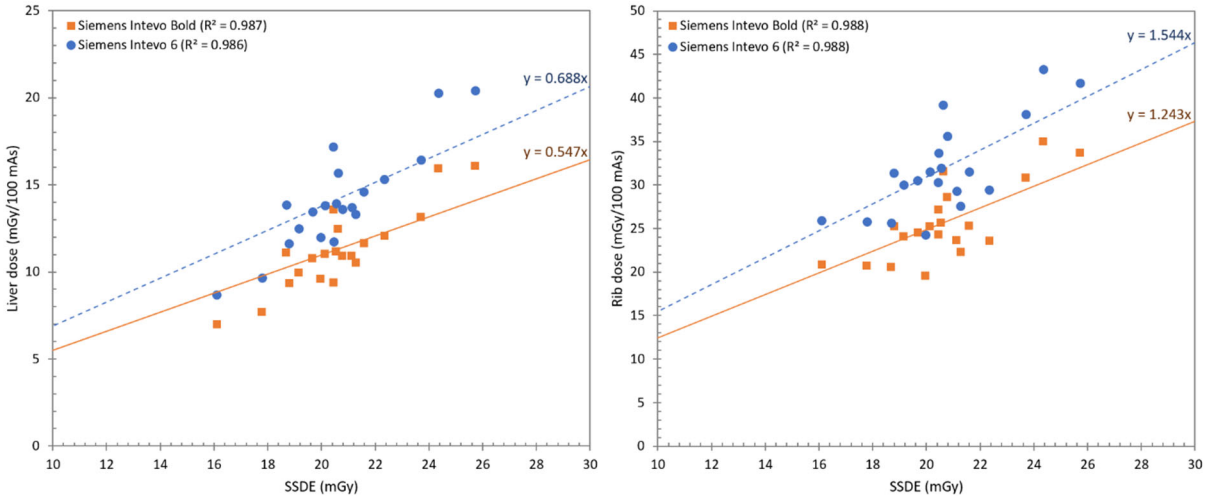

(a) Liver (b) Ribs

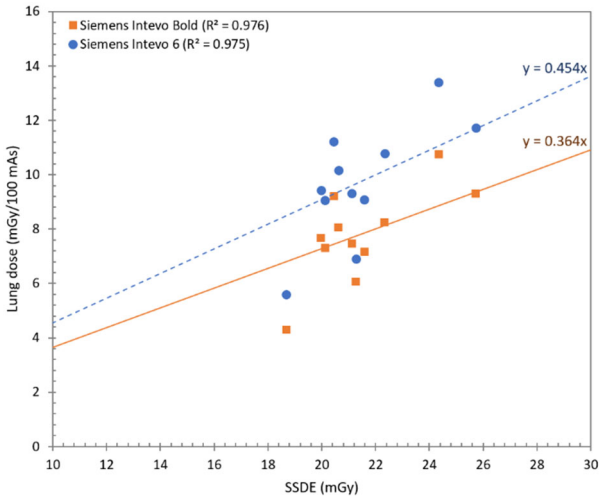

(c) Lungs

Figure 91: Estimated normalised (a) liver, (b) rib and (c) lung dose as a function of size-specific dose estimate (SSDE) for a diagnostic CT scan at 130 kV as part of a lumbar spine SPECT/CT examination. Plot points are patient-specific organ doses for examinations on a Siemens Symbia Intevo Bold (squares) and Siemens Symbia Intevo 6 (circles). Associated exponential regression lines are visualised as a full and dashed line, respectively.

D. Localisation CT of the lumbar spine

Correlation between organ doses and water equivalent diameter

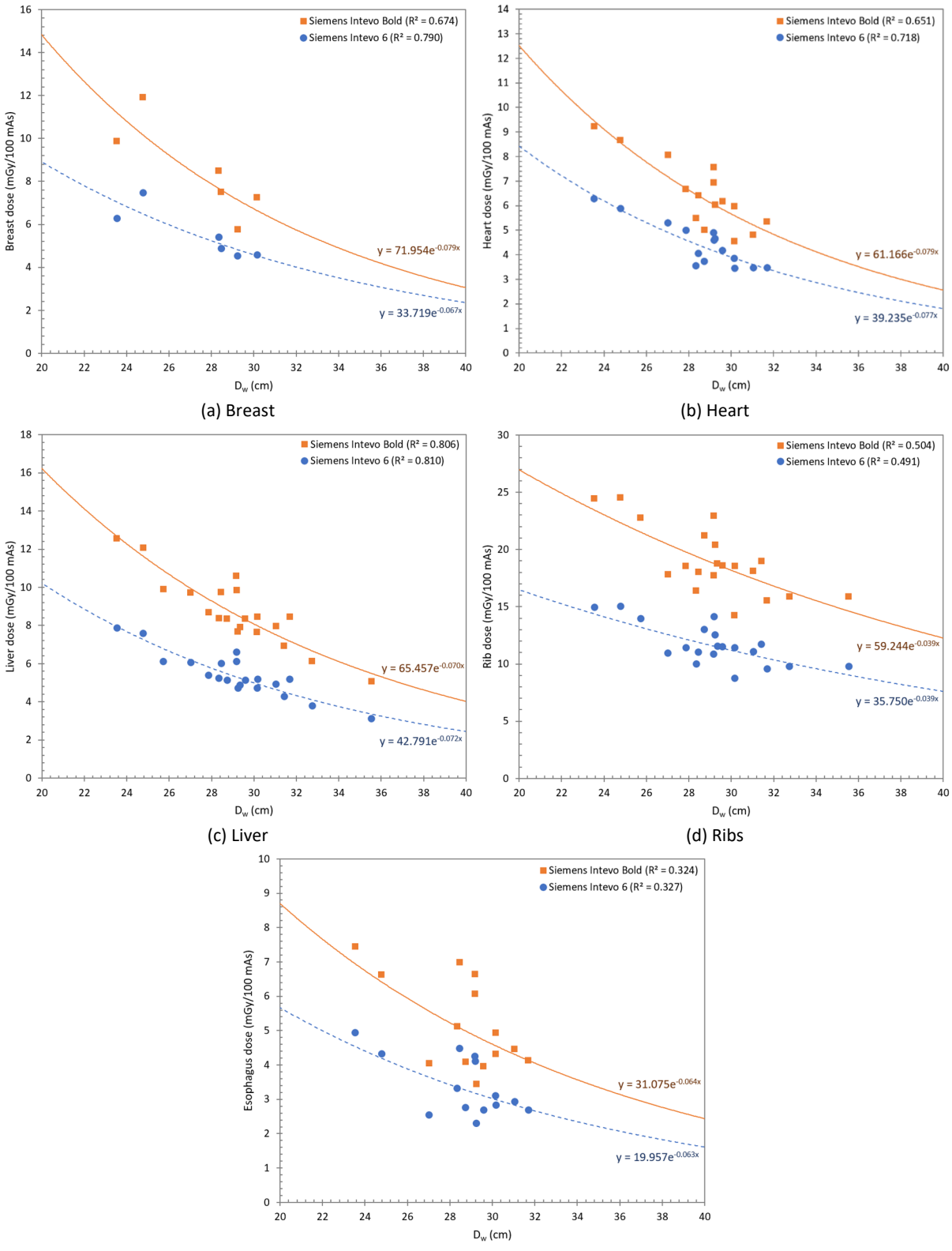

Figure 92: Estimated normalised (a) breast, (b) heart, (c) liver, (d) rib and (e) esophagus dose as a function of water equivalent diameter (D_w) for a localisation CT scan at 130 kV as part of a lumbar spine SPECT/CT examination. Plot points are patient-specific organ doses for examinations on a Siemens Symbia Intevo Bold (squares) and Siemens Symbia Intevo 6 (circles). Associated exponential regression lines are visualised as a full and dashed line, respectively.

Correlation between organ doses and size-specific dose estimate

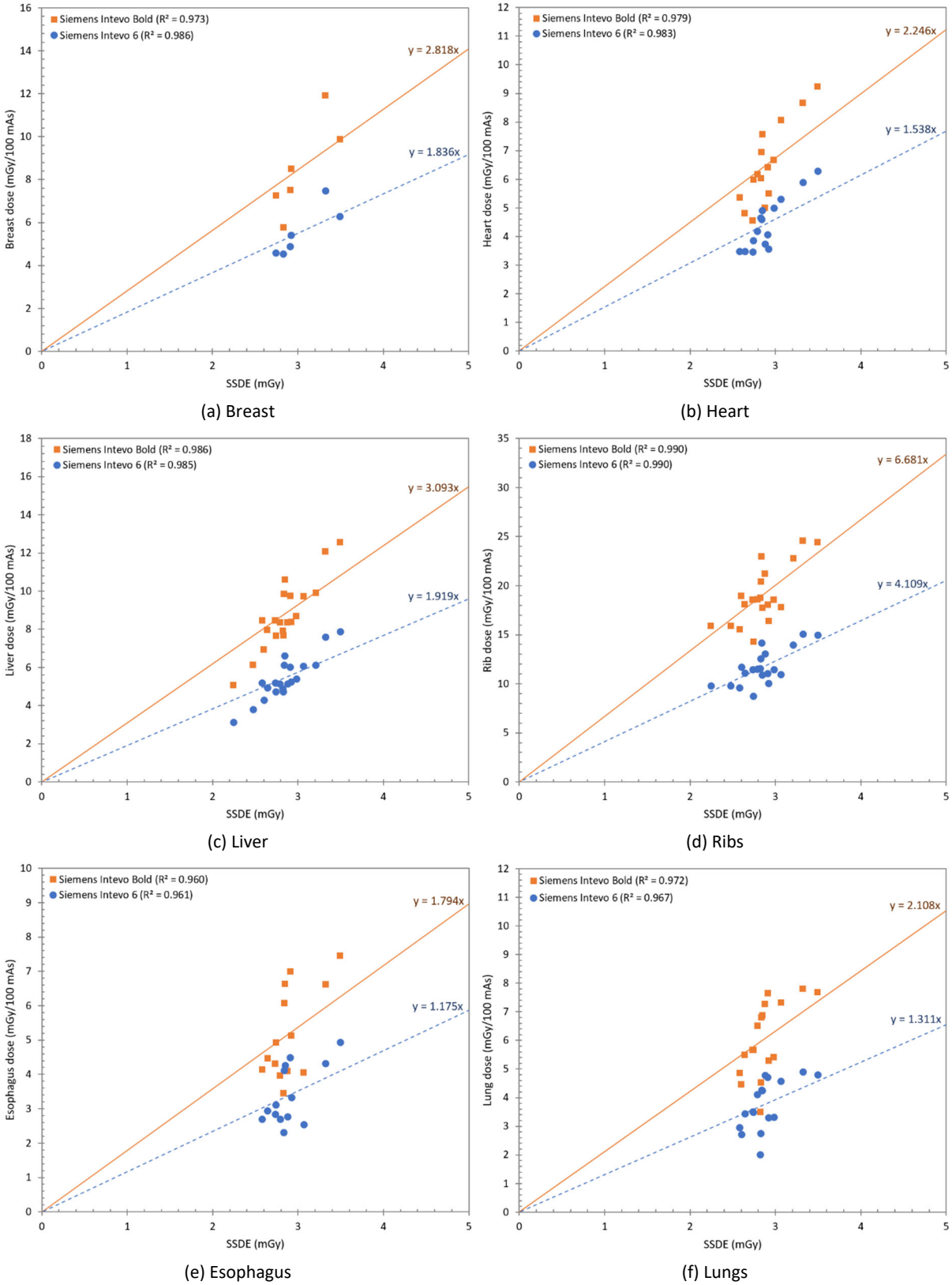

Figure 93: Estimated normalised (a) breast, (b) heart, (c) liver, (d) rib, (e) esophagus and (f) lung dose as a function of size-specific dose estimate (SSDE) for a localisation CT scan at 130 kV as part of a lumbar spine SPECT/CT examination. Plot points are patient-specific organ doses for examinations on a Siemens Symbia Intevo Bold (squares) and Siemens Symbia Intevo 6 (circles). Associated exponential regression lines are visualised as a full and dashed line, respectively.